

ENERGY LABORATORY

MASSACHUSETTS INSTITUTE
OF TECHNOLOGY

AN INVESTIGATION OF THE
NUMERICAL TREATMENT OF CONDENSATION

by

Joseph Sasson and Andrei L. Schor

Energy Laboratory Report No. MIT-EL 85-010

August 1985



Energy Laboratory
and
Department of Nuclear Engineering
Massachusetts Institute of Technology
Cambridge, Mass. 02139

AN INVESTIGATION OF THE
NUMERICAL TREATMENT OF CONDENSATION

by

Joseph Sasson and Andrei L. Schor

August 1984

sponsored by

Northeast Utilities Co.
Foxboro Co.

under

M.I.T. Energy Laboratory Electric Utility Program

Report No. MIT-EL 85-010

"AN INVESTIGATION OF THE
NUMERICAL TREATMENT OF CONDENSATION"

by

Joseph Sasson and Andrei L. Schor

ABSTRACT

The simulation of complete condensation continues to challenge the numerical methods currently used for multi-phase flow modeling; especially at low pressures, the change of phase process from a two-phase mixture to liquid leads to severe pressure field perturbations and often failure of the calculations. During condensation, the local void fraction and pressure decrease rapidly; at the time of complete condensation, the strong nonlinearities of the equations at the phase-change point lead to convergence difficulties and/or unacceptably large mass or energy errors.

Various ad-hoc "fixes" for this phenomenon - often referred to as "water packing" - have been proposed and/or implemented over the last few years. However, they have failed to clarify the core of the problem and are still unsatisfactory. Indeed these solutions cast doubt on the numerical predictions and occasionally are unable to prevent the breakdown of the calculations.

The present investigations have focused on the roots of these difficulties, particularly on the nonlinear effects involved. A time-step control strategy was developed which removes or at least, greatly mitigates the aforementioned computational problems. Numerical

experiments as well as a mathematical analysis have both demonstrated the existence of a critical time-step size beyond which larger time-steps shall accommodate the liquid flow field to any perturbations; smaller time-steps shall cause the pressure to bounce, going out of range as it is indeed witnessed for condensation simulations where the time-steps are drastically reduced when the two phases are still coexisting.

Similar studies have been conducted on variety of numerical methods yielding some unexpected results in terms of time-step limit.

ACKNOWLEDGEMENTS

We wish to express our appreciation for the support provided by the Oak Ridge National Laboratory and the United States Department of Energy.

The fellowship granted one of the authors (Joseph Sasson) by the French Ministry of Foreign Affairs is gratefully acknowledged.

Thanks are due to Mrs. Rachel Morton for her help in computer related matters and Miss Marsha Levine for her readiness in helping locate various references used for this project.

We also wish to thank Mrs. Joel Sasson, for her skill and patience while typing the manuscript.

Finally, we acknowledge the support provided by the M.I.T. Department of Nuclear Engineering in the final stages of the project allowing the successful completion of this work.

The work reported herein is based on the thesis submitted by the first author for the M.S. degree in Nuclear Engineering at M.I.T.

TABLE OF CONTENTS

<u>Item</u>	<u>Page No.</u>
ABSTRACT	2
ACKNOWLEDGEMENTS	4
LIST OF TABLES	8
LIST OF FIGURES	9
NOMENCLATURE	10
CHAPTER I INTRODUCTION	
I.1. Motivation	13
I.2. Objectives	14
I.3. Previous work	14
I.4. Organization of the report	15
CHAPTER II MATHEMATICAL AND PHYSICAL MODELS IN THERMIT	
II.1. The two-phase flow model	16
II.1.1. Introduction	16
II.1.2. The six-equation model	17
II.2. Mixture models	20
II.2.1. The four-equation model	21
II.2.2. The homogeneous equilibrium model (HEM)	24
II.2.3. The exchange terms and the interfacial jump conditions ..	26

TABLE OF CONTENTS (continued)

II.3.	The physical models in THERMIT	26
II.3.1.	Wall friction	26
II.3.2.	Interfacial momentum exchange	30
II.3.3.	Wall heat transfer	33
II.4.	The numerical methods	36
II.4.1.	Introduction	36
II.4.2.	The numerical methods for fluid dynamics	38
II.4.3.	The solution scheme	46
II.4.4.	The Jacobian matrix and the pressure problem	48
CHAPTER III DESCRIPTION OF THE PROBLEM		
III.1.	Introduction	53
III.2.	Typical cases of condensation	54
III.2.1.	Description of the numerical experiments	54
III.2.2.	Analysis of the results	55
III.3.	Review of previous studies	58
III.4.	Preliminary investigations	61
CHAPTER IV A MATHEMATICAL SOLUTION OF CONDENSATION FOR THERMIT - 4E		
IV.1.	Introduction	63
IV.2.	A single-cell problem	65
IV.3.	Application to a multi-cell pipe	72

TABLE OF CONTENTS (continued)

CHAPTER V. COMPARATIVE ANALYSIS WITH OTHER NUMERICAL METHODS	
V.1. An implicit mass convection scheme	77
V.2. The fully explicit scheme	79
V.3. The method of characteristics	81
V.3.1. Introduction	81
V.3.2. Implicit characteristics	84
V.3.3. Explicit characteristics	89
V.4. A generalized approach	92
CHAPTER VI. TESTS OF THE METHOD	
VI.1. Tests with circular pipes	98
VI.2. Tests with loop simulations	104
CHAPTER VII. CONCLUSION	
VII.1. Conclusion and summary of the work	111
VII.2. The limitations of the analysis and recommendations for future work	112
APPENDICES	
Appendix A: Derivation of the momentum equation using the staggered mesh in the continuity equation	A-1
Appendix B: Thermodynamic derivations	B-1
Appendix C: Derivation of the sonic velocity	C-1
Appendix D: Approximation method of Krylov and Bogolyubov	D-1

TABLE OF CONTENTS (continued)

Appendix E: Implemented and modified subroutines	E-1
Appendix F: Code's inputs and outputs for typical cases	F-1
REFERENCES	116

LIST OF TABLES

<u>Table</u>	<u>Page No.</u>
2.1. Two-phase flow models	19

LIST OF FIGURES

<u>Figure</u>	<u>Page No.</u>
2.1. The fluid-wall interaction	25
2.2. Heat transfer selection logic	32
2.3. Minimum computational effort	37
2.4. Typical staggered grid	39
2.5. Sodium internal energy per unit volume versus internal energy	47
4.1. Representation of a single-cell problem	52
4.2. Staggered mesh for the momentum equations	71
4.3. Logic of the subroutine implemented	76
5.1. Sonic characteristic lines	85
5.2. Solution of the equivalent linearized equation for pressure	97
6.1. Test description	99
6.2. Steady state pressure profiles for circular pipe tests	101
6.3. Steady state density profiles for circular pipe tests	102
6.4. Loop modeling geometry	105
6.5. Steady state pressure profiles for loop tests	107
6.6. Steady state density profiles for loop tests	108
6.7. Inlet pressure versus time	109
6.8. Oscillatory loop flow	110
7.1. Pressure profile for assumed density profile	114

NOMENCLATURE

A	flow area	m^2
C	specific heat	$T/(kg \cdot ^\circ K)$
c	sonic velocity	m/sec
cf	contact fraction	-
D	diameter	m
e	internal energy per unit mass	J/kg
F	force	N
f	friction factor	-
G	mass flux, ρU	$kg(m^2 \cdot sec)$
g	gravitational acceleration	m/sec^2
h	enthalpy per unit mass	J/kg
h	heat transfer coefficient	$W/(m^2 \cdot ^\circ K)$
I	identity matrix	-
K	friction coefficient	$N \cdot s/m^4$
k	thermal conductivity	$W/(m \cdot ^\circ K)$
Nu	Nusselt number, hD/k	-
p	perimeter	m
P	pressure	Pa
Pr	Prandtl number, $\mu c_p/k$	-
Pe	Peclet number, $Re \cdot Pr$	-
Q	heat source	W
Re	Reynolds number, $\rho UD/\mu$	-
S	nucleate boiling suppression factor	-
T	temperature	$^\circ K$

NOMENCLATURE (continued)

t	time	sec
U	velocity	m/sec
u	velocity	m/sec
V	fluid volume	m ³
w	mass flow rate	kg/sec
x	quality	-
x,y,z	spatial coordinates	m
α	void (vapor) fraction	-
α	thermal diffusivity, $k(\rho c_p)$	m ² /sec
Γ	phase change rate	kg/m ³ .sec
δ_{\dots}	increment (or change) in...	-
δ	liquid film thickness	m
Δt	time step size	sec
$\Delta x, \Delta y, \Delta z$	mesh spacings	m
ϵ	eddy diffusivity	m ² /sec
η	weighting factor for interfacial velocity	-
θ	angle of a Fourier component	-
λ	amplification factor	-
μ	viscosity	N.sec/m ²
ρ	density	kg/m ³
ρ	spectral radius	-

NOMENCLATURE (continued)

σ	superficial tension	N/m
τ	shear stress	Pa
ω	overrelaxation parameter	-

Subscripts

a	phase "a"
e	equivalent
i	interfacial
l	liquid
P	at constant pressure
sat	saturation
v	vapor
w	wall
w	wetted

I. INTRODUCTION

I.1. Motivation

In order to simulate and investigate flows in test sections of experimental sodium loops and of LMFBR fuel assemblies, a thermal-hydraulic analysis code THERMIT-4e has been implemented along with a one-dimensional loop simulation capability. One of the developments involved in this latter implementation is to present a calculational methodology for treating natural circulation and particularly its application to the primary loop of a sodium-cooled reactor.

Natural circulation along the primary circuit is induced by the differences in both thermal center elevation and the coolant specific weight between the core -the hot region- and the intermediate heat exchangers or condensers -the cold region . Thus there is a possibility that the decay heat due to the reactor shutdown (or scram) could be adequately removed by proper design without the need for forced circulation provided by pumps. While results of single phase calculations are generally in good agreement with the experimental data, however the code has not been able to achieve a stabilized flow configuration when a significant amount of boiling is taking place in the heated section, apparently because of the inability of its original numerical scheme to correctly simulate the extremely violent condensation process occurring in the upper and lower plena of the coolant loop.

Most computer codes utilized in the industry produce a pressure "spike" which at best leads to very short time-steps being needed to ride out the disturbance and at worst causes complete calculation breakdown. This same effect has been and still is encountered in some transients investigated with codes for water systems. The phenomenon came to be referred to as "water-packing".

Its severity increases drastically at lower pressures, as the liquid-to-vapor density ratio increases, thus leading to stronger non-linearities. As expected, for sodium systems, this phenomenon is extreme, given the enormous difference between liquid and vapor densities.

I.2. Objectives

The purpose of this research has been to elucidate the reasons for the breakdown of the numerical schemes used for flow field modeling when a mesh-volume changes state over a time step, from a two-phase mixture to single phase liquid.

Then, our objectives have been to propose a simple problem for which the nonlinear equations involved can be decoupled and solved. We also sought possibilities to linearize the equations with acceptable approximations for a more general case.

The final goal has been to implement a simple subroutine which could be easily incorporated into the THERMIT-4E computer code and would be activated whenever a condensation process is detected.

I.3. Previous works

The problem has been examined before and various ad-hoc "fixes" have been proposed or used in water systems codes. However,

none of them could point to the essence of this peculiar behavior, but focused rather on eliminating (or reducing) the pressure spike itself by modifying and/or adding artificial terms in the basic equations when a water-packing situation is expected or encountered [1-3]. Moreover, they are not guaranteed to work for whatever transient is considered and therefore a more theoretical approach was deemed necessary for further progress.

I.4. Organization of the report

The following chapter presents the code used for this research -THERMIT-4E-, especially the governing differential equations and the numerical methods used to solve them.

The purpose of chapter III is to describe some of the numerical experiments of condensation examined as well as the analysis of the results. We shall emphasize the simplifications that have been made enabling us to neglect the influence of some parameters which do not affect the calculations, as a first approach to the problem itself.

Chapter IV presents the mathematical solutions of condensation for THERMIT-4E, while in chapter V a comparative analysis of other numerical schemes is carried out.

Next, chapter VI discusses tests of the method implemented. Finally, the last chapter summarizes our conclusions and offers some recommendations for future studies on this subject.

II. Mathematical and Physical Models in THERMIT

II.1. The Two-Phase Flow Model

II.1.1. Introduction

Mathematical models for vapor-liquid flows are usually derived starting from the local instantaneous differential conservation laws of mass, momentum and energy and the interfacial jump conditions. Models of varying sophistication result from the specific choices for the averaging procedures and the assumptions made about the nature of the mechanical and thermal coupling between the vapor and the liquid phases.

The most general model is the two-fluid, six-equation model (also referred to as the separated-phase model). It describes each phase by an average temperature and velocity. It could in theory provide the maximum in capability and physical consistency among the two-phase flow models. Various two-phase mixture models also exist. These mixture models use less than six equations and consequently require additional assumptions about the thermal and mechanical coupling between the phases.

II.1.2. The Six-Equation Model

The detailed derivation of the volume-averaged two-phase equations is given in [5]. The working form of these conservation equations is written in one dimension since the proposed method can easily be generalized to two or three dimensions.

Vapor mass equation

$$\frac{\partial}{\partial t} (\alpha \rho_v) + \frac{\partial}{\partial x} (\alpha \rho_v U_v) = \Gamma \quad (2.1.a)$$

Liquid mass equation

$$\frac{\partial}{\partial t} [(1-\alpha)\rho_l] + \frac{\partial}{\partial x} [(1-\alpha)\rho_l U_l] = -\Gamma \quad (2.1.b)$$

Vapor momentum equation

$$\alpha \rho_v \frac{\partial U_v}{\partial t} + \alpha \rho_v U_v \frac{\partial U_v}{\partial x} + \alpha \frac{\partial P}{\partial x} = -F_{wv} - F_{iv} + \alpha \rho_v \vec{x} \cdot \vec{g} \quad (2.1.c)$$

Liquid momentum equation

$$(1-\alpha)\rho_l \frac{\partial U_l}{\partial t} + (1-\alpha)\rho_l U_l \frac{\partial U_l}{\partial x} + (1-\alpha) \frac{\partial P}{\partial x} = -F_{wl} - F_{il} + (1-\alpha)\rho_l \vec{x} \cdot \vec{g} \quad (2.1.d)$$

Vapor internal energy equation

$$\begin{aligned} \frac{\partial}{\partial t} (\alpha \rho_v e_v) + \frac{\partial}{\partial x} (\alpha \rho_v e_v U_v) + P \frac{\partial}{\partial x} (\alpha U_v) + P \frac{\partial \alpha}{\partial t} \\ = Q_{wv} + Q_{iv} + Q_{kv} \end{aligned} \quad (2.1.e)$$

Liquid internal energy equation

$$\begin{aligned} \frac{\partial}{\partial t} [(1-\alpha)\rho_l e_l] + \frac{\partial}{\partial x} [(1-\alpha)\rho_l e_l U_l] + P \frac{\partial}{\partial x} [(1-\alpha)U_l] \\ - P \frac{\partial \alpha}{\partial t} = Q_{wl} + Q_{il} + Q_{kl} \end{aligned} \quad (2.1.f)$$

Note: \vec{x} is a unit vector parallel to the channel's centerline.

where:

Γ = interfacial mass exchange rate

Q_{wa} = phase 'a' wall heat source

Q_{ia} = phase 'a' heat source due to interfacial effects

Q_{ka} = phase 'a' conduction heat transfer rate

F_{ia} = phase 'a' interfacial momentum exchange

F_{wa} = phase 'a' wall momentum exchange

a = liquid or vapor phase

The interfacial momentum exchange terms are extensively presented in section II.3.2.

It should be noted that the internal energy equations are not conservation equations. They are obtained from the total energy conservation equations by subtracting the corresponding mechanical energy equation from the total energy equation.

This form is used for numerical convenience. Also the momentum equations are written in non-conservative form for the same convenience reason, which will later become apparent.

Table 2.1. Two-Phase Flow Models

(General assumption: $p_l = p_v$)

Two-Phase-Flow Model (suggested nomenclature)	Conservation Equations				Imposed Restrictions			Required Constitutive Relations					
	M	E	K	Total	T_a	U_r	Total	External		Interfacial			Total
								Q_w	F_w	Γ	Q_i	F_i	
3 C	1	1	1	3	2	1	3	1	1	0	0	0	2
4 C 2 M	2	1	1	4	1	1	2	1	1	1	0	0	3
4 C 2 E	1	2	1	4	1	1	2	2	1	1*	1	0	5
4 C 2 K	1	1	2	4	2	0	2	1	2	1*	0	1	5
5 C 1 K	2	2	1	5	0	1	1	2	1	1	1	0	5
5 C 1 E	2	1	2	5	1	0	1	1	2	1	0	1	5
5 C 1 M	1	2	2	5	1	0	1	2	2	1*	1	1	7
6 C	2	2	2	6	0	0	0	2	2	1	1	1	7

Legend: M = Conservation of Mass
 E = Conservation of Energy
 K = Conservation of Momentum
 T_a = Phase "a" temperature; a = v or l
 U_r = Relative velocity = $U_v - U_l$

*note that the interface mass exchange, Γ , is needed whenever Q_i and/or F_i are needed.

There are 8 unknowns in equations (2.1). These are α , ρ_v , ρ_l , P , e_v , e_l , U_v and U_l . The wall and interfacial exchange terms as well as the effective fluid conduction heat sources (defined above), are assumed to depend, via constitutive relations, on these variables and the phase temperatures, T_v and T_l , which represent two additional unknowns. Thus we have a total of 10 unknowns.

Equations (2.1) are equivalent to 6 equations, hence we must provide 4 additional equations for closure. These are the equations of state given in the form:

$$\rho_v = \rho_v(P, T_v) \quad (2.2a)$$

$$\rho_l = \rho_l(P, T_l) \quad (2.2b)$$

$$e_v = e_v(P, T_v) \quad (2.3a)$$

$$e_l = e_l(P, T_l) \quad (2.3b)$$

II.2. Mixture models

As mentioned earlier on, a mixture model is a degenerate form of the six-equation model and we should expect consistent results from all models by activating the appropriate constraints or assumptions that led to each model. Table 2.1. gives a summary of the two-phase flow models.

The four-equation model will be discussed in greater detail because of its relevance to the THERMIT-4E code that is used in this work. The homogeneous equilibrium model shall also be

discussed because it provides an easy analytical tool for the treatment of condensation in chapter 4.

II.2. 1. The four-equation model

The detail of the considerations leading to the adoption of the four-equation model in THERMIT-4E has been given in reference [5]. Importantly, the code is developed for the particular applications of the analysis of two-phase sodium coolant flows. The very high conductivity of the liquid sodium precludes significant temperature gradients in the vicinity of the liquid-vapor interface and thus makes the assumption of thermal equilibrium at saturation of the coexisting phases a reasonable one. The assumption of mechanical equilibrium cannot be justified however, because the enormous liquid-vapor density ratio of sodium at near atmospheric pressure coupled with the prevalent low flow conditions lead to substantial slip ratios. It will therefore be necessary to write separate momentum equations for the two-phase in any worthwhile mixture model.

In the 6-equation model, the parameters ρ_v , ρ_ℓ , e_v , e_ℓ are functions of T_v or T_ℓ and P (eqs. 2 and 3) but with the assumption of thermal equilibrium at saturation, $T_v = T_\ell = T_s$, these parameters all become functions only of T_s . Thus, the equations of state become:

$$\rho_v = \rho_v(P) \quad (2.4 \text{ a})$$

$$\rho_\ell = \rho_\ell(P) \quad (2.4 \text{ b})$$

$$e_v = e_v(P) \quad (2.4 \text{ c})$$

$$e_{\ell} = e_{\ell}(P) \quad (2.4 d)$$

$$T_s = T_s(P) \quad (2.4 e)$$

Hence, the 3 unknowns T_v , T_{ℓ} , P in (2.2) and (2.3) reduce to only 1 unknown P in (2.4). The number of conservation equations is also reduced by two, from six to four, yielding the four-equation model as follows:

Mixture mass equation

$$\frac{\partial}{\partial t} \rho + \frac{\partial}{\partial x} [\alpha \rho_v U_v + (1-\alpha) \rho_{\ell} U_{\ell}] = 0 \quad (2.5 a)$$

Momentum equations

$$(\text{identical to 2.1 (c) \& (d)}) \quad (2.5 b,c)$$

Mixture internal energy equation

$$\begin{aligned} \frac{\partial}{\partial t} (\rho_m e_m) + \frac{\partial}{\partial x} [\alpha \rho_v e_v U_v + (1-\alpha) \rho_{\ell} e_{\ell} U_{\ell}] \\ + P \frac{\partial}{\partial x} [\alpha U_v + (1-\alpha) U_{\ell}] = Q_w + Q_{im} + Q_k \end{aligned} \quad (2.5 d)$$

where

$$\rho_m = \alpha \rho_v + (1-\alpha) \rho_{\ell} \quad (2.6 a)$$

$$e_m = [\alpha \rho_v e_v + (1-\alpha) \rho_{\ell} e_{\ell}] / \rho_m \quad (2.6 b)$$

$$Q_w \equiv \text{mixture wall heat source}$$

$$= Q_{wv} + Q_{w\ell}$$

$$\begin{aligned}
 Q_{im} &\equiv \text{mixture heat source due to interfacial effects} \\
 &= Q_{iv} + Q_{il}
 \end{aligned}$$

$$\begin{aligned}
 Q_k &\equiv \text{mixture conduction heat transfer rate} \\
 &= Q_{kv} + Q_{kl}
 \end{aligned}$$

ρ_m and e_m are 2 additional unknowns to the 10 unknowns counted in the six-equation model. Thus we have a total of 12 unknowns. Equations (2.5) and definitions (2.6) represent a total of 6 equations. The 4 equations of state (2.4), and the 2 equations implied in the assumption of thermal equilibrium at saturation:

$$T_v = T_l = T_{sat}(P) \quad (2.7)$$

provide the additional 6 equations required for closure.

By using the four equations (2.5), the two definitions (2.6) and the two constraints (2.7), we shall be able to calculate the following eight quantities α , T_v , T_l , ρ_m , ρ_v , ρ_l , e_v , e_l , for any given P and e_m . This is a very important step in the solution technique in THERMIT.

As shall be shown in a later section, reduction of conservation equations to pressure problem is a dominant feature of the numerical method in the code.

The following terms are neglected in the THERMIT-4E formulation because of their relatively very low magnitudes:

(i) contribution of interfacial effects to mixture heat source,

i.e., work terms due to interfacial momentum exchange and the kinetic energy transport via interfacial mass exchange, the mixture heat source due to interfacial effects, ii) the pseudo-work terms due to wall forces in the wall heat source.

II.2.2. The homogeneous equilibrium model (HEM)

The HEM or the three-equation mixture model is obtained by assuming thermal equilibrium of the co-existing phases at saturation and equal phase velocities. Equilibrium drift flux model would result if a correlation for relative velocity were used.

The resulting HEM conservation equations are given below:

Mixture mass equation

$$\frac{\partial}{\partial t} \rho_m + \frac{\partial}{\partial x} (\rho_m U_m) = 0 \quad (2.8 \text{ a})$$

Mixture momentum equation

$$\rho_m \frac{\partial U_m}{\partial t} + (\rho_m U_m) \frac{\partial U_m}{\partial x} + \frac{\partial P}{\partial x} = -F_w + \rho_m \vec{x} \cdot \vec{g} \quad (2.8 \text{ b})$$

Mixture internal energy equation

$$\frac{\partial}{\partial t} (\rho_m e_m) + \frac{\partial}{\partial x} (\rho_m e_m U_m) + P \frac{\partial U_m}{\partial x} = Q_w + Q_k \quad (2.8 \text{ c})$$

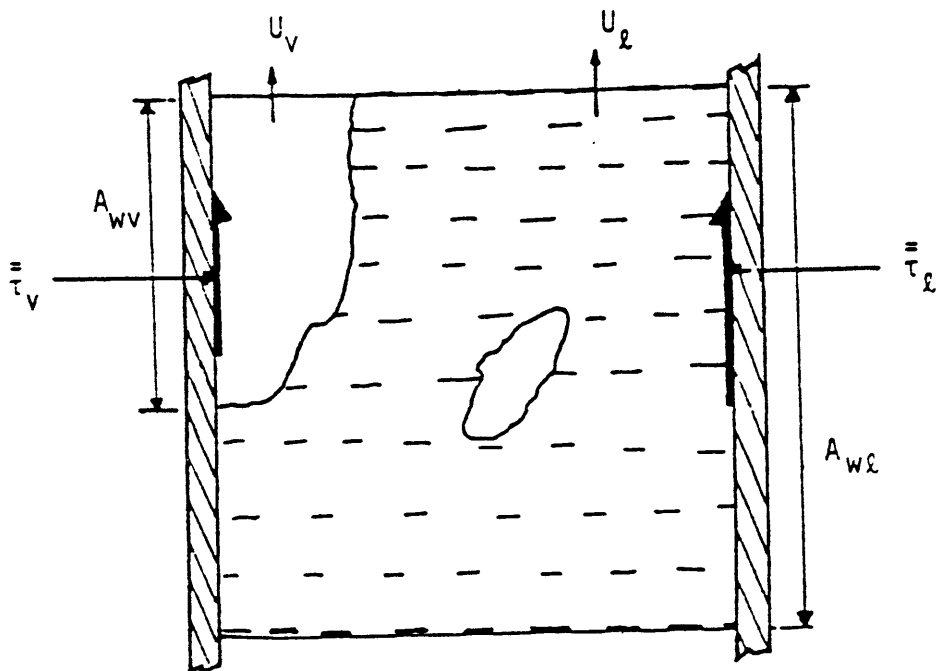


Figure 2.1. The Fluid-Wall Interaction

where

U_m = the mixture velocity

$U_m = U_v = U_l$

II.2.3. The exchange terms and the interfacial jump conditions

The wall and the interfacial exchange terms are the mass, momentum and energy exchanges that take place at the fluid-wall and the fluid-fluid interface respectively. The interfacial jump conditions are essentially the equations of conservation of mass, momentum and energy at the fluid-fluid interface.

The definitions of the exchange terms and the interfacial jump conditions have been given in reference [5].

II.3. The physical models in THERMIT

II.3.1. Wall friction

The fluid-solid interaction at the wall leads to momentum dissipation F_{wa} [force per mixture unit volume] of the phase "a" forming interface with the solid (fig. 2.1).

In fig. 2.1 τ_{wa} represents the average wall shear for the phase "a" and A_{wa} represents the average area 'wetted' by the phase "a".

$$F_{wa} = \left(\frac{A_{wa}}{V} \right) \tau_{wa} \quad (2.9)$$

By analogy to single-phase flow, τ_{wa} can be related to the kinetic energy of phase "a" through a Darcy-type relation.

$$\tau_{wa} = \frac{1}{8} f_{wa} \rho_a |U_a| U_a \quad (2.10)$$

where

$$f_{wa} \equiv \text{friction factor for phase a.}$$

The wetted area per unit volume for phase "a" is given as:

$$\begin{aligned} \frac{A_{wa}}{V} &= \frac{P_{wa} L}{AL} = \frac{P_w}{A} C_{fa} \\ &= \frac{4}{D_e} C_{fa} \end{aligned} \quad (2.11)$$

where

$$P_{wa} = \text{wetted perimeter for phase "a"}$$

$$L = \text{'length' of the control volume}$$

$$A = \text{total flow area}$$

$$P_w = \text{total wetted perimeter}$$

$$D_e = \text{equivalent hydraulic diameter}$$

$$= 4A/P_w$$

$$C_{fa} = \text{contact fraction of phase a} = P_{wa}/P_w$$

Combining (2.11), (2.10) and (2.9) we obtain the final forms of the wall frictional force per unit volume for phase a as:

$$F_{wa} = \frac{C_{fa}}{2D_e} f_{wa} \rho_a |U_a| U_a \quad (2.12 a)$$

$$= K_{wa} U_a \quad (2.12 b)$$

We shall refer to K_{wa} as the wall friction coefficient for phase a.

The factor C_{fa} and f_{wa} must be defined with proper considerations to the two-phase situations.

An assumption which has been deemed adequate is that whenever two-phase flow exists, an annular flow regime prevails, with the liquid coating the solid surfaces. At very high void fractions, some vapor wall contact is allowed. Accordingly, C_{fa} is prescribed as:

$$C_{fl} = \begin{cases} 1.0 & ; \alpha < 0.89 \\ 10(0.99-\alpha) & ; 0.89 < \alpha < 0.99 \\ 0.0 & ; \alpha > 0.99 \end{cases} \quad (2.13)$$

and

$$C_{fv} = 1 - C_{fl}$$

For f_{wa} , the following postulate is made by analogy to the single-phase flows:

$$f_{wa} = C Re_a^{-b} \quad (2.14)$$

The Reynold's number Re_a of the phase "a" is defined to take into account the actual flow area of phase "a".

$$Re_a = \frac{\rho_a U_a D_{e,a}}{\mu_a} \quad (2.15)$$

where

$$\begin{aligned}
 D_{e,a} &= \frac{4A_a}{P_w} \\
 &= \frac{4\alpha_a A}{P_w} \\
 &= \alpha_a D_e \qquad (2.16)
 \end{aligned}$$

We shall now provide the working form correlation (equation (2.14)) for the axial flow condition that is relevant to our 1-D loop flow problem.

The correlations that follow are formulated for wire-wrapped rod bundle flow-channels; they are specific forms of equation (2.14).

Axial flow

$$(f_{wa})_{\text{laminar}} = \frac{32}{\sqrt{H}} \left(\frac{P}{D} \right)^{1.5} \frac{1}{Re_a}, \text{ for } Re_a < 400 \quad (2.17a)$$

$$(f_{wa})_{\text{turbulent}} = \frac{0.316M}{Re_a^{0.25}}, \text{ for } Re_a > 2600 \quad (2.17b)$$

$$\begin{aligned}
 (f_{wa})_{\text{transition}} &= (f_{wa})_{\text{turbulent}} \sqrt{\psi} + (f_{wa})_{\text{laminar}} \\
 &\quad \times \sqrt{1-\psi}, \text{ for } 400 < Re_a < 2600 \quad (2.17c)
 \end{aligned}$$

where:

$$M = \left[\frac{1.034}{(P/D)^{0.124}} + \frac{29.7(P/D)^{6.94} Re_a^{(0.086)}}{(H/D)^{2.239}} \right]^{0.885}$$

$$\psi = (Re_a - 400)/2200$$

H = wire-wrap lead length (meters),

P/D = pitch-to-diameter ratio,

H/D = helical pitch-to-diameter ratio

The laminar flow correlation was proposed by Engel et al, and the correlation used in turbulent flow is a slightly modified version of the correlation due to Novendstern. To avoid unrealistic situations for bare rods (i.e. $H \rightarrow \infty$), a cut-off is imposed on the laminar correlation by requiring $f_{\text{laminar}} Re > 60$. The hydraulic diameter has been recommended to be calculated as :

$$D_e = 4 \times A (\text{bundle}) / P_w (\text{rods} + \text{ducts}) \quad (2.18)$$

II.3.2. Interfacial momentum exchange

The interfacial momentum exchange F_{ia} in (2.2) is made up of two components, one due to interfacial mass exchange, the other due to form and shear drag at the interface.

The form of the correlation used in THERMIT-4E for F_{ia} are given below

$$\begin{aligned}
 F_{iV} &= K_{iV} (U_V - U_\ell) \\
 F_{i\ell} &= K_{i\ell} (U_V - U_\ell)
 \end{aligned}
 \tag{2.19}$$

where

$$\begin{aligned}
 K_{iV} &= \eta \Gamma + K_i \\
 K_{i\ell} &= (1-\eta) \Gamma + K_i
 \end{aligned}
 \tag{2.20}$$

η is a weighting factor defined (empirically) for the present by a donor-like formulation [5].

$$\begin{aligned}
 \eta &= 1, \text{ if } \Gamma > 0 \text{ (evaporation)} \\
 \eta &= 0, \text{ if } \Gamma < 0 \text{ (condensation)}
 \end{aligned}$$

Γ and K_i must be specified in (2.19) in order to obtain the momentum exchange coefficients K_{iV} and $K_{i\ell}$ in (2.20).

Γ is obtained from the equation of conservation of mass on any one of the phases. Thus for the vapor phase;

$$\Gamma = \frac{\partial}{\partial t} (\alpha \rho_V) + \frac{\partial}{\partial x} (\alpha \rho_V U_V)
 \tag{2.21}$$

The following correlations for K_i are obtained using the Wallis correlation [5] for friction factor.

$$\begin{aligned}
 (K_i)_{\text{turbulent}} &= \frac{0.01}{D_e} \sqrt{\alpha} [1 + 150 (1 - \sqrt{\alpha})] \rho_V |U_r| \\
 (K_i)_{\text{laminar}} &= \frac{32\mu_V}{D_e^2}
 \end{aligned}
 \tag{2.22}$$

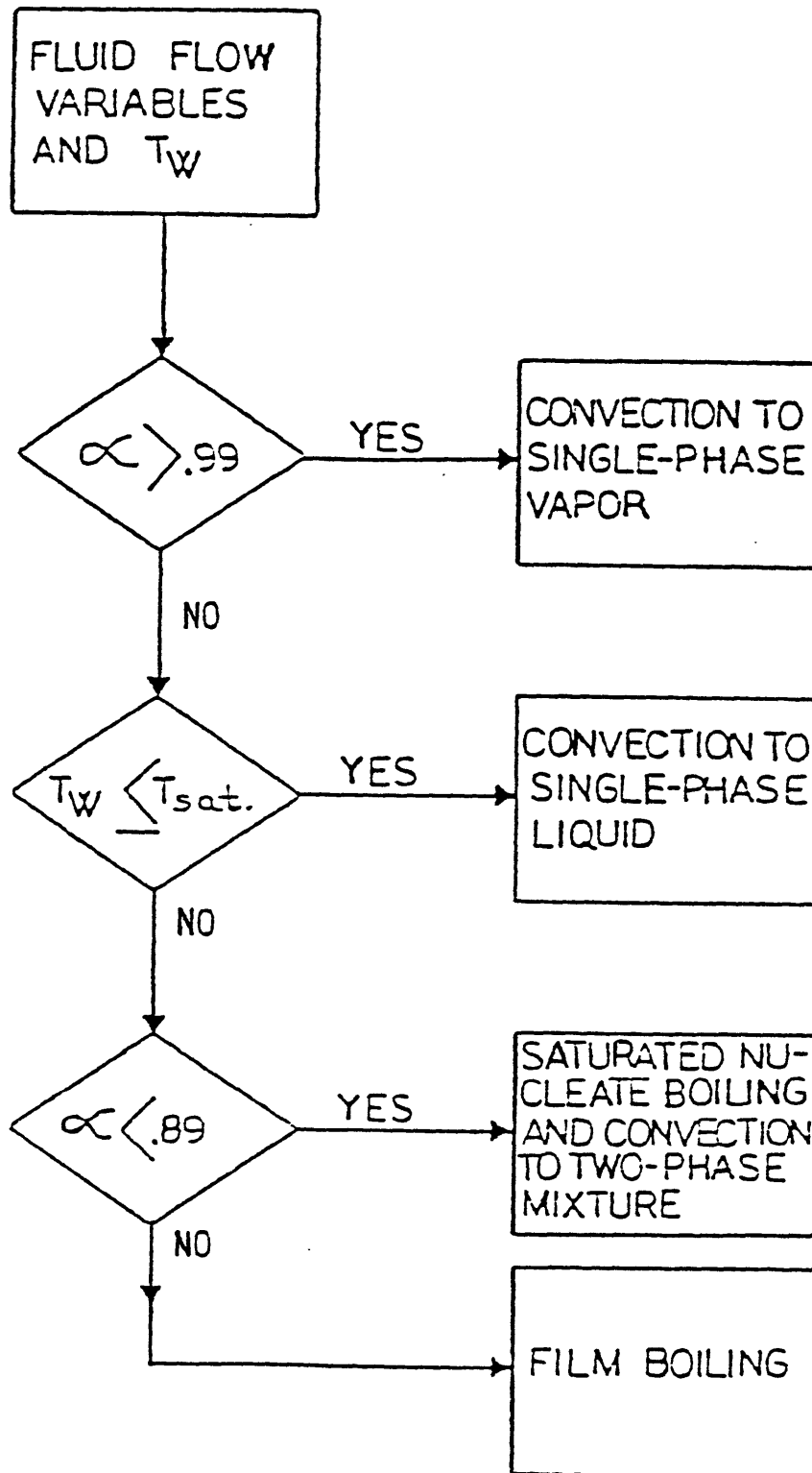


Figure 2.2. Heat Transfer Selection Logic

where

$$U_r = \text{relative velocity} = U_v - U_l$$

II.3.3. Wall heat transfer

The heat transfer correlations between the fluid and the solid surfaces (heater or fuel rods and the hex can) that are used in the code are given in this section.

Fuel or heater rods

The heat transfer regime selection logic is presented in fig. 2.2 adapted from reference [5]. The correlation for single-phase liquid in triangular - arrayed bundle due to Schad is adopted.

$$\begin{aligned} \text{Nu} &= \text{Nu}_0 (\text{Pe}/150)^{0.3} & \text{Pe} > 150 \\ &= \text{Nu}_0 & \text{Pe} < 15 \end{aligned} \quad (2.24)$$

where

$$\text{Nu}_0 = 4.5 [-16.15 + 24.96 (P/D) - 8.55 (P/D)^2]$$

$$\text{and Pe} = \text{Re} \cdot \text{Pr}$$

The single-phase vapor heat transfer correlation used is the well-known Dittus-Boelter's correlation:

$$\text{Nu} = 0.023 \text{Re}^{0.8} \text{Pr}^{0.4} \quad (2.25)$$

For two-phase fluid heat transfer, the total heat transfer coefficient for two-phase flow boiling with no liquid deficiency is given by:

$$h_{TP} = h_c + h_{NB} \quad (2.26)$$

as suggested by Manahan [5].

The convective component h_c could be represented by the Schad's correlation in which the Peclet number for two-phase (Pe_{TP}) is given by:

$$Pe_{TP} = Re_{TP} Pr_\ell \quad (2.27)$$

and the two-phase Reynold's number (Re_{TP}) is obtained through the factor F defined as

$$F = (Re_{TP}/Re_\ell)^{0.8} \quad (2.28)$$

F depends on the Martinelli's parameter, x_{tt} .

$$x_{tt} = \left(\frac{1-x}{x} \right)^{0.9} \left(\frac{\rho_v}{\rho_\ell} \right)^{0.5} \left(\frac{\mu_\ell}{\mu_v} \right)^{0.1} \quad (2.29)$$

The heat transfer correlation for nucleate boiling due to Forster-Zuber's analysis is [5]:

$$h_{NB} = 0.00122 \left[\frac{K_\ell^{0.79} C_{P\ell}^{0.45} \rho_\ell^{0.49}}{\sigma^{0.5} \mu_\ell^{0.29} h_{fg}^{0.24} \rho_\ell^{0.24}} \right] \Delta T_{sat}^{0.24} \Delta P_{sat}^{0.75} S \quad (2.30)$$

where

ΔT_{sat} = wall superheat,

ΔP_{sat} = pressure difference corresponding to T_{sat} ,

S = nucleate boiling suppression factor,

$$= (\Delta T_{sat,e}/\Delta T_{sat})^{0.99},$$

$\Delta T_{\text{sat,e}}$ = effective wall superheat.

The following fits for F and S are given in reference [5].

$$F = \begin{cases} 1.0, & x_{\text{tt}}^{-1} < 0.10 \\ 2.35(x_{\text{tt}}^{-1} + 0.213)^{0.736}, & x_{\text{tt}} > 0.10 \end{cases} \quad (2.31)$$

$$S = \begin{cases} [1.0 + 0.12 (Re'_{\text{TP}})^{1.14}]^{-1}, & Re'_{\text{TP}} < 32.5 \\ [1.0 + 0.42 (Re'_{\text{TP}})^{0.78}]^{-1}, & 32.5 \leq Re'_{\text{TP}} \leq 70.0 \\ 0.1, & Re'_{\text{TP}} \geq 70.0 \end{cases} \quad (2.32)$$

where

$$Re'_{\text{TP}} = Re_{\text{TP}}(10^{-4})$$

At high void regimes, ($0.89 < \alpha < 0.99$), film begins to blanket the surface. Heat transfer decreases and is approximated by:

$$h_{\text{film}} = \psi^2 h_{\text{TP,c}} + (1-\psi^2) h_{\text{vapor}} \quad (2.33)$$

where

$$\psi = 10(0.99 - \alpha)$$

II.4. The numerical methods

II.4.1. Introduction

THERMIT is a lumped parameter component code that can handle up to three-dimensional two-phase flows. An Eulerian numerical approach is used for the fluid dynamics. This approach follows the evolution of the volume- (and time-) averaged values of material parameters and other quantities of interest at fixed points in space. The reactor is divided by a mesh into a collection of cells and the parameters and quantities are calculated at each cell as a function of time. The smearing of transported entities within the cells due to this technique is minimized by reducing the sizes of the averaging volumes wherever there is a strong spatial variation of the quantity being averaged.

The numerical method in THERMIT is a modified form of the successful I.C.E. (Implicit Continuum Eulerian) technique. Like the I.C.E. method, it uses a staggered grid, treats sonic propagation implicitly and convective transport explicitly and obtains a pressure-field solution from which the other variables are inferred. In THERMIT, all the equations (mass, momentum and energy) are blended simultaneously to obtain the pressure-field solution while in the I.C.E., the energy equation is treated explicitly. This choice of treatment is necessary in THERMIT because the change in density with energy can no longer be assumed a small correction to the flow field in two-phase flows as can be done in single-phase flows [8].

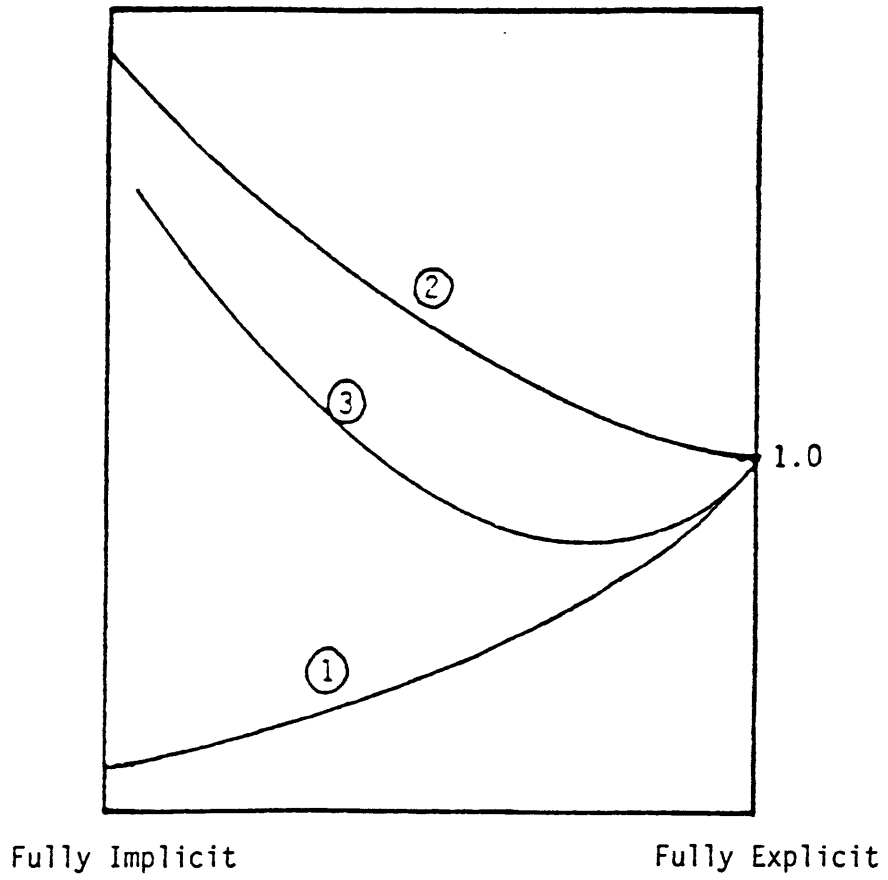


Figure 2.3. Minimum Computational Effort

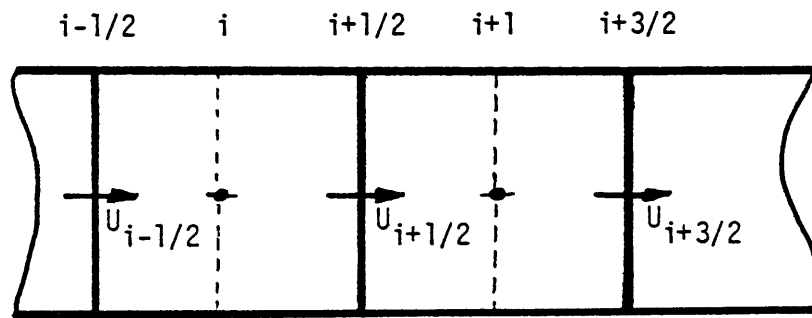
The next subsection gives a review of the numerical method used in the four-equation model THERMIT-4E simplified to a one-dimensional formulation. The detail of the analysis for multidimensional flows has been given in Schor and Todreas [5].

II.4.2. The numerical methods for fluid dynamics

The finite difference equations

The choice of the method of treatment of the time discretization of a system of partial differential equations can be obtained from a spectrum of schemes, ranging from fully explicit to fully implicit ones. Whatever the choice, stability and consistency must be ascertained in order to guarantee convergence. A judicious choice can be qualitatively inferred from the curve of minimum computational efforts (figure 2.3. [7]) and from the knowledge of the time scales of the phenomena involved. In light of the above, we seek a numerical method that treats local phenomena (couplings) and sonic propagation in a fully or highly implicit manner, while describing explicitly transport mechanisms by convection and diffusion.

In space, a fully donor-cell differencing is used accompanied by additional averaging whenever quantities are required at the locations other than those at which they are originally defined. The widely used staggered-mesh approach is adopted, whereby the scalar quantities are defined at the



cell center (i):

α , p , ρ_v , ρ_l , ρ_m ,

e_m , e_v , e_l , T_v , T_l

Figure 2.4. Typical Staggered Grid

cell center while the fluxes are defined at the cell faces to which they are normal (fig 2.4).

The discrete analogs of the partial differential equations describing our two phase model will now be presented.

The mixture mass equation

$$v(\rho_m^{n+1} - \rho_m^n)/\Delta t + \{A[(\alpha\rho_v)^n(U_v)^{n+1} + ((1-\alpha)\rho_\ell)^n(U_\ell)^{n+1}]\}_{i+1/2} - \{A[(\alpha\rho_v)^n(U_v)^{n+1} + ((1-\alpha)\rho_\ell)^n(U_\ell)^{n+1}]\}_{i-1/2} = 0 \quad (2.38)$$

In the above, the convected quantities are needed at cell faces, where fluxes are defined. Full donor-cell differencing being used to define these quantities, let C stand for any cell-centered quantity (see fig. 2.4) and consider the face $(i + 1/2)$, normal to the direction of flow in the loop. The quantity $C_{i+1/2}$ is then determined as:

$$C_{i+1/2} = \begin{cases} C_i & , \text{ if } (U)_{i+1/2}^n \geq 0 \\ C_{i+1} & , \text{ if } (U)_{i+1/2}^n \leq 0 \end{cases}$$

It is important to note that donor-cell decisions are made only with regard to quantities at time level n , using velocities at the same time level. As a result no difficulty arises even if a velocity sign change occurs during a time step.

The mixture energy equation

A number of variants for the finite difference equation exists. The conservative/semi-implicit convection (CSIC) scheme is given below:

$$\begin{aligned}
 & V[(\rho_m e_m)^{n+1} - (\rho_m e_m)^n]/\Delta t + [P^n + (\rho_v e_v)_{i+1/2}^n][A\alpha^n (U_v)^{n+1}]_{i+1/2} \\
 & + [P^n + (\rho_\ell e_\ell)_{i+1/2}^n][A(1-\alpha)^n (U_\ell)^{n+1}]_{i+1/2} \\
 & - [P^n + (\rho_v e_v)_{i-1/2}^n][A\alpha^n (U_v)^{n+1}]_{i-1/2} \\
 & - [P^n + (\rho_\ell e_\ell)_{i-1/2}^n][A(1-\alpha)^n (U_\ell)^{n+1}]_{i-1/2} \\
 & = Q_w^{n+1/2} + Q_K^{n+1/2} \tag{2.39}
 \end{aligned}$$

The difference forms of energy and the mass equations, (2.38) and (2.39) are a strict adaptation of the scheme used for a six-equation model to a four-equation "mixture" model. The schemes for both models are equivalent for single-phase, either liquid or vapor. For two-phase however, the four-equation adaptation suffers a subtle flaw, namely the lack of monotonicity of the mixture internal energy density $(\rho_m e_m)$ with respect to e_m . This feature is undesirable for the Newton method used to solve our system of equation.

To avoid the problem raised by the product $\rho_m e_m$, a non-conservative/semi-implicit convection (NCSIC) form of the energy equation is used. To this end, the mass equation is multiplied by e_m and then subtracted from the conser-

-vative form of the energy equation. The resulting difference equation is

$$V(\rho_m)^n [(e_m)^{n+1} - (e_m)^n] / \Delta t + [\text{conv}_e - \text{conv}_m]^{n+1/2} \\ = (Q_w + Q_K)^{n+1/2}$$

where $\text{conv}_m^{n+1/2}$ and $\text{conv}_e^{n+1/2}$ stand for the semi-implicit convective terms in the mass and energy equations, respectively. The heat sources appear with superscript $n+1/2$, indicating a combination of implicit / explicit components in the constitutive relations used for them.

The phasic momentum equations

The momentum equations are used in the non-conservative form, particularly convenient to our method. The control volume for which the momentum equation is written is offset by half mesh with respect to that used for the scalar quantities (fig. 2.4). The momentum equations are written below:

Vapor momentum equation

$$(\alpha \rho_v)^n_{i+1/2} \frac{[(U_v)^{n+1} - (U_v)^n]_{i+1/2}}{\Delta t} \\ + (\alpha \rho_v)^n_{i+1/2} [(U_v)_{i+1/2} \left(\frac{\Delta U_v}{\Delta x} \right)_{i+1/2}]^n \\ + \alpha^n_{i+1/2} \frac{(P_{i+1} - P_i)^{n+1}}{\Delta x_{i+1/2}} \\ = - (F_{wv})^{n+1/2}_{i+1/2} - (F_{iv})^{n+1/2}_{i+1/2} - (\alpha \rho_v)^n \vec{x} \cdot \vec{g} \\ (2.41 \text{ a})$$

Liquid momentum equation

(similar to (2.41 a))

In the above equations $(\frac{\Delta U_a}{\Delta x})_{i+1/2}$ represents a difference approximation for the spatial derivatives $\partial U_a / \partial x$ evaluated at the point $i+1/2$, where $a = \ell$ or v .

Again the cell-centered quantities $\alpha, \rho_v, \rho_\ell$ are now needed at the cell faces. Donor-cell differencing can be used in case of single-phase liquid where the properties in the adjacent cells are not greatly different. Things are different, however, once the face in question separates a liquid cell and a two-phase cell. In this case the mixture density (mainly through α) may vary by as much as two orders of magnitude. In such a situation a change in the sign of the velocities at the face, for donor-cell scheme, would lead to very large changes in terms of the momentum equations, which in turn could generate large pressure spikes and even ruin the solution, by imposing an impractically short time steps. As a result, a weighted average scheme is adopted. Let C be a cell-centered quantity, then its value at the cell surface is specified as:

$$C_{i+1/2} = (C_i \Delta x_i + C_{i+1} \Delta x_{i+1}) / (\Delta x_i + \Delta x_{i+1}) \quad (2.42)$$

for the product $\alpha_a \rho_a$ for instance, we define

$$(\alpha_a \rho_a)_{i+1/2} = (\alpha_a)_{i+1/2} (\rho_a)_{i+1/2} \quad (2.43)$$

The difference approximation of the convective derivatives are defined through a donor-cell logic:

$$\left(\frac{\Delta U_v}{\Delta x}\right)_{i+1/2} = \begin{cases} \frac{(U_v)_{i+3/2} - (U_v)_{i+1/2}}{\Delta x_{i+1}}, & \text{if } (U_v)_{i+1/2} < 0 \\ \frac{(U_v)_{i+1/2} - (U_v)_{i-1/2}}{\Delta x_i}, & \text{if } (U_v)_{i+1/2} > 0 \end{cases} \quad (2.43)$$

and the mesh spacing $(\Delta x)_{i+1/2}$ needed in the pressure gradient is given by:

$$(\Delta x)_{i+1/2} = (\Delta x_i + \Delta x_{i+1})/2 \quad (2.44)$$

In the momentum equations, the wall and the interfacial exchange terms have a linear dependence on the new time phase velocities or they can be linearized in these new time velocities about the old time velocities [5]. The following forms of constitutive relations are adopted in our calculations.

$$(F_{wa})_{i+1/2}^{n+1/2} = (K_{wa})_{i+1/2}^n (U_a)_{i+1/2}^{n+1} \quad (2.45)$$

$$(F_{ia})_{i+1/2}^{n+1/2} = (K_{ia})_{i+1/2}^n (U_v - U_\ell)_{i+1/2}^{n+1} \quad (2.46)$$

The coefficients K_{wa} and K_{ia} can be complex functions of any variables, the only requirement being its evaluation using old time quantities.

With equations (2.45) and (2.46) the momentum equations (2.41 a) and (2.41 b) can be written in the form:

$$\begin{aligned} U_v^{n+1} &= a_v \Delta P^{n+1} + b_v \\ U_\ell^{n+1} &= a_\ell \Delta P^{n+1} + b_\ell \end{aligned} \quad (2.47)$$

where the coefficients a_v , a_ℓ , b_v and b_ℓ contain old time quantities only.

$\Delta P^{n+1} = (P_{i+1} - P_i)^{n+1}$ is the pressure drop between two consecutive cell centers.

The spatial subscripts have been dropped in (2.47) with the understanding that the velocities are evaluated at the faces of a node.

The quantities a_v , a_ℓ , b_v , b_ℓ are defined below [5]

$$a_v = - \frac{\Delta t}{\Delta x} [\alpha e_2 + \Delta t K_{iv} (1-\alpha)]/d \quad (2.48 a)$$

$$a_\ell = - \frac{\Delta t}{\Delta x} [(1-\alpha)e_1 + \Delta t K_{i\ell}\alpha]/d \quad (2.48 b)$$

$$b_v = (f_1 e_2 + \Delta t K_{iv} f_2)/d \quad (2.48 c)$$

$$b_\ell = (f_2 e_1 + \Delta t K_{i\ell} f_1)/d \quad (2.48 d)$$

$$e_1 = \alpha \rho_v + \Delta t (K_{wv} + K_{iv}) \quad (2.49 a)$$

$$e_2 = (1-\alpha)\rho_\ell + \Delta t(K_{w\ell} + K_{i\ell}) \quad (2.49 \text{ b})$$

$$f_1 = \alpha\rho_v[U_v - \Delta t(\text{conv}_v + \vec{x} \cdot \vec{g})] \quad (2.49 \text{ c})$$

$$f_2 = (1-\alpha)\rho_\ell[U - \Delta t(\text{conv}_\ell + \vec{x} \cdot \vec{g})] \quad (2.49 \text{ d})$$

$$d = e_1 e_2 - (\Delta t)^2 K_{iv} K_{i\ell} \quad (2.49 \text{ e})$$

In equations (2.48) and (2.49), everything is evaluated at the old time. Consequently the coefficients a's and b's can be calculated only once at the beginning of the current time step and stored.

II.4.3. The solution scheme

The finite difference equations described in the preceding section combined with the equations of state (equations 2.3) form a large system of non-linear equations. The following seven new time variables appear as unknowns for all cells in the domain of the problem:

$$\rho_m^{n+1}, p^{n+1}, e_m^{n+1}, T_\ell^{n+1}, T_v^{n+1}, U_v^{n+1} \text{ and } U_\ell^{n+1}$$

The new time temperatures appear from the fully-implicit treatment of the heat sources and sinks that is adopted for this formulation. The high heat transfer coefficient and the low heat capacity of the plenum material that are required to keep the plenum temperature constant during transients may give rise to instabilities for a fully explicit or a semi-implicit treatment, hence the decision to use a fully-implicit treatment for tests of our method on a loop version of THERMIT.

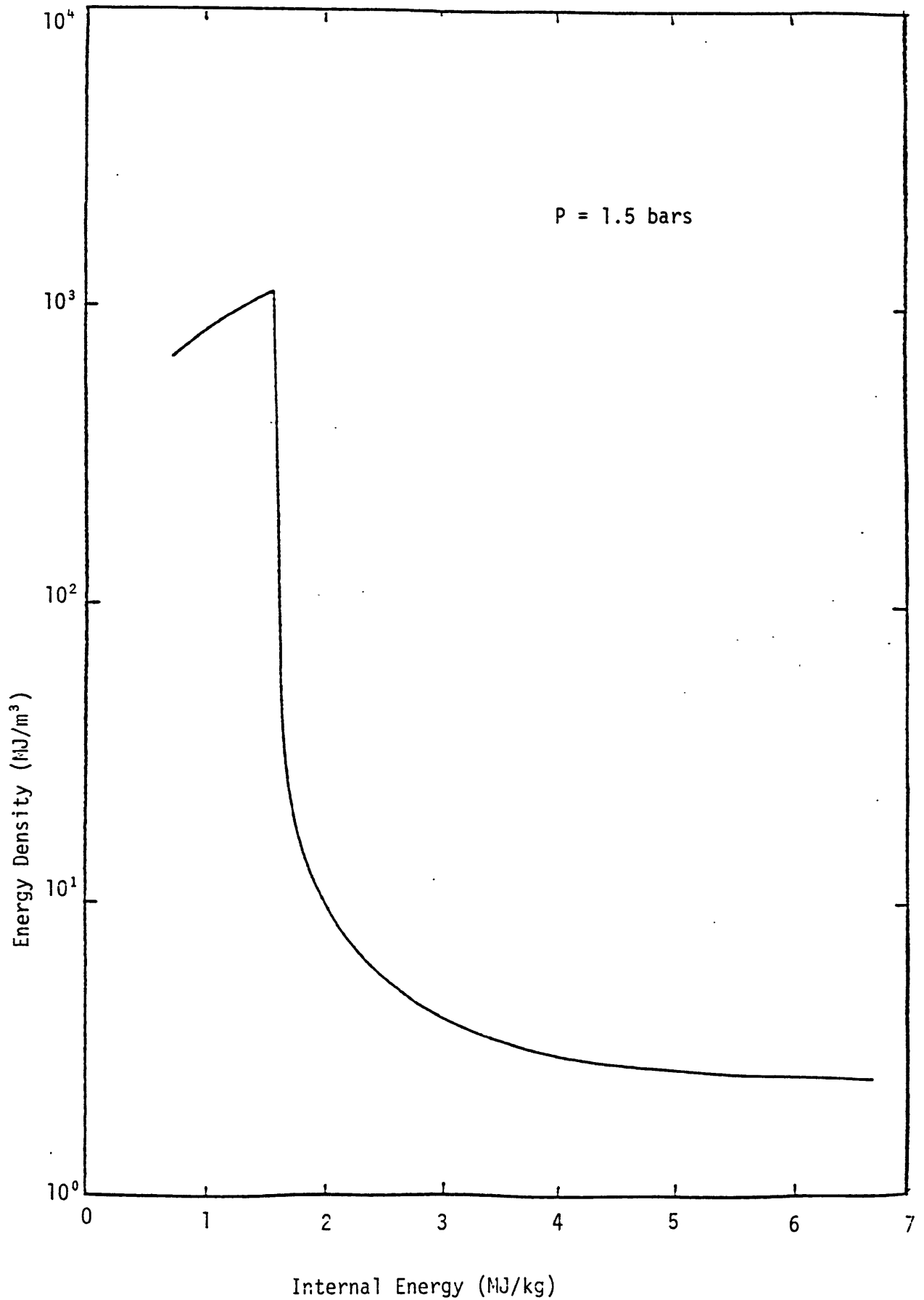


Figure 2.5. Sodium Internal Energy Per Unit Volume versus Internal Energy

Note also that ρ_m^{n+1} and e_m^{n+1} now appear as separate unknowns due to the non-conservative form of the energy equation adopted (equation 2.40). This splitting of the product $(\rho_m e_m)^{n+1}$, which otherwise would appear as an unknown from the conservative form (equation 2.39), is highly desirable. The product $\rho_m e_m$ is a non-monotonic function of e_m for sodium and also for water at low pressure (fig. 2.5). This behavior have the tendency of ruining the Newton-Raphson method adopted to solve our non-linear system. Generally, the Newton-Raphson method is destroyed when an extremum point exists between the guess and the solution.

II.4.4. The Jacobian matrix and the pressure problem

The new time velocities that appear in the mass and the energy equations are eliminated in favor of the new time pressures using the momentum equations in the form of (2.47). Thus for each cell we now have two scalar conservation equations namely the mass and the energy equations. The appropriate equations of state are combined with these scalar conservation equations for closure. In our one-dimensional formulation, the elimination of the new time velocities leads to the appearance of the new time local and two neighboring pressures in the mass and the energy equations for each node.

Note that our numerical scheme uses the internal energy as primary variable, therefore the temperature must be inferred. It is determined through an iterative procedure applied to equations (2.3c,d).

The resulting mass and energy together with the state equations can be written in functional form for node 'i' as follows [7]:

$$R_{mi}(\rho_{mi}, P_{i-1}, P_i, P_{i+1}) = 0 \quad (2.50 \text{ a})$$

$$R_{ei}(\rho_{mi}, e_{mi}, P_{i-1}, P_i, P_{i+1}) = 0 \quad (2.50 \text{ b})$$

$$\rho_{mi} - \rho_{mi}(P_i, e_{mi}) = 0 \quad (2.50 \text{ c})$$

where

R_{mi} refers to the mass equation for node 'i'

R_{ei} refers to the mass equation for node 'i'

and all the quantities inside the parentheses are now evaluated at the new time level.

Equations (2.50) are generally highly non-linear, the source of non-linearity being mainly the state equation.

The pressure P and the mixture internal energy e_m are taken as the main variables and the mixture density ρ_m is eliminated through the equation of state. Consequently we obtain two non-linear scalar equations in P 's and e_m for each node. These equations can be written symbolically as:

$$\bar{R}(\bar{U}) = 0 \quad (2.51)$$

where

$$\bar{R} = [R_{m1}, R_{e1}, \dots, R_{mN}, R_{eN}]^T$$

$$\bar{U} = [P_1, e_{m1}, \dots, P_N, e_{mN}]^T$$

Applying Newton's method to solve (2.51) we have

$$\bar{J}(\bar{U})\delta\bar{U} = -\bar{R}(\bar{U}) \quad , \quad (2.52)$$

where the jacobian $\bar{J}(\bar{U})$ is given by

$$\bar{J}(\bar{U}) = \frac{\partial \bar{R}}{\partial \bar{U}} \quad .$$

Let K be the counter for the Newton iteration. Then the scheme becomes:

$$\bar{J}(\bar{U}) (\bar{U}^{K+1} - \bar{U}^K) = -\bar{R}(\bar{U}^K). \quad (2.53)$$

The entries of the jacobian matrix for a particular node 'i' are obtained from the following partial derivatives

$$\begin{array}{cccc} \frac{\partial R_{mi}}{\partial P_{i-1}} & \frac{\partial R_{mi}}{\partial P_i} & \frac{\partial R_{mi}}{\partial e_{mi}} & \frac{\partial R_{mi}}{\partial P_{i+1}} \\ \frac{\partial R_{ei}}{\partial P_{i-1}} & \frac{\partial R_{ei}}{\partial P_i} & \frac{\partial R_{ei}}{\partial e_m} & \frac{\partial R_{ei}}{\partial P_{i+1}} \end{array}$$

We denote these generally non-zero entries by "x" and thus obtain a matrix form for equation (2.52), for cell i:

$$\begin{array}{c} \left[\begin{array}{ccc|ccc} x & 0 & & x & x & & x & 0 \\ & & & & & & & \\ x & 0 & & x & x & & x & 0 \end{array} \right] \begin{array}{c} \delta P_{i-1} \\ \delta e_{mi-1} \\ \delta P_i \\ \delta e_{mi} \\ \delta P_{i+1} \\ \delta e_{mi+1} \end{array} \stackrel{K+1}{=} - \begin{array}{c} \left[\begin{array}{c} R_{mi} \\ R_{ei} \end{array} \right]^K \end{array}$$

(2.54)

Equation (2.54) forms a total of $2N$ equations, where N is the total number of nodes. The full 2×2 block in (2.54) provides local (within cell) coupling while the sparse 2×2 blocks provides spatial coupling, indicating a field coupling through pressure only.

The next step in the solution is to solve the main diagonal block to eliminate δe_{mi} in favor of the neighboring pressures. This procedure effectively reduces the problem to a pure pressure problem in N equations. The pressure problem in matrix form becomes:

$$\begin{vmatrix} x & & \\ & x & \\ & & x \end{vmatrix} \begin{vmatrix} \delta P_{i-1} \\ \delta P_i \\ \delta P_{i+1} \end{vmatrix}^{K+1} = R_i^K \quad (2.55)$$

Equation (2.55) when written for the N -cell domain gives rise to an $N \times N$ tridiagonal jacobian matrix in the left hand side while right hand side becomes an $N \times 1$ vector.

The pressure increments are solved in (2.55) by a direct technique (i.e., LU decomposition). The increment δe_{mi}^{k+1} is then obtained from the second equation of (2.54) in each cell. This completes a Newton iteration. The process is then repeated until successive changes in the main variables become very small.

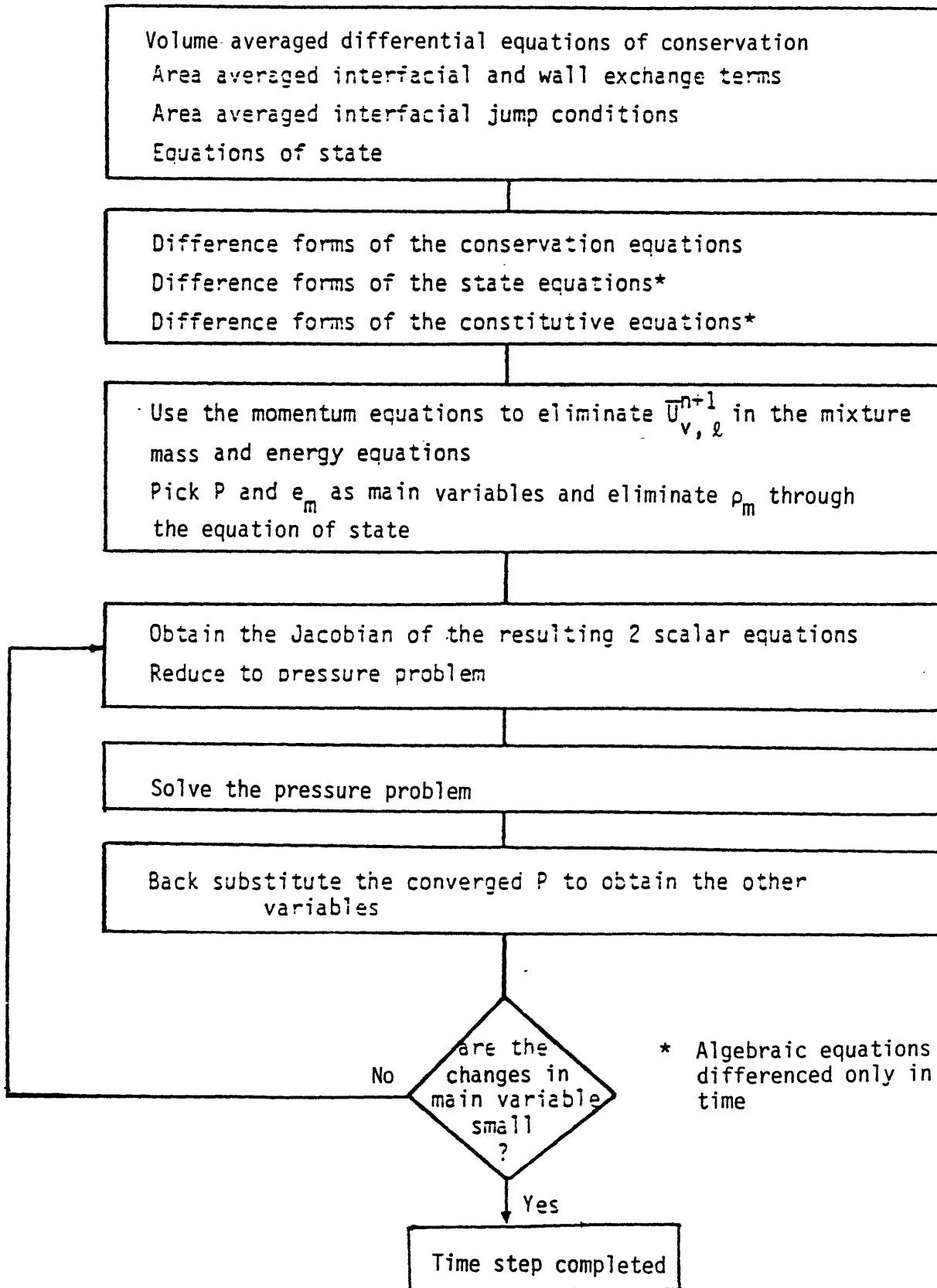


Figure 2.6. Summary of the Solution Technique in THERMIT-4E.

III. Description of the problem

III.1. Introduction

Experiments suggest that the condensation process is basically the reciprocal of boiling: both can be represented as a mere change in phase. However because of the difference in density of vapor and liquid, small pressure pulses cannot be absorbed as easily for liquid as it is for vapor. Indeed this aspect of condensation will prove to be determinant for the final understanding and the resolution of this phenomenon.

The intuitive physical model considered in order to encounter a condensation problem has been a channel with a test section in which heat would be removed through the structure walls maintained at very low temperature. An incoming two-phase mixture flow would then condense in this test section. Other conditions involving less computation were investigated: those conditions were designed so that they would re-create the same situation leading to high pressure spikes as they were witnessed indeed in the loop simulation of THERMIT.

In this latter case condensation is taking place in the neighboring cells of the upper and lower plenum [4].

The following studies shall essentially focus on one dimensional channels, and also using simple legitimate simplifications such as:

- no transverse flow
- no heat input
- adiabatic flow
- pressure-pressure boundary conditions

This last choice of boundary conditions will enable us to avoid imposing the flow in and/or out of the channel and to observe a natural behavior of the flow, especially flow reversal during change of phase as the case may be.

III.2. Typical cases of condensation

III.2.1. Description of the numerical experiments

The first series of benchmarks that have been investigated features a flow of two-phase mixture injected into stagnant subcooled liquid. The same flow pattern is indeed observed in the heated section of the upcomer of the reactor loop simulation: a two-phase mixture reverses and flows back into the lower plenum which contains subcooled liquid at approximately 840° K. Pressure-pressure boundary conditions is imposed, the expected result being a pressure gradient throughout the channel.

Results showed the interface-cell pressure increasing rapidly and exceeding the upper limit of the pressure range prescribed by the equation of states (20.0 bars): simultaneously the incoming flow starts to reverse direction and to push the liquid away, but not sufficiently to alter substantially the

pressure increase.

The second series of benchmarks represents water-hammer-like problems: a flow of subcooled liquid is injected into stagnant two-phase mixture at higher temperature. Other conditions of the tests remained similar to previous calculations. Condensation occurs also at the interface-cell and leads to pressure going out of range.

III.2.2. Analysis of the results

It is important to note that all calculations were run keeping a tight allowable conservation error (on the order of 0.5%) since larger mass error would artificially and non-physically "solve" the problem; when the code reached this limit it automatically reduced the time-step and reiterated the calculations.

Also, for simplicity reason, no slip was assumed; actually this condition is a much more severe situation than if slip existed since the flow has more difficulties in reversing for liquid than for a two-phase mixture or vapor: the obvious advantages of using the HEM is to eliminate a variable and an equation making hand-calculations possible.

A final reduction in computing will consist of considering a one-cell volume filled with stagnant two-phase mixture in which very subcooled liquid is injected at a given pressure.

The results of these numerical tests exhibited most interesting anomalies leading to some instabilities

of the flow yet to be defined. The pressure and the void fraction in the cell start dropping due to condensation effects, while mass flows and velocities at both cell interfaces are directed inward with increasing absolute value in order to compensate this trend. When condensation is completed, pressure rises abruptly because of the inward flows; at this point of the experiments the channel contains only subcooled liquid.

The code will recover from the above described behavior for an initial void fraction in the cell lower than a critical void fraction. However for larger initial void fractions pressure as well as velocities at the interfaces oscillate with growing amplitudes preventing the flow from reaching steady-state. The calculations eventually stop because of the pressure going out of range of state functions.

Besides the dependency on the initial void fraction in the cell, different tests demonstrated also that the final state of the flow is greatly affected by effective quantity of subcooled liquid injected on the the two-phase mixture and not by the number of cells of subcooled liquid.

During the process of condensation, when the mesh-volume still contains a two-phase mixture, the sonic velocity in the cell becomes small compared with the sonic velocity in liquid or vapor (approximately 320 m/sec at 1 bar). In cases of larger initial void fraction than the critical void fraction mentioned above, the flow becomes supersonic until the

condensation ends: the flow returns to a subsonic regime as the sonic velocity becomes large. SHAPIRO [6], referring to steady state flows, predicted that the transition from subsonic to supersonic flow is stable whereas the transition from supersonic to subsonic is unstable. However, thus far, the case of the latter situation during transients has been unexplored; in fact, one of the consequences of our tentative findings is the possibility of a stable supersonic-subsonic transition for short transients such as condensation.

A decisive feature of these tests as far as the final solution of the problem is concerned is deeply related to the time step control of the code. At the first stage of the runs, vapor in a cell condenses and causes the time steps to be appreciably reduced because of the large mass error involved. The final stage of the runs corresponds to a fully condensed state.

During this period, the time steps remain relatively small compared with the time step limit due to the convective term, even though the system is basically quasi-linear; indeed linearization errors in pressure, mass and energy are very small. We have noted the importance of the inertia effect of the system for liquid sodium: pressure undershoots or overshoots the estimated pressure at steady state because the velocities at the cell edges are still respectively directed outward or inward. In many cases, the velocities fail to reverse this trend soon enough before pressure reaches the upper or lower limits defined by the state functions -0.0 and 20.0 bars-. This inertia effect

has been determined as being responsible for the code's breakdown. The observation of this phenomenon lead us to restart the problem from the point of terminated condensation using a time-step size of the order of the convective limit; the problem is in fact equivalent to a liquid-filled channel with an initial pressure perturbation. Surprisingly, steady-state was reached within few time-steps. Clearly, a definite influence of the time-step size on the code's behavior toward condensation was actually perceived: these effects are extensively discussed and thoroughly examined in chapters IV and V.

III.3. Review of previous studies

As stated before, studies have been done on this subject by various workers and it is worthwhile reviewing some of them here since they have been most useful at the very beginning of this research by giving some ideas of what was wrong.

-a) A major effort has been going on at Los Alamos Scientific Laboratory [1] where the research has been based on the TRAC computer code.

Like THERMIT, in differencing the governing equations, a staggered grid is used in which velocities are evaluated on mesh cell edges and the remaining are cell centered. They proposed a procedure that consists of a correction to the pressure gradient term in the momentum equation.

The correction needs to be made only if a packing situation is expected. Generally, the equation for the change in velocity will be written as

$$\delta V_{i+1/2} = F_1[\delta P_{i+1} - \delta P_i] + F_2 ,$$

where δP_i is the change in pressure in cell i , $\delta V_{i+1/2}$ is the change in velocity at cell edge $i + \frac{1}{2}$, and F_1 and F_2 contain the remaining terms of the momentum equation.

If a packing situation is expected, say within the i -th cell, this equations is then rewritten as

$$\delta V_{i+1/2} = F_1[\delta P_{i+1} - S\delta P_i] + F_2 ,$$

where S is the scaling factor chosen to minimize the pressure spike. Generally, a constant factor of 1000 was found sufficient and it need only be applied for a single time step in most cases. The scaling factor is only applied to the cell being packed. Caution must be exercised not to apply the scaling factor to two adjacent cells simultaneously since this may preclude a real water-hammer effect.

Even though the method appears to solve the problem, it affects results in ways that are not readily apparent.

- b) Water packing anomalies in thermal-hydraulics codes have been investigated at Lawrence Livermore Laboratory by Lyczkowski [2].

The source of these pressure spikes has been conjectured to be caused by nonuniform enthalpy distribution or wave reflec-

tion off the closed end of a pipe or abrupt changes in pressure history when the fluid changes from subcooled to two-phase conditions. It was demonstrated that many of the faults can be attributed to inadequate modeling of the average volume flow and the sharp fluid density front crossing a junction.

General corrective models are difficult to devise since the causes of the problems touch on the very theoretical bases of the differential field equations and associated solution scheme. This is why simple corrective models, economical to implement and use, were developed.

When incorporated into the one-dimensional homogeneous transient thermal-hydraulic analysis computer code, RELAP-4, they help mitigate many of the code's difficulties related to average volume flow and water-packing anomalies.

- c) Another approach on the problem comes from Padilla and Rowe [3]. They have developed a donor flow formulation for momentum flux differencing, that have been incorporated into the CAPRICORN subchannel code. Originally CAPRICORN has, as THERMIT a staggered grid formulation where the momentum cells are shifted by one-half a computational cell from the continuity-energy cells. However their implementation was prompted by anomalies which do not occur in THERMIT and therefore it seemed reasonable to dismiss this new approach for our final solution.

III.4. Preliminary investigations

- a) The relatively large linearization errors due to mass conservation during the condensation process suggested to write the continuity equation in difference form using the momentum cell which is translated a half-cell away from the usual mass cell (see Appendix A).

However, qualitative considerations showed that the large mass errors involved are solely due to high non-linearity of the system when two-phase are present and no evidence of improvement emerged from this calculations as far as the stability of the flow is concerned.

- b) Earlier on, we have mentioned the abnormal variation of pressure still decreasing while flow is coming in or increasing pressure while flow is going out of the mesh-volume. It seemed oportune to find an expression of the variation of pressure in terms of density, energy and their respective derivatives using basic thermodynamic derivations (see Appendix B) .

These derivations have been most helpful in understanding of the pressure's dependancy on other variables and its effect on the stability of the system.

- c) The low pressures attained during condensation of the two-phase mixture, and the corresponding large velocities that were witnessed in our tests indicated that a transonic flow situation may have occured.

Therefore sonic velocities and Mach number have been derived (see Appendix C) and inserted in the code's calculations. Indeed, in many cases supersonic flow situation did exist and its consequences are discussed in the following chapter.

IV. A Mathematical Solution of Condensation for THERMIT-4E

IV.1. Introduction

In the previous chapter, we have emphasized on the importance of the time step strategy that has been noticed in our numerical experiments run on THERMIT-4E especially when complete condensation is achieved. The system examined here is an adiabatic channel filled with very subcooled liquid and an initial pressure perturbation imposed somewhere in that channel; inlet and outlet pressures are imposed and finally we assume that the temperature and the energy remain constant throughout the tests which is a very reasonable assumptions in our case.

Consequently, the state function [5] of liquid density becomes a linear function of pressure (T constant):

$$\rho_l = a + b.P \quad (4.1)$$

where

$$a = A_5 + A_6 + A_7 T^2 - P_{\text{ref}}/c_l^2$$

$$b = 1/c_l^2$$

$$A_5 = 1.0042 \times 10^3$$

$$c_l^2 = 2.0 \times 10^{-7}$$

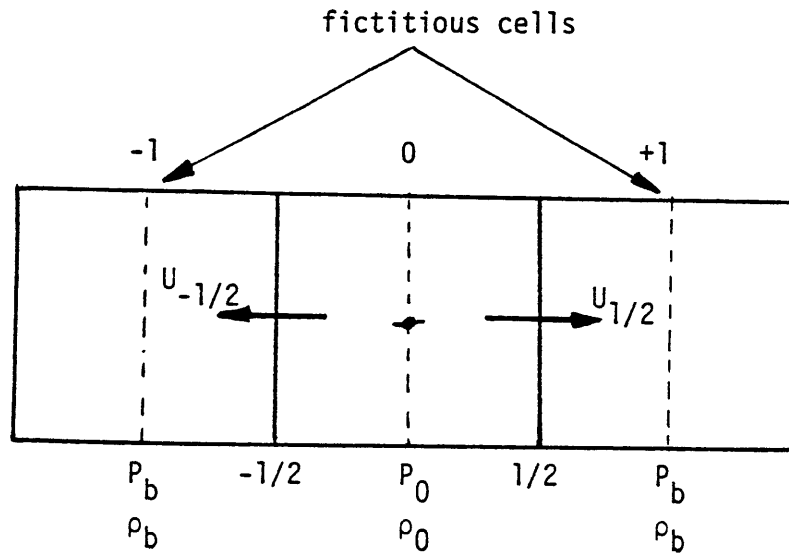
$$A_6 = -2.1390 \times 10^{-1}$$

$$P_{\text{ref}} = 1.5 \times 10^5$$

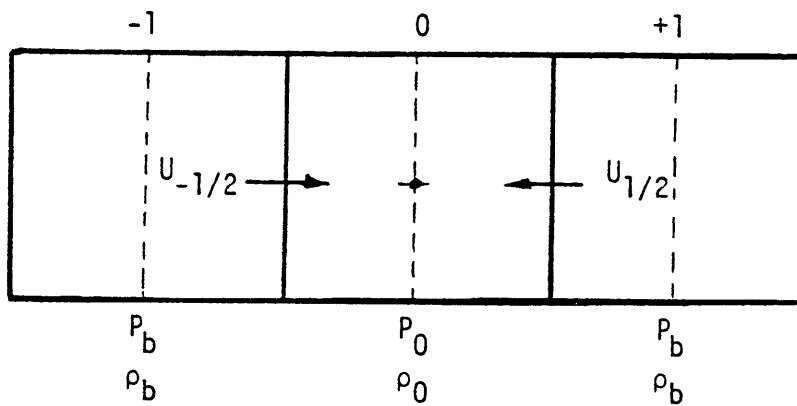
$$A_7 = -1.1046 \times 10^{-5}$$

T is in °K and P in Pa . Range of validity: 550 < T < 2270 °K

In the next subsection, we shall study a simple one-dimensional problem of a channel defined by a single cell for which a pressure perturbation is applied given



-a) outward flow



-b) inward flow

Figure 4.1. Representation of a single-cell problem.

the assumptions stated before while the following subsection applies the results for a multi-cell case.

IV.2. A single-cell problem

As stated before inlet and outlet pressures are imposed as boundary conditions. The initial pressure pulse condition is applied on the cell itself.

Because of the symmetry of the problem (fig. 4.1) the velocities at both cell edges are always equal in absolute value and opposite in direction

$$U_{\frac{1}{2}} = -U_{-\frac{1}{2}} \quad (4.2)$$

Therefore we are left with 2 unknowns only: the pressure in the cell and the velocity at the cell face (P_o and $U_{\frac{1}{2}}$).

Writing the mass equation using (2.38), (4.1) and (4.2), we obtain:

$$b (P_o^{n+1} - P_o^n) \frac{\Delta x}{\Delta t} + 2\rho_{\frac{1}{2}} U_{\frac{1}{2}}^{n+1} = 0 \quad (4.3)$$

where:

$$\rho_{1/2} = \begin{cases} \rho_o^n & \text{if } U_{1/2}^n \geq 0 \\ \rho_b & \text{if } U_{1/2}^n < 0 \end{cases}$$

$$\rho_b = a + b \cdot P_b$$

$$P_b = \text{constant pressure at boundaries}$$

$$U = U_{1/2}$$

$$\rho_{1/2} = \rho_{1/2}^n \quad (4.4)$$

We now write the momentum equation using expression (2.41a) and the same conventions mentioned above. For the purpose of the generality we are writing a mixed friction term:

$$F_w^{n+1/2} = (1-\theta)K^n U^{n+1} + \theta K^n U^n \quad (4.5)$$

where $-1 \leq \theta \leq +1$. For $\theta = +1$, the treatment of wall friction becomes fully explicit; while $\theta = 0$ corresponds to a semi-implicit one. K^n can be deduced from equation (2.12a) and we simplify the notation by writing K with the understanding that it is an old time parameter. The momentum equation can be written as:

$$U^{n+1} [\bar{\rho} + (1-\theta)K\Delta t] = (P_o^{n+1} - P_b)\Delta t/\Delta x + \bar{\rho}U^n(1 - \Delta t.\text{conv} - \theta K\Delta t/\bar{\rho}) \quad (4.6)$$

where

$$\text{conv} = \begin{cases} 2U^n/\Delta x & \text{if } U^n = U_{1/2}^n \geq 0 \\ 0 & \text{if } U^n < 0 \end{cases} \quad (4.7a)$$

$$\bar{\rho} = 1/2(\rho_o^n + \rho_b) \text{ from (2.47)} \quad (4.7b)$$

Re-arranging equation (4.6) so that we have an expression of the new time velocity in terms of the new time pressure yields:

$$U^{n+1} = \frac{P_o^{n+1} - P_b}{(\bar{\rho} + (1-\theta)K\Delta t)} (\Delta t/\Delta x) + \frac{\bar{\rho}U^n(1-\text{conv}.\Delta t-\theta K\Delta t/\bar{\rho})}{(\bar{\rho} + (1-\theta)K\Delta t)} \quad (4.8)$$

Inserting equation (4.8) into (4.3) yields an expression of P_o^{n+1} as a function of old time quantities that are already known.

However, being rather interested in having the pressure variation over the time step, we subtract by P_o^n so that we obtain the following relation:

$$P_o^{n+1} - P_o^n = \frac{A X^2 + B X}{A' X^2 + B' X + C'} \quad (4.9)$$

where

$$\begin{aligned} X &= \Delta t \\ A &= 2\rho_{1/2}[P_b - P_o^n + U^n \Delta x (\bar{\rho}_{conv} + \theta K)] \\ B &= -2\rho_{1/2} \bar{\rho} U^n \Delta x \\ A' &= 2\rho_{1/2} \\ B' &= (1-\theta) K b (\Delta x)^2 \\ C' &= b \bar{\rho} (\Delta x)^2 \end{aligned} \quad (4.10)$$

A' , B' , C' are always positive and therefore there is no real positive time step size for which the pressure variation ($P_o^{n+1} - P_o^n$) will be infinite.

We now concentrate on the critical situations that lead to the code's breakdown after completed condensation:

1) pressure decreasing and undershooting the steady state pressure which is here equal to P_b ($P_o^n < P_b$). We are also placing ourself in the most critical condition where P_o is very close to 0.0 bar and the velocity is still positive accentuating the trend (fluid extracted from the cell, $U_{1/2} > 0$). We then look for the Δt 's for which a flow reversal

is possible before P_o goes to nonphysical values.

2) The second critical condition is the opposite of the first one: it corresponds to the pressure increasing and overshooting the steady state pressure situation ($P_o^n > P_b$, and $P_o \approx 20.0$ bars), while the velocity is still negative (fluid injected into the cell, $U_{\frac{1}{2}}^n < 0$).

Examining the first case described above, we can easily note that B is negative and A is positive when U is positive and P_o is smaller than P_b (especially when $P_o \approx 0.0$ bar).

If Δt_o is the non-zero root that cancels the numerator of (4.9), Δt_o is equal to:

$$\Delta t_o = -B/A = \frac{\bar{\rho} U^n \cdot \Delta x}{[P_b - P_o^n + U^n \Delta x (\bar{\rho} \cdot \text{conv} + \theta K)]} \quad (4.11)$$

Let Δt_c be the convective time step limit

$$\Delta t_c = \frac{\Delta x}{|U^n|} \quad (4.12)$$

We check that Δt_c is always larger than Δt_o :

$$\Delta t_o < \Delta t_c \quad (4.13)$$

Proof:

$$\begin{aligned} & \frac{\bar{\rho} U^n \cdot \Delta x}{[P_b - P_o^n + U^n \Delta x (\bar{\rho} \cdot \text{conv} + \theta K)]} < \frac{\Delta x}{|U^n|} \\ \rightarrow & \frac{\bar{\rho} U^n \cdot |U^n| - P_b + P_o^n - U^n \Delta x (\bar{\rho} \cdot \text{conv} + \theta K)}{|U^n| \cdot [P_b - P_o^n + U^n \Delta x (\bar{\rho} \cdot \text{conv} + \theta K)]} < 0 \end{aligned} \quad (4.14)$$

after dividing by Δx from each side of the inequality.

Since $U^n > 0$, $\text{conv} = \frac{2U^n}{\Delta x}$ from equation (4.11). Therefore in the numerator of equation (4.14), the following expression

$$[\bar{\rho}U^n \cdot |U^n| - U^n \cdot \Delta x \cdot (\bar{\rho} \cdot \text{conv} + \mathcal{K})]$$

is necessarily negative. P_o being smaller than P_b the numerator of (4.14) is also negative. The denominator is positive, therefore (4.13) is true. We can easily check that $\Delta t_o > 0$ when $U^n > 0$ and $P_o^n < P_b$ from equation (4.11).

The study of equation (4.9) where ΔP_o is a function of Δt and using equation (4.3) yields the following results:

$$\begin{aligned} \text{for } \Delta t = \Delta t_o ; P_o^{n+1} &= P_o^n \text{ and } U^{n+1} = 0 \\ \text{for } \Delta t_o < \Delta t < \Delta t_c ; P_o^{n+1} &> P_o^n \text{ and } U^{n+1} < 0 \\ \text{for } 0 \leq \Delta t < \Delta t_o ; P_o^{n+1} &\leq P_o^n \text{ and } U^{n+1} > 0 \end{aligned} \quad (4.15)$$

Important conclusions can be drawn from these expressions. We see that too small time steps keep the pressure decreasing and prevent any flow reversal, whereas time steps larger than Δt_o allow a flow reversal and the pressure to increase. This demonstrates that the semi-implicit scheme has a lower time step limit, and we will show in the next chapter the reasons for the existence of such unexpected limit.

Two additional remarks are to be made at this point.

- a) Considering the same experiment for vapor, the equations remain unchanged the only difference being in the value of the density: the changing terms are $\bar{\rho}$ and $\rho_{\frac{1}{2}}$.

Specifically, the expression of Δt_o (4.11) is unchanged: $\bar{\rho}$ is smaller while other variables are the same. $\bar{\rho}$ appears in the numerator and the denominator of (4.11). A study of this function, $\bar{\rho}$ being then the only variable, indicates a decrease of

the whole expression when $\bar{\rho}$ decreases. Practically, Δt_0 , which is our previously defined lower limit of "pseudo-stability" of the system, is much smaller for vapor and therefore seldom noticeable compared to the situation for liquid.

- b) When $p_0^n < p_b$, $p_0^n \cong 0.0$ bar and $U^n < 0$ so that the flow has already reversed, we can see that Δt_0 is negative meaning that $p_0^{n+1} - p_0^n$ is always positive whatever the time step size. We have checked that the pressure has to increase when flow is injected in the cell which is a normal behavior. We now turn to the aforementioned second critical condition which turns out to be very similar to the former one:

$$p_0^n > p_b, \quad p_0^n \cong 20.0 \text{ bars}, \quad U^n < 0 \quad \text{and} \quad \text{conv} = 0.$$

Inequality (4.14) remains the same; however here, we note that the denominator is negative. In order to have $\Delta t_0 < \Delta t_c$, the numerator has to be positive; the velocity must verify the following inequality:

$$(U^n)^2 \leq (p_0^n - p_b) / \bar{\rho}$$

Considering a typical case where $p_b = 1.0$ b, $\bar{\rho} = 800 \text{ kg/m}^3$, U^n must be less than 50 m/sec; if $p_b = 16.0$ b, U^n must be less than 22 m/sec. For our numerical experiments of condensation, these situations were never encountered and therefore for our analysis inequality (4.14) is always true.

Also $\Delta t_0 > 0$ when $U^n < 0$ and $p_0^n > p_b$ from (4.11). Similarly to (4.15)

we have:

$$\begin{aligned} \text{for } \Delta t = \Delta t_0 & ; p_0^{n+1} = p_0^n \quad \text{and} \quad U^{n+1} = 0 \\ \text{for } \Delta t_0 < \Delta t < \Delta t_c & ; p_0^{n+1} < p_0^n \quad \text{and} \quad U^{n+1} > 0 \\ \text{for } 0 < \Delta t < \Delta t_0 & ; p_0^{n+1} > p_0^n \quad \text{and} \quad U^{n+1} < 0 \end{aligned} \quad (4.16)$$

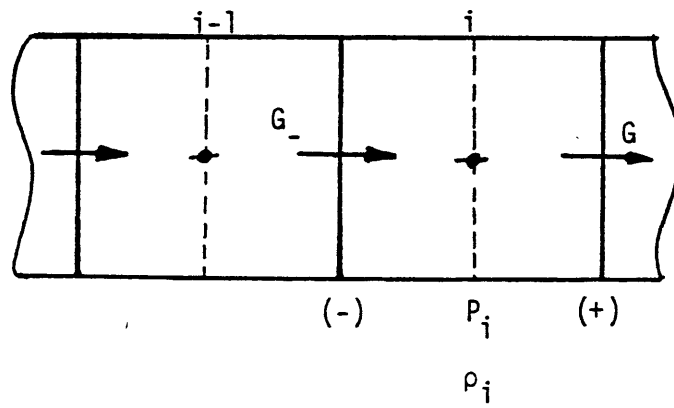


Figure 4.2. Staggered mesh for the momentum equations.

Again, in this case, flow reversal occurs if the time step size is larger than Δt_0 , which sets the same lower limit for the code's ability to simulate a pressure perturbation and condensation.

If $P_0^n \approx 20.0$ bars and $U^n > 0$ then $\Delta t_0 < 0$; meaning here again that pressure can only decrease whatever the time step size.

We have finally demonstrated in this subsection the existence of a lower limit to the time step beyond which the numerical scheme in THERMIT-4E cannot reverse the flow of subcooled liquid following either an undershooting or an overshooting of the expected pressure level. This is a rather surprising finding and it is a result of the intrinsic non-linear dependency of the pressure on the time step. We shall now try to generalize this result to multi-cell channels.

IV.3. Application to multi-cell pipes

For our one-dimensional, barotropic and multi-cell analysis, let $G = \rho U$ and $co = \partial(\rho U U) / \partial x$. Then the finite difference analogs of the mass and momentum equations are (THERMIT's semi-implicit numerical method):

$$\frac{1}{\Delta t} (\rho_i^{n+1} - \rho_i^n) + \frac{1}{\Delta x} (G_+^{n+1} - G_-^{n+1}) = 0 \quad (4.17)$$

$$\frac{1}{\Delta t} \begin{matrix} (G_+^{n+1} \\ (-) \end{matrix} - \begin{matrix} G_+^n \\ (-) \end{matrix}) + \begin{matrix} co_+^n \\ (-) \end{matrix} + \frac{1}{\Delta x} \begin{matrix} (P_{i+1}^{n+1} \\ (i) \end{matrix} - \begin{matrix} P_i^{n+1} \\ (i-1) \end{matrix}) = \begin{matrix} F_+^n \\ (-) \end{matrix} \quad (4.18)$$

where the (-) and (+) refers to the two cell boundaries of our familiar staggered mesh arrangement (fig 4.2) and F

represents the friction term. Substituting the two momentum equations (for the (-) and (+) cell edges) into the mass equation for cell (i) results in

$$\begin{aligned} \frac{1}{\Delta t^2} (P_i^{n+1} - P_i^n) + \frac{1}{\Delta t \Delta x} (G_+^n - G_-^n) - \frac{1}{\Delta x^2} (P_{i+1}^{n+1} - 2P_i^{n+1} + P_{i-1}^{n+1}) \\ = \frac{1}{\Delta x} (co_+^n - co_-^n) - \frac{1}{\Delta x} (F_+^n - F_-^n) \end{aligned} \quad (4.19)$$

We now eliminate the density in favor of the pressure, using the equation of state (4.1) in the form:

$$\rho_i^{n+1} - \rho_i^n = \frac{1}{c_\lambda^2} (P_i^{n+1} - P_i^n) \quad (4.20)$$

Substitute equation (4.20) into (4.19):

$$\begin{aligned} (\Delta t / \Delta x)^2 \{ P_i^{n+1} [2 + (\Delta x / c_\lambda \Delta t)^2] - P_{i-1}^{n+1} - P_{i+1}^{n+1} \} = (1 / c_\lambda^2) P_i^n \\ - (\Delta t / \Delta x) (G_+^n - G_-^n) + (\Delta t^2 / \Delta x) [(co_+^n - co_-^n) - (F_+^n - F_-^n)] \end{aligned} \quad (4.21)$$

The right-hand-side of the above equation contains only old-time quantities; we have indeed an equation for the new pressure. We now cast equation (4.21) in the way that gives the variation of pressure in a cell over the time step as it was done in equation (4.9):

$$P_i^{n+1} - P_i^n = \frac{\Delta t^2 [P_{i-1}^{n+1} + P_{i+1}^{n+1} - 2P_i^n + (\Delta co^n - \Delta F^n) \cdot \Delta x] + \Delta x \Delta t \Delta G^n}{2\Delta t^2 + (\Delta x / c_\lambda)^2} \quad (4.23)$$

where:

$$\Delta\phi = \phi_+^n - \phi_-^n$$

and $\phi = \text{co, F or G}$

We can deduce from equation (4.22) the critical time step that

was defined in equation (4.11) and for which $P_i^{n+1} - P_i^n = 0$:

$$\Delta t_{0,i} = (\Delta x \Delta G^n) / [P_{i+1}^{n+1} + P_{i-1}^{n+1} - 2P_i^n + \Delta \text{co}^n - \Delta F^n] \quad (4.23)$$

We see that $\Delta t_{0,i}$ is expressed in terms of the new time pressure of the neighboring cells. If N is the number of cells composing the pipe, in order to find $\Delta t_{0,i}$ for which $P_i^{n+1} = P_i^n$, we have to solve a linear system of N equations and N unknowns - the δP_i 's - with a parameter - $\Delta t_{0,i}$ - that appears in both the right-hand-side and in the Jacobian matrix of equation (2.55).

More specifically, we have to find the right parameter corresponding to the solution which would include $\delta P_I = 0$, if I is the cell number where the critical time step ($\Delta t_{0,i}$) calculation is needed.

Numerically, we decouple the system into two linear sub-systems of equations.

The first sub-system has (I-1) equations and (I-1) unknowns: $\delta P_1, \delta P_2, \dots, \delta P_{I-1}$. The second sub-system has (N-I) equations and (N-I) unknowns: $\delta P_{I+1}, \delta P_{I+2}, \dots, \delta P_N$.

Therefore, we can obtain the δP_i 's ($i = 1, N$ and $i \neq I$)

in terms of $\Delta t_{o,i}$. Considering now the I^{th} equation which contains δP_{I-1} , δP_I and δP_{I+1} , knowing $\delta P_{I-1}(\Delta t_{o,I})$, $\delta P_{I+1}(\Delta t_{o,I})$ previously calculated and $\delta P_I = 0$, we then solve this equation for $\Delta t_{o,i}$.

This procedure has to be repeated for every cell encountering a condensation problem; we will then consider only the maximum of all the $\Delta t_{o,i}$'s computed at every time step.

However, this operation has proved to be very costly in computing time; it seemed more reasonable to call for the convective time step limit whenever a critical time step is needed since; it has been demonstrated in (IV.2) that the former is always larger and in these circumstances flow reverses avoiding the breakdown of the calculation.

In order to implement the method we have described before, a subroutine presented in Appendix E performs a series of tests on the void fraction at each cell: the subroutine is activated by a flag which is turned on whenever the void fraction of any cell decreases especially when the void fraction goes from some value to zero. The flag is also turned on when all the cells are filled with liquid. Once it is turned on, the code will use the minimum of the convective time step limit calculated for the whole channel and the $(\Delta t)_{\text{max}}$ prescribed by the user in the input file. A flowchart of the subroutine is given on figure 4.3.

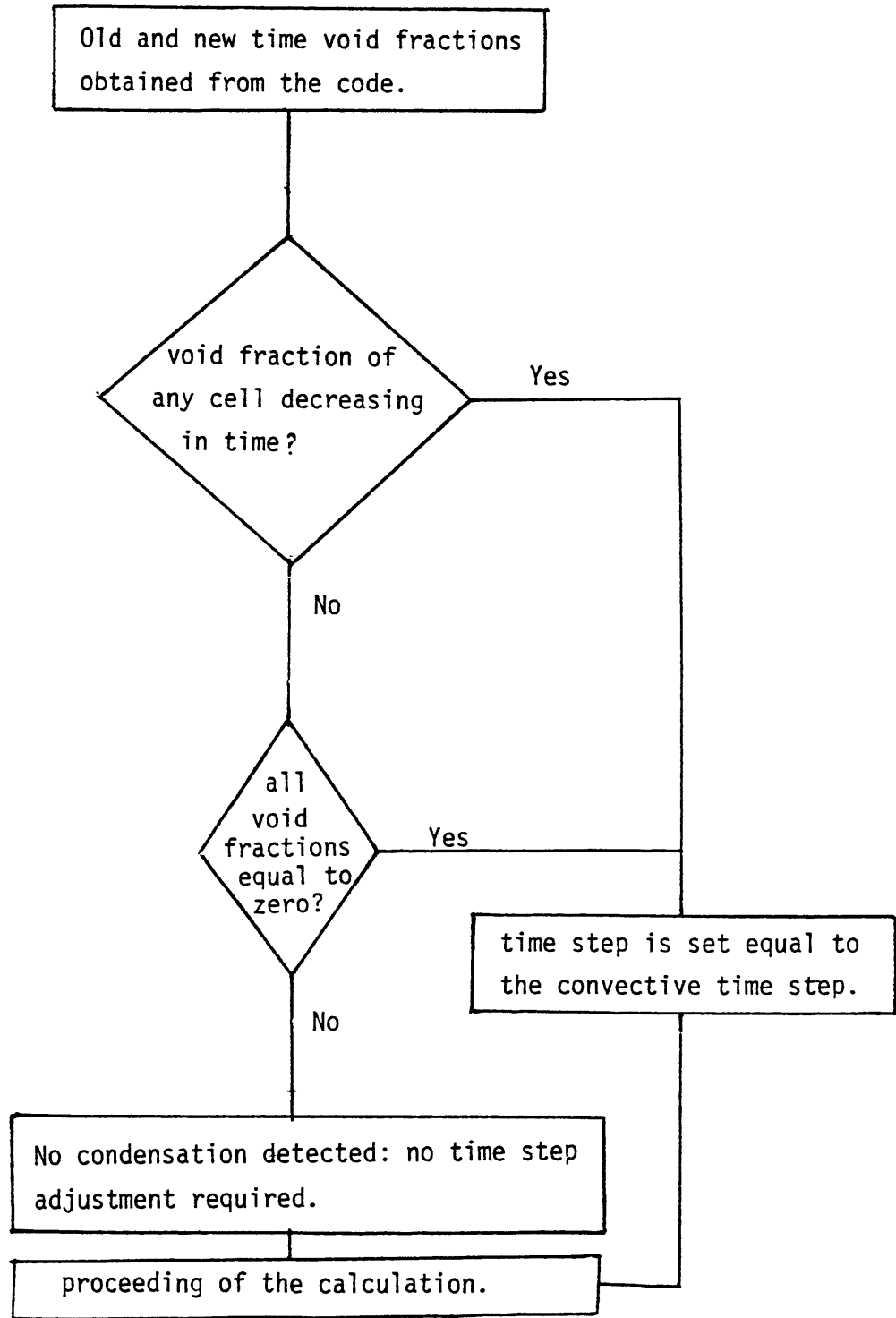


Figure 4.3. Logic of the subroutine implemented.

V. Comparative Analysis with other Methods

This chapter is devoted to the investigation of a spectrum of numerical methods and the possible existence of a minimum time step necessary for condensation simulations.

For the review of the following schemes, the conventions and notations remain unchanged and the assumptions made are those listed in sub-section (IV.2). Also, for the simplicity of the calculations, a one-cell control volume is considered all throughout our work: same results can be obtained for a multi-cell channel since the problem is basically equivalent.

V.1. An implicit mass convection scheme

The difference between the semi-implicit scheme examined in chapter IV and a fully implicit mass equation scheme is that the densities in the mass equation (the convective term) are treated implicitly: the momentum equation remains the same. With these considerations, the equations can be written as:

Mixture Mass Equation:

$$b \cdot \Delta P_o \frac{\Delta x}{\Delta t} + 2\rho_{\frac{1}{2}}^{n+1} U^{n+1} = 0 \quad (5.1)$$

where:

$$\rho_{\frac{1}{2}}^{n+1} = \begin{cases} \rho_o^{n+1} & \text{if } U^n \geq 0 \\ \rho_b & \text{if } U^n < 0 \end{cases} \quad (5.2)$$

Momentum equation:

identical to equation (4.6)

In order to linearize the mass equation we denote:

$$\begin{aligned} p_o^{n+1} &= \Delta P_o + p_o^n \\ U^{n+1} &= \Delta U + U^n \end{aligned} \quad (5.3)$$

Using equations (5.3) into the momentum equation, we have:

$$\Delta U = R \cdot \Delta P_o + S \quad (5.4a)$$

where:

$$\begin{aligned} R &= \frac{\Delta t}{\Delta x} / [\bar{\rho} + (1-\theta) \cdot K \Delta t] \\ S &= [(P_o^n - P_b) \frac{\Delta t}{\Delta x} - U^n \Delta t \cdot (K\theta + \bar{\rho} \text{conv})] / [\bar{\rho} + (1-\theta) K \Delta t] \end{aligned} \quad (5.4b)$$

If $U^n < 0$, then from equation (5.2) $\rho_{\frac{1}{2}}^{n+1} = \rho_b$ and therefore the mass equation is identical to the one for the semi-implicit scheme: the results pertaining to the case of pressure overshooting are also the same. However, for $U^n \geq 0$, $\rho_{\frac{1}{2}}^{n+1} = \rho_o^{n+1}$; in this case, the mass equation is written as follows after combining equations (5.1), (5.2), (5.3) and (4.4) and neglecting the second order term:

$$b \cdot \Delta P_o \frac{\Delta x}{\Delta t} + 2a(\Delta U + U^n) + 2b(U^n \Delta P_o + P_o^n \Delta U + P_o^n U^n) = 0 \quad (5.5)$$

Replacing the expression for ΔU from equation (5.4a) into equation (5.5) and solving for ΔP_o yields:

$$\Delta P_o = \frac{A \cdot \Delta t + B}{C} \quad (5.6a)$$

where:

$$\begin{aligned} A &= -U^n \cdot [\bar{\rho} \cdot \text{conv} + (2\theta - 1) \cdot K] + (P_o^n - P_b) / \Delta x \\ B &= U^n \cdot \bar{\rho} \\ C &= -\frac{\Delta t}{\Delta x} - \frac{b}{\rho_o} [\bar{\rho} + (1-\theta) K \Delta t] (U^n + \frac{1}{2} \frac{\Delta x}{\Delta t}) \end{aligned} \quad (5.6b)$$

since: $\rho_0^n = a + b P_0^n$ from equation (4.1).

For our case, B is positive and C is negative. Considering a critical situation of a pressure undershooting where $P_0^n < P_b$ and $U^n \geq 0$, then A is negative. The function for $\Delta P_0 = P_0^{n+1} - P_0^n$ in equation (5.6a) leads us to define a time step Δt_0 which has a similar significance to those defined in (4.2) and (4.3):

$$\begin{aligned} \Delta t_0 &= -B/A = \bar{\rho} U^n / [U^n (\bar{\rho} \cdot \text{conv} + (2\theta - 1) \cdot K) + (P_b - P_0^n) / \Delta x] \\ &\approx (\Delta t_0)_{\text{semi-implicit}} \end{aligned}$$

This result shows that an implicit mass equation scheme behaves like the semi-implicit one toward condensation or any pressure perturbation: in case of a pressure undershooting or overshooting of the steady state pressure level (here P_b), it can be easily overcome by using a time step larger than Δt_0 . Moreover, work done on this particular implicit scheme by S. Free and A. Schor [14] demonstrated that it is unconditionally stable, (for subsonic flow) so that there is no upper limit on the time step.

V.2. The fully explicit scheme

Once again, the same single-cell control volume is considered, its simplicity enabling us to gain insight into the problem. The mass equation can be written:

$$b \cdot \Delta_t P_0 \cdot \Delta x / \Delta t + 2 \rho_{\frac{1}{2}} U^n = 0 \quad (5.7)$$

where: $\Delta_t P_0 = P_0^{n+1} - P_0^n$

Re-arranging (5.7), P_0^{n+1} can be calculated by:

$$P_0^{n+1} = P_0^n - (2\rho_{\frac{1}{2}} \cdot U^n \Delta t) / b \Delta x \quad (5.8)$$

Considering a pressure undershooting such that:

$$0 < P_0^n < P_b \quad \text{and} \quad U^n > 0 \quad (5.9)$$

Calculating the adequate Δt 's for which P_o^{n+1} is positive using (5.8) yields:

$$\Delta t \leq \frac{P_o^n b \Delta x}{2\rho_{\frac{1}{2}} U^n} = (\Delta t)_{\text{mass}} \quad (5.10)$$

The momentum equation can be written as:

$$U^{n+1} = U^n + \frac{P_o^n - P_b}{\bar{\rho}} (\Delta t / \Delta x) - U^n \Delta t (\text{conv} + K/\bar{\rho}) \quad (5.11)$$

Since $U^n > 0$, we need to find the adequate Δt 's that give a negative U^{n+1} which corresponds to a flow reversal; (5.11) yields

$$\Delta t \geq \frac{U^n \bar{\rho} \Delta x}{U^n \bar{\rho} \Delta x (\text{conv} + K/\bar{\rho}) + P_b - P_o^n} = (\Delta t)_{\text{mom}} \quad (5.12)$$

In conclusion, in order to have a successful reversed flow before P_o becomes negative we need to choose Δt such as:

$$(\Delta t)_{\text{mom}} \leq \Delta t \leq (\Delta t)_{\text{mass}} \quad (5.13)$$

Therefore, we have to check that such Δt 's do exist by verifying that:

$$(\Delta t)_{\text{mom}} < (\Delta t)_{\text{mass}} \quad (5.14)$$

using (5.10) and (5.11) into (5.14) gives:

$$\frac{2 (U^n)^2 \bar{\rho}}{U^n \bar{\rho} \Delta x (\text{conv} + K/\bar{\rho}) + P_b - P_o^n} < P_o^n b/\rho_{\frac{1}{2}} \quad (5.15)$$

Practically, the inequality (5.15) turns out to be invalid, especially for low P_b 's; for example, for $P_o^n = 0.5$ bar and $P_b = 1.0$ bar while $U^n = 2.0$ m/sec, the flow will not reverse and P_o will keep decreasing and become negative.

The relatively large density of subcooled liquid renders $(\Delta t)_{\text{mom}}$ larger and $(\Delta t)_{\text{mass}}$ smaller so that eventually we rather have:

$$(\Delta t)_{\text{mom}} > (\Delta t)_{\text{mass}}$$

This result shows that unlike the implicit scheme, explicit schemes cannot correctly simulate either a condensation process or an important pressure perturbation.

V.3. The Method of Characteristics

V.3.1. Introduction

The basic equations of the HEM (2.8) are transformed into the characteristic form, leading to a set of ordinary differential equations. One of the most attractive features of the characteristic method is that the numerical schemes based on it conserve the physical properties of the system. Basically, the characteristic method tracks the propagation of waves and calculates their strength. Therefore, it is comparatively easy to simulate a fluid system including fluid discontinuities or shock waves.

Considering our one-dimensional homogeneous flow of subcooled liquid in a conduit of uniform cross-section, the equations of continuity and motion are respectively equations (2.8a) and (2.8b) (repeated below for convenience), and the energy equation is cast in terms of specific enthalpy:

$$\frac{\partial}{\partial t} \rho_m + \frac{\partial}{\partial x} (\rho_m U_m) = 0 \quad (2.8a)$$

$$\rho_m \frac{\partial U_m}{\partial t} + (\rho_m U_m) \frac{\partial U_m}{\partial x} + \frac{\partial P}{\partial x} = -F_w + \rho_m \vec{x} \cdot \vec{g} \quad (2.8b)$$

$$\rho_m \left(\frac{\partial h}{\partial t} + U \frac{\partial h}{\partial x} \right) - \left(\frac{\partial P}{\partial t} + U \frac{\partial P}{\partial x} \right) = 0 \quad (5.16)$$

Note that no heat input is being considered. The partial derivatives of h may be written as:

$$\frac{\partial h}{\partial t} = \frac{\partial h}{\partial \rho} \frac{\partial \rho}{\partial t} + \frac{\partial h}{\partial P} \frac{\partial P}{\partial t} \quad (5.17)$$

$$\frac{\partial h}{\partial x} = \frac{\partial h}{\partial \rho} \frac{\partial \rho}{\partial x} + \frac{\partial h}{\partial P} \frac{\partial P}{\partial x} \quad (5.18)$$

The square of sonic velocity can be defined as (App.C, eq. C-20):

$$c^2 = \frac{-\partial h / \partial \rho}{\partial h / \partial P - 1/\rho} \quad (5.19)$$

Using equations (2.8a), (5.17), (5.18) and (5.19) equation (5.16) is transformed to:

$$\rho c^2 \frac{\partial U}{\partial x} + \left(\frac{\partial P}{\partial t} + U \frac{\partial P}{\partial x} \right) = 0 \quad (5.20)$$

The set of equations (2.8a), (2.8b) and (5.20) are the basic equations used to derive the characteristic equations.

Let us first consider the set of equations (2.8b) and (5.20):
 along an arbitrary chosen curve on the x-t plane we have the
 following equations:

$$dU = \frac{\partial U}{\partial t} dt + \frac{\partial U}{\partial x} dx \quad (5.21)$$

$$dP = \frac{\partial P}{\partial t} dt + \frac{\partial P}{\partial x} dx \quad (5.22)$$

Equations (2.8b), (5.20), (5.21) and (5.22) provide a sufficient
 set to determine $\partial U/\partial t$, $\partial U/\partial x$, $\partial P/\partial t$ and $\partial P/\partial x$ along this curve if
 the determinant of the coefficients is not zero. Being however
 interested in the family of curves for which the determinant is zero,
 we have:

$$\begin{vmatrix} \rho & \rho U & 0 & 1 \\ 0 & \rho c^2 & 1 & U \\ dt & dx & 0 & 0 \\ 0 & 0 & dt & dx \end{vmatrix} = 0 \quad (5.23)$$

Expanding the determinant and solving for dx/dt we obtain:

$$\frac{dx}{dt} = U + c \quad (5.24)$$

$$\frac{dx}{dt} = U - c \quad (5.25)$$

where (5.24) and (5.25) are referred to as sonic character-
 istic lines. When (5.24) is satisfied by a curve on the
 x-t plane, the set of equations (2.8b), (5.20), (5.22) and
 (5.24) are consistent only if the following determinant

becomes zero:

$$\begin{vmatrix} \rho & \rho U & 0 & F \\ 0 & \rho c^2 & 1 & 0 \\ dt & dx & 0 & dU \\ 0 & 0 & dt & dP \end{vmatrix} = 0 \quad (5.26)$$

where F is the friction term in the momentum equation (2.8b).
 (5.26) and (5.24) yields:

$$\rho c \frac{dU}{dt} + \frac{dP}{dt} = cF \quad (5.27)$$

Similarly along a curve satisfying (5.25) we have:

$$- \rho c \frac{dU}{dt} + \frac{dP}{dt} = -cF \quad (5.28)$$

In our case, we have assumed constant temperature and energy of the fluid (subcooled liquid) and therefore (5.24), (5.27), (5.25) and (5.28) are used to calculate P and U along the sonic characteristic lines. We shall now apply this method of solution to our sample problem using successively an implicit and an explicit scheme.

V.3.2. Implicit characteristic method

The lines represented by (5.24) and (5.25) in a time and space mesh box are referred to as positive and negative characteristic lines respectively, or simply as sonic characteristic lines. They are illustrated in fig. 5.1.

Recalling the configuration of our problem, consisting of a single-cell and equal pressures at boundaries, its symmetry allows us to consider the equivalent problem of only a half of the cell with imposed pressure at the inlet and zero velocity at the outlet as boundary conditions.

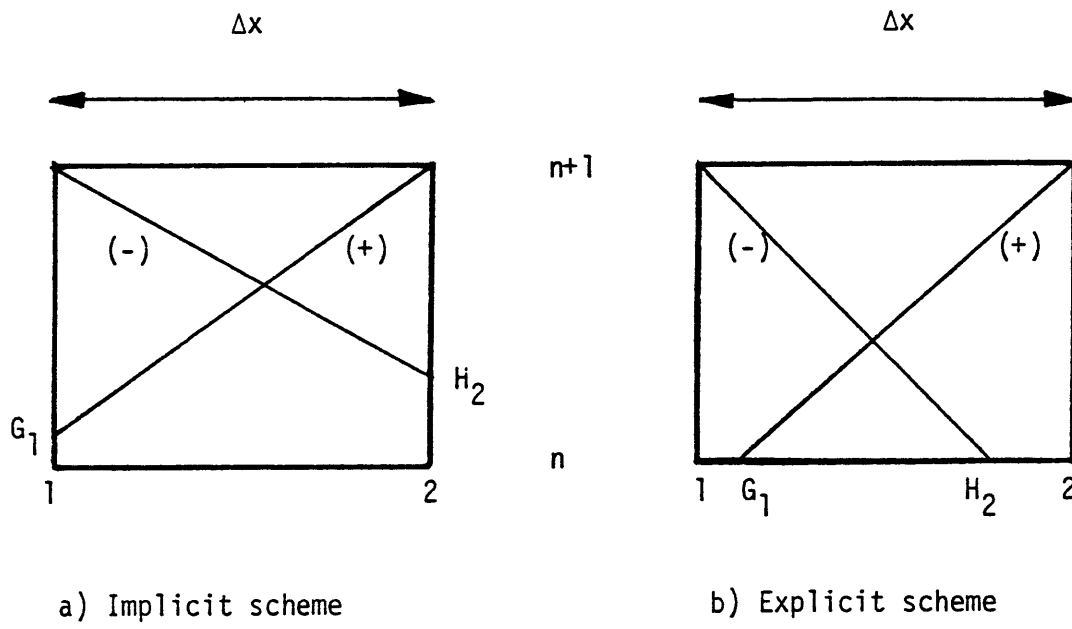


Figure 5.1. Sonic Characteristic lines

If subscripts 1 and 2 refer to the inlet and outlet,
we have:

$$\begin{aligned} p_2^n &= p_2^{n+1} = p_2 = \text{constant} \\ U_1 &= 0 \end{aligned} \quad (5.29)$$

The difference approximation to equations (5.27)
and (5.28) along the characteristic lines may be written,
respectively, as:

$$\frac{p_2 - p_G}{\Delta t} + (\rho c)_+ \frac{U_2^{n+1} - U_G}{\Delta t} = (cF)_+ \quad (5.30)$$

$$\frac{p_1^{n+1} - p_H}{\Delta t} - (\rho c)_- \frac{0 - U_H}{\Delta t} = -(cF)_- \quad (5.31)$$

Implicit difference schemes for characteristic
equations are obtained in accordance with fig. 5.1a where
the points G and H are located on the vertical sides
of each mesh box. The values of P and U at those points are
interpolated between the values of (1,n) and (1,n+1) for G
and between (2,n) and (2,n+1) for H applying equations (5.29):

$$\begin{aligned} p_G &= (1 - \eta_+) p_1^{n+1} + \eta_+ p_1^n \\ U_G &= (1 - \eta_+) U_1^{n+1} + \eta_+ U_1^n = 0 \\ p_H &= (1 - \eta_-) p_2^{n+1} + \eta_- p_2^n = p_2 \\ U_H &= (1 - \eta_-) U_2^{n+1} + \eta_- U_2^n \end{aligned} \quad (5.32)$$

where:

$$\begin{aligned}\eta_+ &= \frac{\Delta x}{\Delta t} \frac{1}{(c + U_2)_+} \\ \eta_- &= \frac{\Delta x}{\Delta t} \frac{1}{(c - U_2)_-}\end{aligned}\quad (5.33)$$

$()_+$ and $()_-$ denote averages along the positive and negative sonic characteristic lines. With the following change of variables :

$$\begin{aligned}\Delta U_2 &= U_2^{n+1} - U_2^n \\ \Delta P_1 &= P_1^{n+1} - P_1^n\end{aligned}$$

and using equations (5.32) and (5.33) into (5.30) and (5.31) we finally obtain:

$$\begin{aligned}-(1 - \eta_+) \Delta P_1 + (\rho c)_+ \Delta U_2 &= \frac{\Delta x}{(c + U_2)_+} (cF)_+ - (\rho c)_+ U_2^n \\ &\quad - \Delta_x P^n\end{aligned}\quad (5.34)$$

$$\begin{aligned}\Delta P_1 + (\rho c)_- (1 - \eta_-) \Delta U_2 &= \frac{\Delta x}{(c - U_2)_-} (cF)_- - (\rho c)_- U_2^n \\ &\quad + \Delta_x P^n\end{aligned}\quad (5.35)$$

where $\Delta_x P^n = P_2^n - P_1^n$

We now have to solve at every time step, a system of 2 equations and 2 unknowns, ΔP_1 and ΔU_2 . However, being concerned only with the pressure variation over the time step when critical situations are expected, ΔU_2 is eliminated between equations (5.34) and (5.35) to give:

$$\Delta P_1 = \frac{A \Delta t + B}{\Delta t \cdot C} \quad (5.36)$$

where:

$$A = \frac{\Delta x}{(c + U_2)_+} c_+ c_- \rho_- F_+ - \frac{\Delta x}{(c - U_2)_-} c_+ c_- \rho_+ F_- - (\rho_- c_- + \rho_+ c_+) \Delta_x P^n$$

$$B = \frac{\Delta x}{(c - U_2)_-} c_- \rho_- (c_+ \rho_+ U_2 + \Delta_x P^n - \frac{\Delta x}{(c + U_2)_+} c_+ F_+)$$

$$C = (\eta_+ - 1)(1 - \eta_-)(\rho c)_- - (\rho c)_+ \quad (5.37)$$

Since $\eta_+ \leq 1$ and $\eta_- \leq 1$, C is always negative, as well as the denominator of equation (5.36). Defining Δt_0 such as $\Delta t_0 = -B/A$ (5.38), if $-B/A > 0$ then $\Delta P_1 = 0$ for $\Delta t = \Delta t_0$. Considering the case of pressure undershooting where $P_1^n \approx 0.0$ bar so that $\Delta_x P^n > 0$, and $U_2 > 0$, equations (5.37) shows that practically the first two terms in the expression of A are comparable in magnitude and opposite so that the third term turns out to be dominant: in this case, A is negative. Also, in the expression of B , the last term is always negligible compared to the first and second terms so that B is positive here. Since C is negative, from equation (5.36) we deduce that ΔP_1 is positive if $\Delta t > \Delta t_0$ and ΔP_1 is negative if $0 \leq \Delta t < \Delta t_0$.

For the case of pressure overshooting where $P_1^n \approx 20.0$ bars and $U_2 < 0$, the assumptions previously made concerning the expressions of A and B remain valid so that now A is positive and B is negative. Since C is negative, from equation (5.36) we deduce that ΔP_1 is negative if $\Delta t > \Delta t_0$ and ΔP_1 is positive for $0 \leq \Delta t < \Delta t_0$.

These results mean that in order to have a flow reversal which is necessary to avoid having pressure going out of range (negative pressure or exceeding 20.0 bars), we need to impose a time step larger than some critical value Δt_0 . This conclusion is entirely similar to our findings in chapter V for the treatment of the implicit finite difference.

Furthermore, the implicit method of characteristic requires a time step larger than:

$$\Delta t \geq \frac{\Delta x}{c - |U_2|}$$

so that it will be always possible to reverse the flow in these particular "critical" conditions described before, resulting from complete condensation.

V.3.3. Explicit characteristic method

For the explicit scheme, points G and H are on the bottom line of the mesh-box as shown in figure 5.1b.

The values of P and U at those points may be calculated by interpolating the known values at (1,n) and (2,n); using (5.29) we have:

$$P_G = \left(1 - \frac{x_G}{\Delta x}\right) P_1^n + \frac{x_G}{\Delta x} P_2^n \quad (5.39)$$

$$U_G = \left(1 - \frac{x_G}{\Delta x}\right) U_1^n + \frac{x_G}{\Delta x} U_2^n = \frac{x_G}{\Delta x} U_2^n \quad (5.40)$$

$$P_H = \left(1 - \frac{x_H}{\Delta x}\right) P_1^n + \frac{x_H}{\Delta x} P_2^n \quad (5.41)$$

$$U_H = \left(1 - \frac{x_H}{\Delta x}\right) U_1^n + \frac{x_H}{\Delta x} U_2^n = \frac{x_H}{\Delta x} U_2^n \quad (5.42)$$

Substituting the values of P_G , U_G , P_H and U_H into (5.30) and (5.31) while recalling that $U_1 = 0$ and P_2 is constant at all times, those equations can be written as:

$$\Delta P_1 = \frac{x_H}{\Delta x} [P_2 - P_1^n - (\rho c)_- \cdot U_2^n] \quad (5.43)$$

$$\Delta U_2 = \frac{1}{(\rho c)_+} [\Delta t c_{F,+} U_2^n + (1 - \frac{x_G}{\Delta x}) (P_1^n - P_2 - (\rho c)_+ U_2^n)] \quad (5.44)$$

where $\Delta P_1 = P_1^{n+1} - P_1^n \quad (5.45)$

and $\Delta U_2 = U_2^{n+1} - U_2^n \quad (5.46)$

As for the implicit scheme, $()_+$ and $()_-$ refers to the average quantity along the positive and the negative characteristic lines respectively.

In equations (5.43) and (5.44), $x_G/\Delta x$ and $x_H/\Delta x$ need to be calculated.

From equation (5.24) which corresponds to the positive characteristic line we have:

$$x_G = \Delta x - \Delta t (\bar{U} + c_+) \quad (5.47)$$

where $\bar{U} = 0.5 (U_G + U_2^{n+1}) \quad (5.48)$

Using equations (5.40) in (5.48) and then in (5.47) yields, after dividing by Δx :

$$\frac{x_G}{\Delta x} = \frac{2 \Delta x - \Delta t (U_2^{n+1} + 2c_+)}{2 \Delta x + U_2^n \Delta t} \quad (5.49)$$

Similarly, x_H is computed from equation (5.25) using the negative characteristic line;

$$x_H = \Delta t (c_- - \bar{U}) \quad (5.50)$$

$$\text{where } \bar{U} = 0.5 (U_H + U_1^{n+1}) \quad (5.51)$$

Equation (5.42) substituted into equation (5.51) yields:

$$\bar{U} = \frac{x_H}{\Delta x} \frac{U_2^n}{2} \quad (5.52)$$

Then equations (5.50) and (5.52) combined give after dividing by Δx :

$$\frac{x_H}{\Delta x} = \frac{2c_- \Delta t}{2 \Delta x + U_2^n \Delta t} \quad (5.53)$$

Introducing the equation for $x_H/\Delta x$ from (5.53) into (5.43)

we obtain :

$$\Delta P_1 = \frac{2c_- \Delta t}{2 \Delta x + U_2^n \Delta t} [(P_2 - P_1^n) - (\rho c)_- U_2^n] \quad (5.54)$$

Considering a pressure undershooting due to condensation, where the most critical condition already described is encountered:

$$P_1^n \approx 0.0 \text{ bar and } U_2^n > 0$$

(5.54) shows that the pressure trend will not reverse if

$$U_2^n > \frac{P_2}{(\rho c)_-}$$

whatever the time step is. Considering now a pressure

overshooting situation where $P_1^n \approx 20.0$ bars and $U_2^n < 0$
 (5.54) shows again that the incorrect pressure trend will not
 reverse whatever the time step size if:

$$|U_2^n| > \frac{P_1^n - P_2}{(\rho c)_-}$$

These results prove that the explicit characteris-
 tic method will not adapt to a situation of large pressure
 perturbation created by such tests as a condensation or a water-
 hammer phenomenon. This is indeed consistent with the reported
 behavior of the explicit finite difference examined in V.2..

V.4. A generalized approach

At this point of the research, when some of the
 reviewed numerical methods seemed to exhibit difficulties in simu-
 lating a condensation process without the remedial use of relati-
 vely large time steps, and other schemes have been proved to be
 totally ineffective even with such remedy, an approximated analy-
 tical solution has been sought for the same problem that have
 been tested all throughout this work.

As previously done for the method of characteristics, only a
 half of the one-cell control volume is considered, with fixed
 pressure boundary condition at the outlet and zero velocity at
 the inlet. Furthermore, constant temperature and energy is also
 assumed so that density becomes a linear function of pressure and
 therefore only mass and momentum equations are used: namely eqs.

(2.8a) and (2.8b) from the HEM and equation (4.4) for the equation of state. Denoting by subscript 1 the boundary corresponding to the inlet and 2 for the outlet, we make the additional approximation that the mesh-size is small enough so that the following assumption can be justified.

Let $\phi = P, \rho U$ or ρU^2

$$\frac{\partial \phi}{\partial x} = \frac{\phi_2 - \phi_1}{\Delta x} \quad (5.55)$$

We also recall that P_2 is constant and $U_1 = 0$. (5.56)

Using (4.4), (5.55), (5.56) and (2.8a) the mass equation can then be written as:

$$b \frac{dP_1}{dt} + \rho_2 \frac{U_2}{\Delta x} = 0 \quad (5.57)$$

We now consider the density at the boundary constant so that:

$$\frac{\partial}{\partial t} (\rho U) = \rho \frac{\partial U}{\partial t} + U \frac{\partial \rho}{\partial t} \approx \rho_2 \frac{dU_2}{dt} \quad (5.58)$$

Using (5.55), (5.56), (5.57) and (2.8b) the momentum equation can be written as:

$$\rho_2 \frac{dU_2}{dt} + \rho_2 \frac{U_2^2}{\Delta x} + \frac{P_2 - P_1}{\Delta x} = -K \cdot U_2 \quad (5.59)$$

Equation (5.57) is re-arranged as written below :

$$U_2 = - \frac{b \cdot \Delta x}{\rho_2} \cdot \frac{dP_1}{dt} \quad (5.60)$$

Substituting equation (5.60) and its derivative into (5.59)

(recalling that ρ_2 is assumed constant) yields:

$$\ddot{P} (b \cdot \Delta x) + \dot{P} (Kb \cdot \Delta x / \rho_2) - \dot{P}^2 (b^2 \cdot \Delta x / \rho_2) + P (1/\Delta x) = P_2 (1/\Delta x) \quad (5.61)$$

where:

$$\begin{aligned} P &= P_1 \\ \dot{P} &= \frac{dP_1}{dt} \\ \ddot{P} &= \frac{d^2P_1}{dt^2} \end{aligned} \quad (5.62)$$

Let

$$\begin{aligned} a_0 &= b \cdot \Delta x \\ a_1 &= Kb \cdot \Delta x / \rho_2 \\ a_2 &= 1/\Delta x \\ a_3 &= - b^2 \cdot \Delta x / \rho_2 \\ a_4 &= P_2 / \Delta x \end{aligned} \quad (5.63)$$

With the change of variable defined by $\bar{P} = P - P_2$, equation (5.61) becomes:

$$a_0 \ddot{\bar{P}} + a_1 \dot{\bar{P}} + a_2 \bar{P} + a_3 \dot{\bar{P}}^2 = 0 \quad (5.64)$$

The approximation method of Krylov and Bogolyubov [13] yields an equivalent linearization of the given differential equation (5.64) with an error of the order of $(1/\rho_2)^2$ which is a very good approximation for subcooled liquid as it is the case here. The details of the approximation method are given in appendix D. Therefore, the linearized form of equation (5.64) is:

$$a_0 \ddot{\bar{P}} + a_1 \dot{\bar{P}} + a_2 \bar{P} = 0 \quad (5.65)$$

$$\text{Let } \Delta = a_1^2 - 4(a_0 a_2) \quad (5.66)$$

Then, using equations (5.63) :

$$\Delta = (Kb \cdot \Delta x / \rho_2)^2 - 4b \quad (5.67)$$

Since we made the initial assumption of small Δx ,

we necessarily have:

$$\Delta x < \frac{2\rho_2}{K\sqrt{b}} \quad (5.68)$$

Typically, for $\rho_2 = 800 \text{ kg/m}^3$, $U_2 = 1 \text{ m/sec}$, $b = 2 \cdot 10^{-7}$ and $\Delta x = 0.1 \text{ m}$ and using equation (2.12) for K , the right-hand-side of inequality (5.68) is indeed greater than the mesh size assumed; we can see that inequality (5.68) does not restrict the generality of our analysis and therefore from equation (5.67), we conclude that Δ is always negative. This means that the differential equation (5.65) has an underdamped (oscillatory) solution of the form:

$$\bar{P}(t) = R \cdot e^{\sigma t} \cdot \sin(\omega_N t + \alpha) \quad (5.69)$$

where:

σ is the damping constant

$$\sigma = -a_1/2a_0 = -K/2\rho_2 \quad (5.70)$$

ω_N is the natural circular frequency

$$\omega_N = (\sqrt{4a_0 a_2 - a_1^2})/2a_0 \quad (5.71)$$

R and α are chosen so as to match given initial conditions.

$$\text{Let } P(t=0) = P_0 \quad (5.72)$$

$$\text{and } \dot{P}(t=0) = 0 \quad (5.73)$$

because $U_2(t=0) = 0$

Equations (5.69), (5.72) and (5.73) yield:

$$\tan \alpha = -\frac{\omega_N}{\sigma} \quad \text{and} \quad R = (P_0 - P_2)/\sin \alpha \quad (5.74)$$

Then, equations (5.4.15) can be re-written as:

$$P(t) = P_2 + \frac{P_0 - P_2}{\sin\alpha} \cdot e^{\sigma t} \cdot \sin(\omega_N t + \alpha) \quad (5.75)$$

The above equation for P (5.75) shows that if $P_0 > 2 \cdot P_2$, P will go through negative values since for the damping constant for sub-cooled liquid (σ_ℓ), which is a function of density, is too small and thus does not provide enough damping to prevent these oscillations from reaching negative minima (figure 5.2).

Similarly, the phenomenon can be observed for a pressure overshooting case with the maxima of the oscillations reaching the upper limit of the pressure range (20.0 bars) as shown on figure 5.2.

In the case of vapor however, from equation (5.70), it is interesting to note that since the density is much smaller in the denominator, the damping constant for vapor (σ_v) is much larger and thus this effect is actually not felt.

Moreover, the time step strategy that has been recommended as a remedy to avoid pressure spikes mainly for semi-implicit and fully implicit schemes can now be understood as a method which predicts the time at which the minima of these oscillations cease to be negative and will remain positive until steady state is reached.

Also, the method enables us to evaluate the time for which the maximum of the oscillations (for pressure overshooting situations) do not exceed the upper limit of the pressure range as shown on figure 5.2.

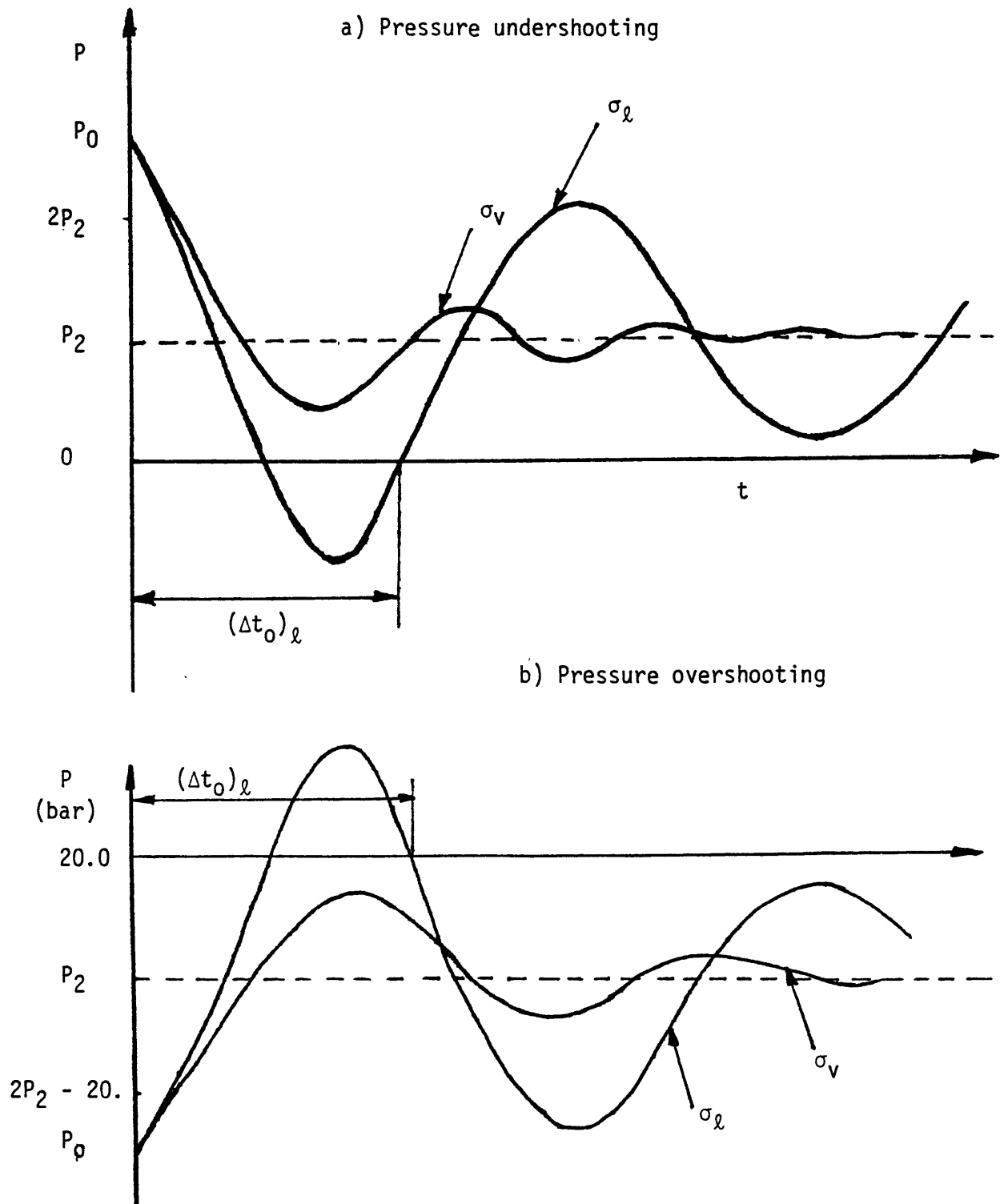


Figure 5.2. Solution of the equivalent linearized equation for pressure.

VI. Tests of the method

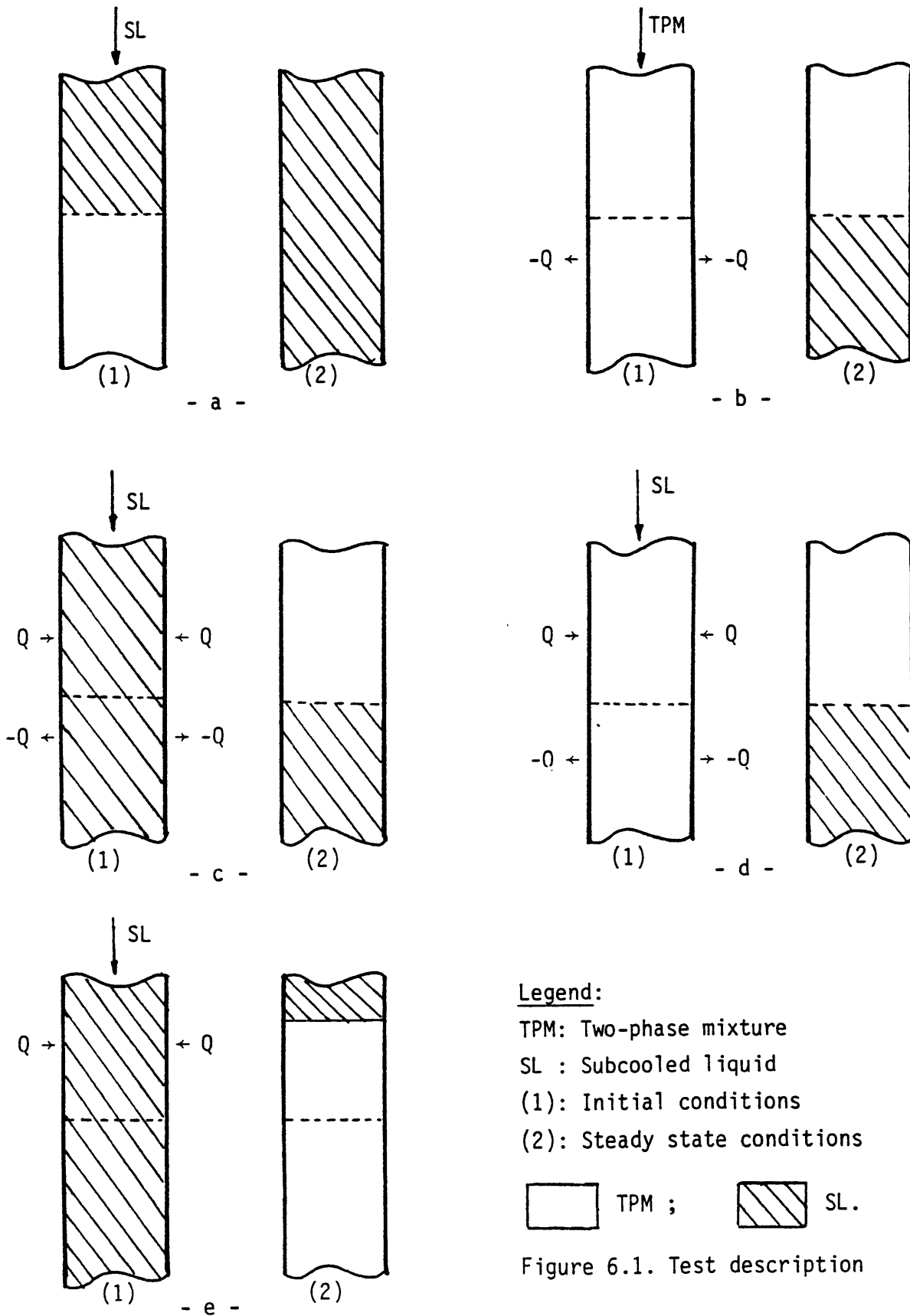
VI.1. Tests with a circular pipe

Several numerical experiments have been examined, each of them involving a condensation phenomenon, using the computer code THERMIT-4E and its modified version for loop simulation with our proposed algorithm. Computer outputs illustrating sample problems for each of these tests are given in Appendix F. First series of tests consist of a one-dimensional channel designed to generate a condensation process alone whereas a second series of tests is essentially considering a boiling-condensation combination.

First runs already described in chapter III feature subcooled liquid injected into two-phase mixture assumed initially stagnant (figure 6.1a). The two-phase mixture fully condenses so that only subcooled liquid flows in the channel at steady state. The corresponding computer code results are given in pages F-1 to 3.

The second type of runs feature a channel in which a two-phase mixture is injected: the first half of the channel is maintained at adiabatic conditions while heat is withdrawn at a constant rate from the fluid in the second half downstream. The boundary conditions are prescribed pressures at the inlet and the outlet; as expected, the two phase mixture fully condenses to liquid (figures 6.1b and 6.2; pages F-4 to 6).

For the tests described above where only condensation is taking place, the method implemented here enabled the code to reach steady state within a reasonable elapsed time.



Legend:

TPM: Two-phase mixture

SL : Subcooled liquid

(1): Initial conditions

(2): Steady state conditions

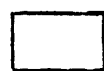
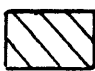
 TPM ;  SL.

Figure 6.1. Test description

The second series of tests considers a channel where the heat input in the first half of the total axial length is removed in the second half (figure 6.1c), thus creating essentially symmetrical density, enthalpy and velocity profiles. The boundary conditions are inlet mass flow rate and outlet pressure. The code reached steady state in this particular case of boiling-condensation experiments with the help of our algorithm. As expected, the results show here the coexistence of two-phase mixture-filled cells in the top half with subcooled liquid-filled cells in the bottom half of the channel and thus an interface of density gradient is correctly simulated (figures 6.2 and 6.3; pages F-7 to 12).

Furthermore, by keeping the same boundary conditions and the same heat input in the first half of the channel as before while maintaining the second half adiabatic (figure 6.1e) so that only boiling is taking place, we could check that the steady state obtained features now a two-phase mixture-filled pipe with some subcooled liquid at the inlet due to the inertia of the system (figures 6.2 and 6.3; pages F-13 to 20).

However, some remarks are to be made at this point, as far as these applications are concerned.

First, it is interesting to mention that the time step control algorithm is indeed turned on only whenever the void fraction of a cell changes from some value to zero. This situation takes place in the condensation test (figure 6.1b) and the boiling-condensation test (figure 6.1c) when in both cases, the channel initially

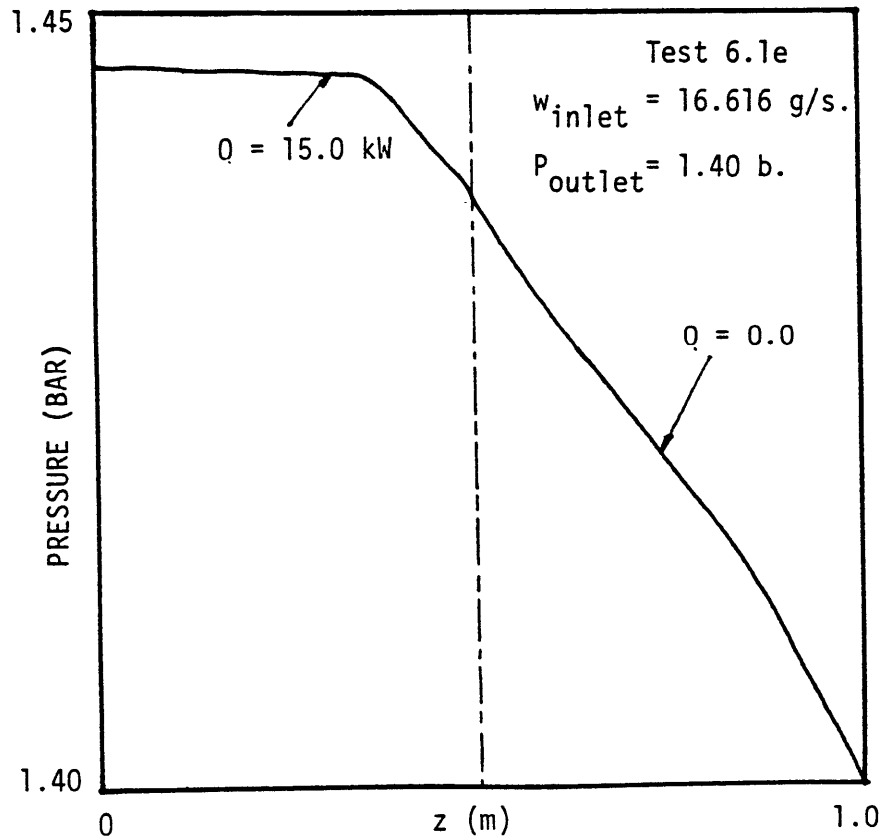
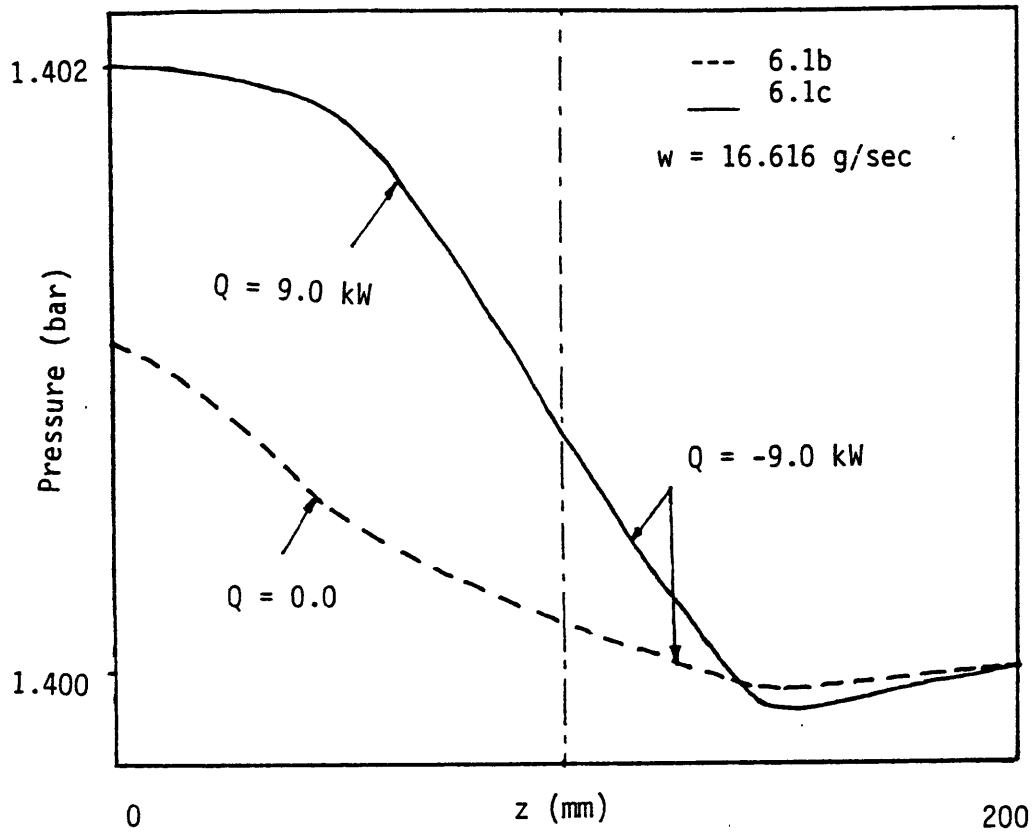


Figure 6.2. Steady state Pressure profiles for circular pipe tests.

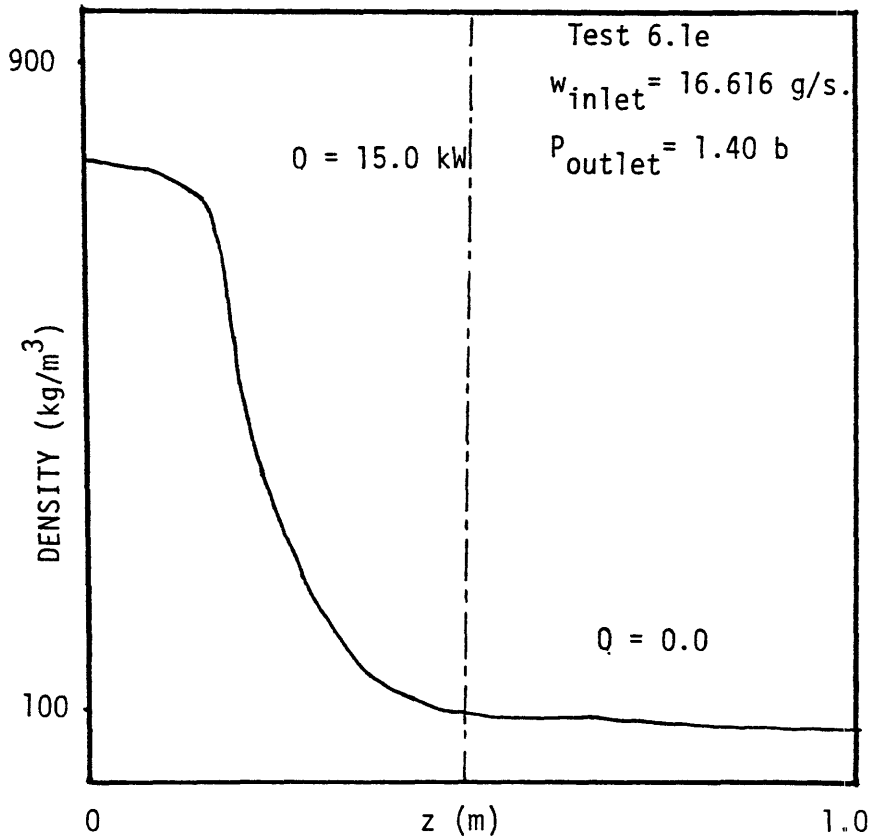
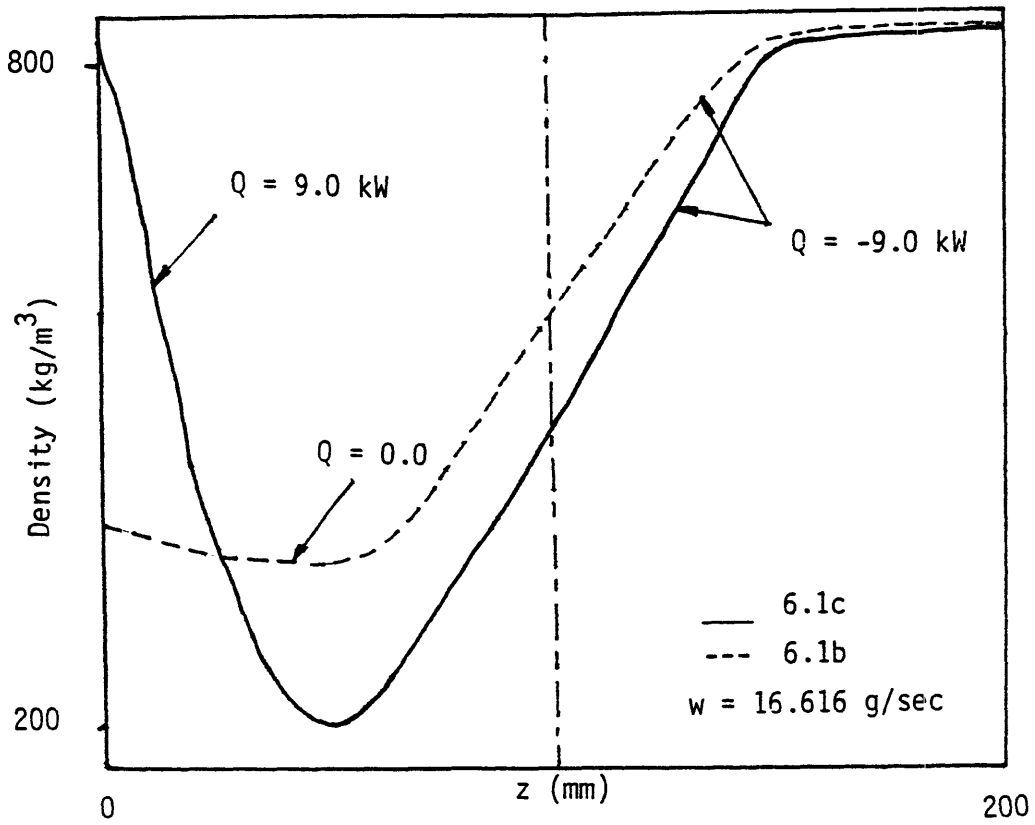


Figure 6.3. Steady state Density profiles for circular pipe tests.

contains two-phase mixture. For a subcooled liquid initial state (figure 6.1d), the flow evolves toward a final steady state without encountering a transition such as the one described above.

Secondly, when boiling numerical experiments were performed (figure 6.1e), we have noted the following behavior of the code: the flow is rejected from each side of the heated section of the channel in spite of the incoming flow at the inlet-side of the heated section; physically, the fluid flashes, entailing a very drastic density change. This trend causes the Newton iterations to diverge if the option of multiple Newton is invoked, eventually leading to pressure going out of range in the neighboring cells of the heated test section and finally to the code breaking down. However, a single Newton iteration i.e., a linearization only about old time values enables the code to overcome this trend successfully.

Whereas the code demonstrates the capability of simulating boiling with inlet mass flow and outlet pressure boundary conditions, it is not possible to achieve a boiling situation at steady state for a fixed inlet pressure as a boundary condition at the inlet of the channel. A tentative explanation of this behavior can be drawn from the numerous tests performed using such particular boundary conditions.

When sufficient heat input is provided for at least one cell to boil, the flow slows down substantially because of the relatively large friction factor of vapor. This leads to the boiling cell's pressure exceeding the pressure at the boundary such as to create a flow reversal from this particular cell to the inlet, while for the

downstream cells, the flow keeps the same direction. Eventually, the boiling cell being depleted and heated at the same time reaches a state of superheated steam and the vapor temperature rapidly goes out of range of state functions (1649 K).

VI.2. Tests with loop simulations

Last series of tests were performed using the loop version of THERMIT-4E. The loop geometry used for our numerical tests of loop simulations (figure 6.4) was developed by O. Adekugbe [4].

This geometry was found to be well adapted to the series of experiments performed in the sodium boiling test facility loop at the Oak Ridge National Laboratory.

Basically, the fluid undergoes a combination of the five simple processes previously described when flowing in the simulated loop. Considering the results from previous tests using the basic version of the computer code THERMIT-4E, it should be noted that in a reactor loop, the coolant undergoes a combination of our simple tests reviewed before. It was therefore expected that we would encounter difficulties in simulating natural circulation loop since in that case, it would imply a fixed pressure at the inlet as boundary conditions, whatever the location of the cut used for our simulations [4].

Indeed, a similar pattern of the code's breakdown to the one described in section VI.1 was observed. However, forced circulation loop tests simulated by using inlet mass flow-outlet pressure boundary conditions were successfully performed. Various power levels were

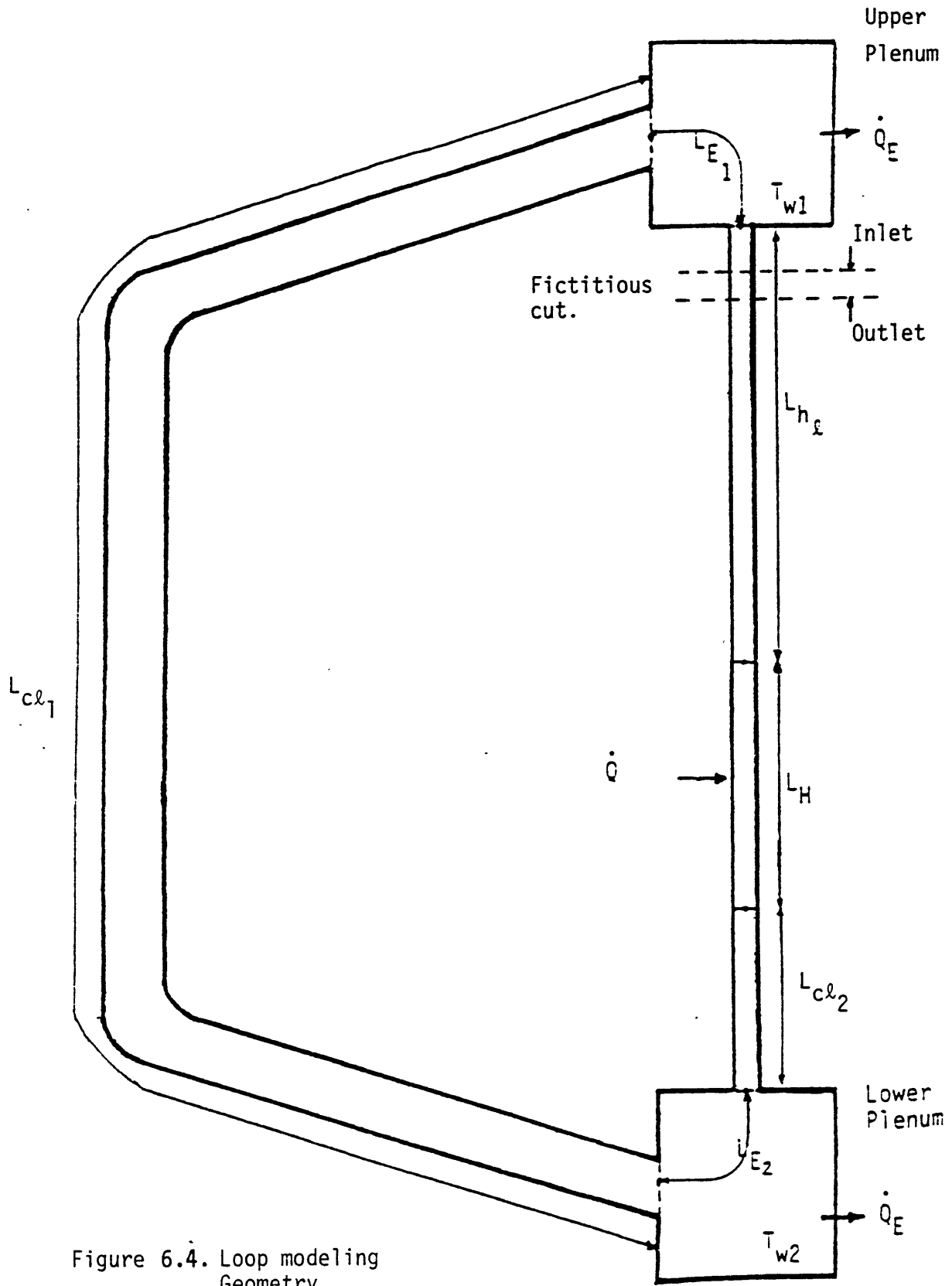


Figure 6.4. Loop modeling Geometry.

assumed and steady state was achieved (Appendix F, pages F-24 to 33); figures 6.5 and 6.6 (pages F-28 to 33) present two such cases.

For a given power input in the heated section, a given inlet mass flow rate and outlet pressure as boundary conditions, the pressure at the inlet varies non-monotonically for some time before reaching the steady state level (figure 6.7).

This behavior can be interpreted as being due to the pressure gradient necessary to prevent the flow reversal tendency caused by flashing cells in the heated region of the loop.

It should also be noted that the location of the fictitious cut (figure 6.4) which is required in our loop simulation, has not proved determinant as far as the code's behavior toward condensation is concerned; for all our calculations, this cut has been located at the inlet of the upper plenum.

Keeping the same heat input as well as the same outlet pressure, an oscillatory flow behavior was observed for lower inlet mass flow rates. Figure 6.8 indicates this behavior for one such case. This behavior is similar to the oscillatory loop flow encountered in single-phase by Adekugbe [4].

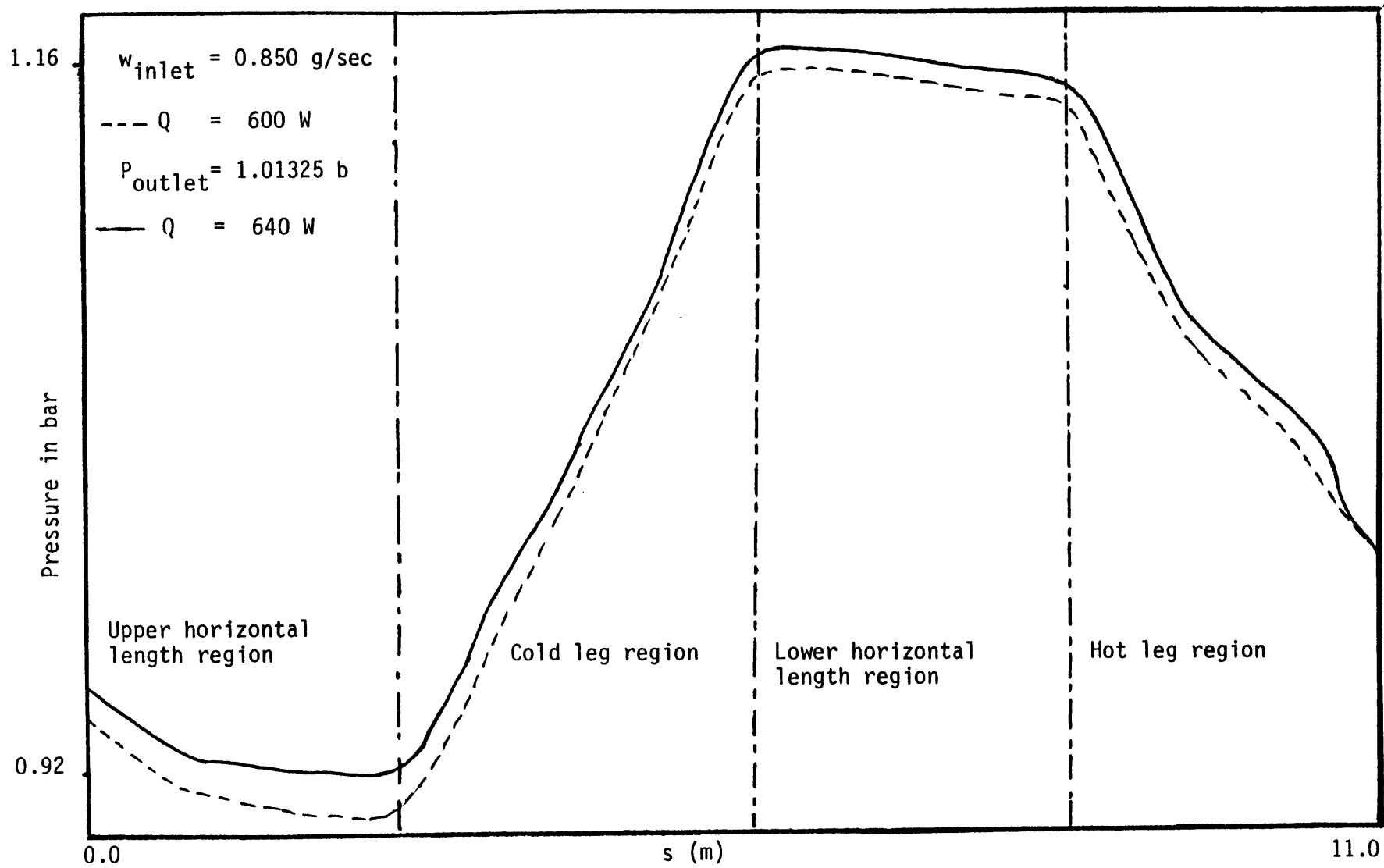
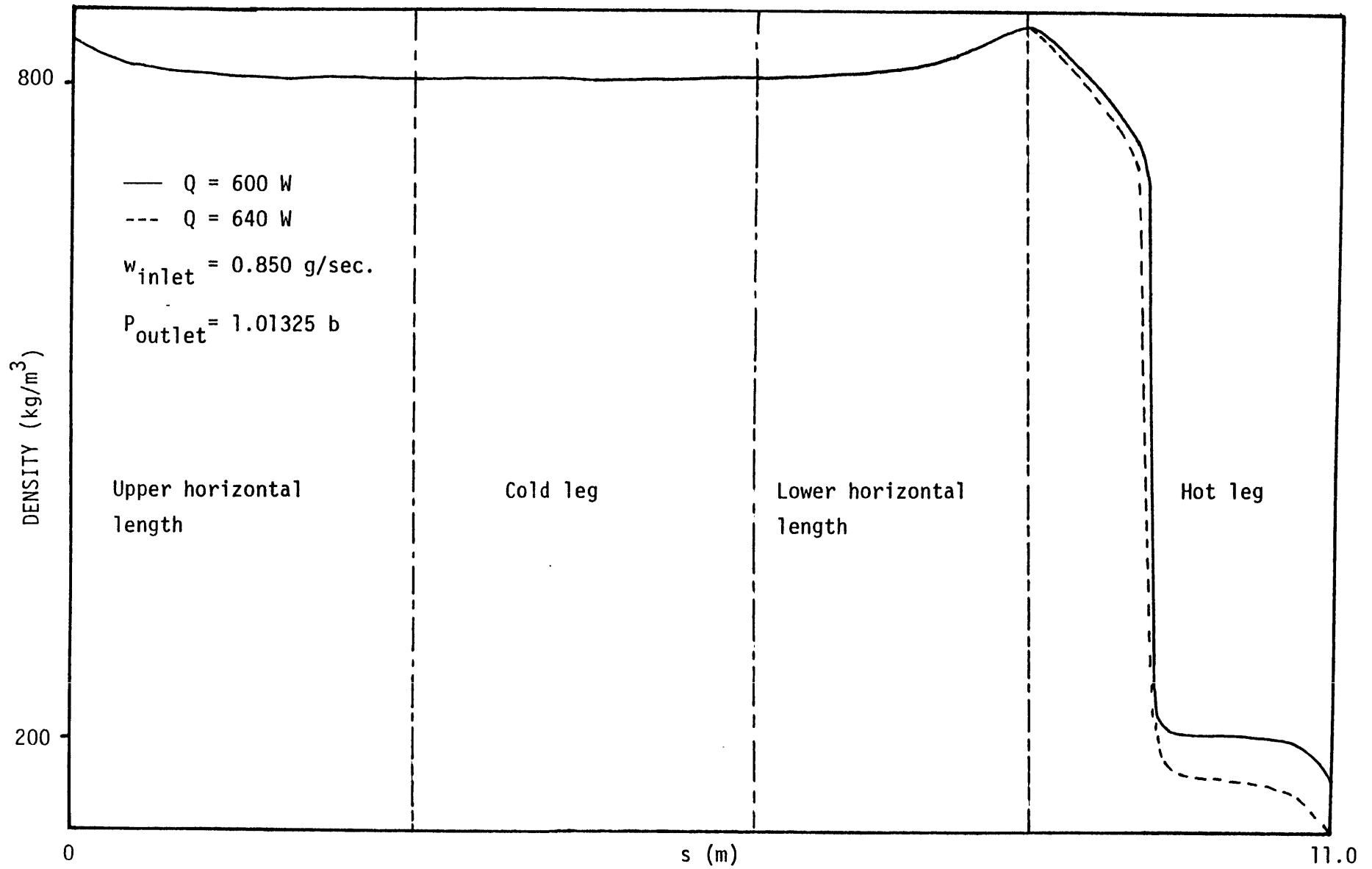


Figure 6.5. Pressure profile at steady-state for loop tests.

Figure 6.6. Steady state density profile for loop tests.



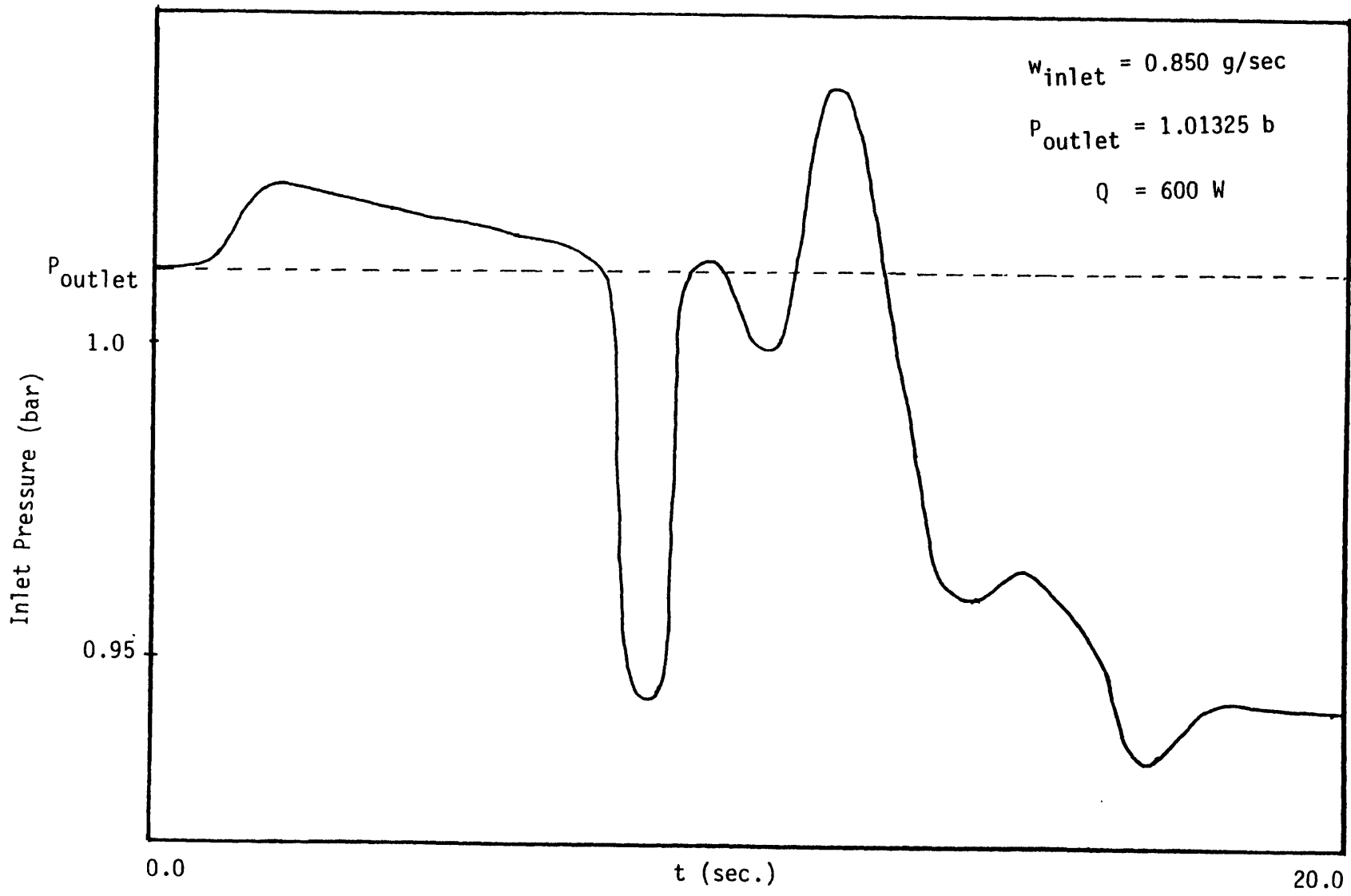


Figure 6.7. Inlet Pressure vs. time.

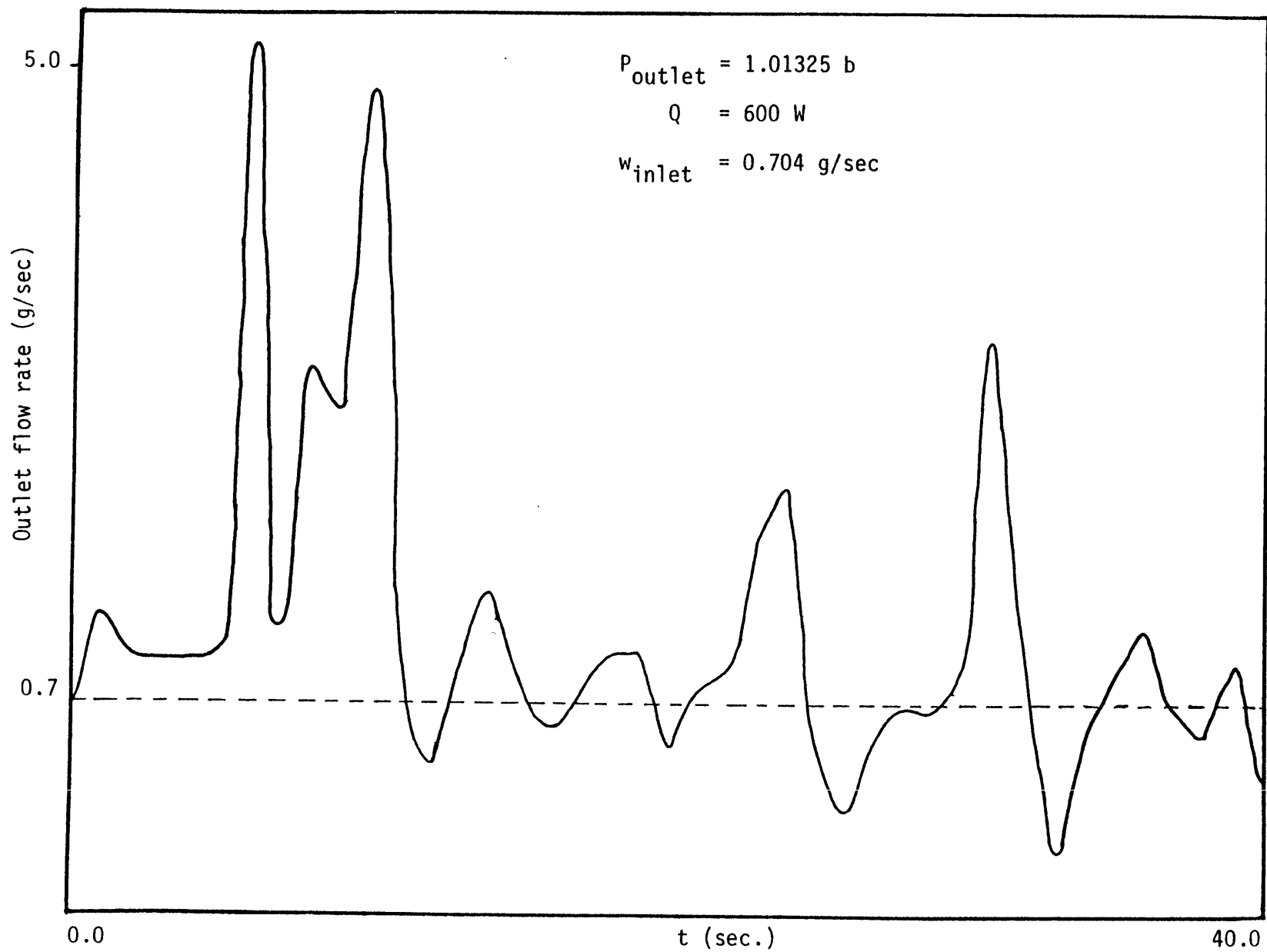


Figure 6.8. Oscillatory loop flow.

VII. CONCLUSION

VII.1. Conclusion and summary of the work

A general analysis of the effects of a vapor or two-phase mixture to liquid phase change has been carried out.

A number of numerical methods commonly used to solve the mass, momentum and energy equations for a thermo-hydraulic system were reviewed with regard to their behavior following complete condensation. The pressure perturbation generated following a full condensation process was proved to be damped differently by the system depending on the degree of explicitness of the equations.

Specifically, fully implicit and semi-implicit numerical methods are capable to absorb any pressure perturbation caused by condensation whereas a fully explicit scheme may encounter situations of large pressure spikes for which the calculations will fatally break down.

Furthermore, our findings cast doubt on the friction factor in the particular case of complete condensation and subsequent large pressure pulses: it appears from subsection V.4. that indeed the friction factor correlated in [5] and presented in chapter II is under-estimated leading to a small damping factor for the approximate solution of the mass and momentum equations. In addition, it is now ascertained that numerical methods and the corresponding legitimate approximations involved

are not the source of the breakdown of the basic numerical scheme used in the computer code THERMIT-4E, as far as these types of problems are concerned.

The outcome of this research which leads to a time step strategy by applying a time step increase (as opposed to a time step reduction originally implemented) whenever condensation conditions are met, is finally an optimized time step since it is also computed so as to maintain a small allowable mass conservation error. The ultimate results are very appreciable savings in computing time, and in many cases, making actually possible a broad range of calculations.

VII.2. The limitations of the analysis and recommendations for future work

An adequate friction factor should be investigated in those situations of sudden large pressure gradients for subcooled-liquid-filled channel. It would enable us to use time steps as small as it is needed, when a detailed picture of the physics of the channel is sought.

Also the use of a new donor flow formulation for momentum flux differencing has been investigated. Even though the convective term in the momentum equations do not affect the code's global behavior for our tests of boiling and condensation a new formulation would help eliminate the small pressure and velocity anomalies caused by fictitious momentum sources that arise when the actual numerical formulation is used to characterize the large density gradients associated with sodium boiling. To illustrate the incentive for a new formulation of the momentum

flux, let us consider the following situation: one dimensional steady-state flow with constant area and without gravity and friction.

The momentum equation used for this situation is cast in a non-conservative form:

$$\rho U \frac{dU}{dx} + \frac{dP}{dx} = 0 \quad (7.2.1)$$

since ρU is constant, equation (6.1.1) can be integrated as:

$$P_2 - P_1 = (\rho U) \cdot (U_1 - U_2) \quad (7.2.2)$$

where U_1 and U_2 are the velocities at the cells center.

The code's formulation however uses the velocities placed at the boundaries of the cells.

To compare the numerical solution used in THERMIT-4E with the analytical solution, a simple case can be considered (see Figure 7.1) where two low-densities cells ($\rho = 1$) are separated from high-density cells ($\rho = 2$) on both ends, the flow is steady with $\rho U = 20$. Figure 7.1 shows the pressure profiles pertaining to the numerical and analytical solutions.

As expected, the analytical solution produces a symmetrical pressure profile but the numerical solution gives a different pressure profile which is translated downstream from the geometric symmetry axis of the channel. In order to remedy

this discrepancy a new donor flow formulation, adapted from the one proposed by Rowe and Padilla [3] should be applied to the THERMIT-4E computer code.

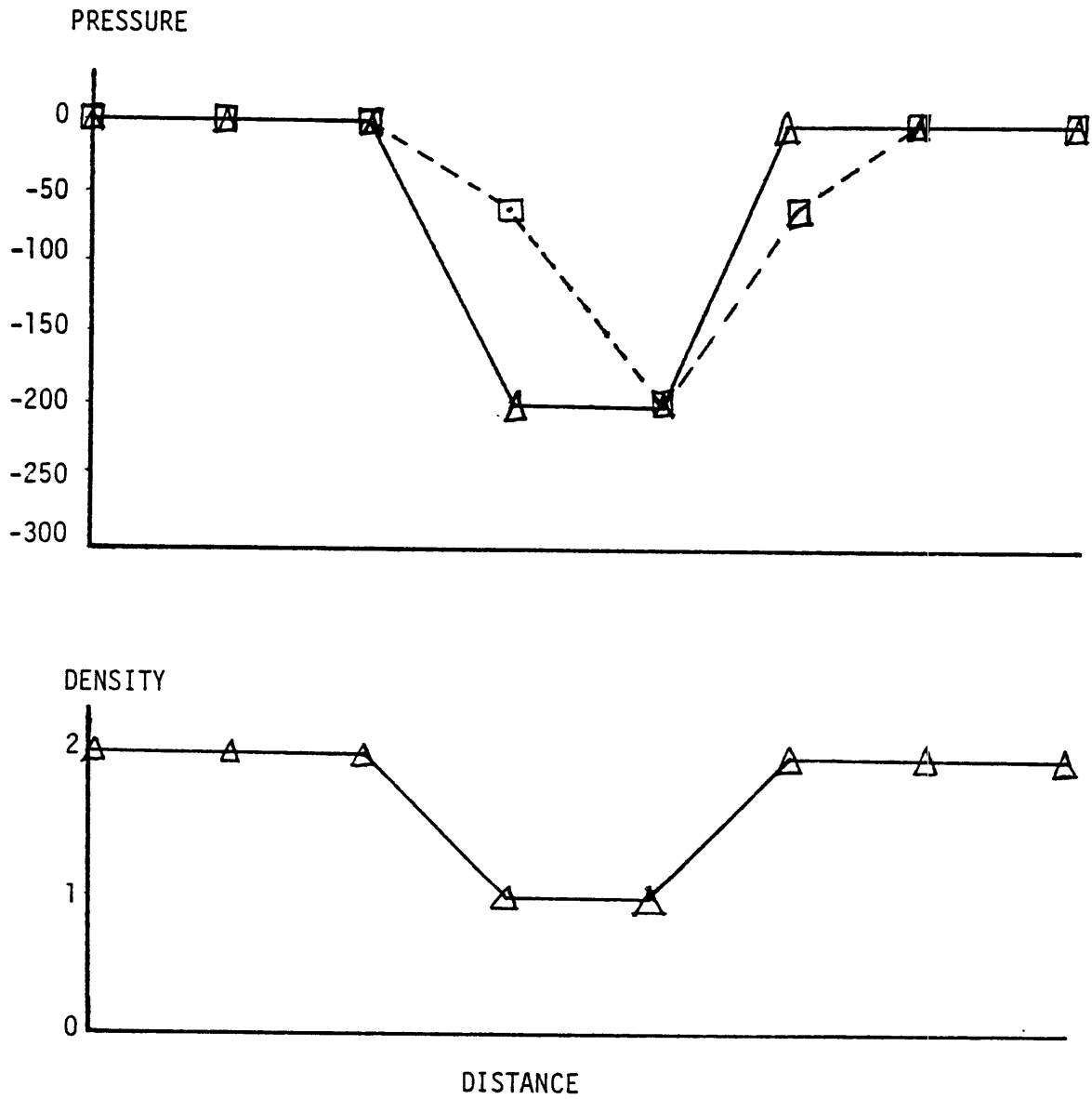


Figure 7.1 Pressure profile for assumed density profile.

However, it should be pointed out that the above mentioned formulation is applicable to the conservative form of the momentum equations, and its modification to a non-conservative momentum form (as used in THERMIT-4E) does not appear straightforward.

REFERENCES:

1. R.J. Pryor, D.R. Liles, J.H. Mahaffy (LASL), "Treatment of Water Packing Effects", A.N.S. Transactions (1978).
2. R.W. Lyczkowski, J.T. Ching, D.C. Mecham, "Studies Concerning Average Volume Flow and Water-Packing Anomalies in Thermal-Hydraulics codes", A.N.S. Thermal Reactor Safety Meeting (1977).
3. A. Padilla, D.S. Rowe, "A Donor Flow Formulation for Momentum Flux Differencing", A.N.S. Second Proceeding of Nuclear Thermal-Hydraulics (1984).
4. O. Adekugbe, A.L. Schor, "Loop Simulation Capability for Sodium Systems", M.I.T. Energy Laboratory Report: N°. M.I.T. - EL 84-013.
5. A.L. Schor, N.E. Todreas "A Four-Equation Two-Phase Flow Model for Sodium Boiling Simulation of LMFBR Assemblies", M.I.T. Energy Laboratory Report: N°. M.I.T. - EL 82-039
6. Asher H. Shapiro, "The Dynamics and Thermodynamics of Compressible Fluid Flow", Mc. Graw Hill book Company (1969).
7. Lecture Notes. M.I.T. Course 22.43 (Spring 1984)
8. A. L. Schor, "Numerical Method in THERMIT/TRAC Course Notes, Nuclear Engineering Department, MIT.
9. James E. A. John, "Gas Dynamics", Allyn and Bacon Inc. (1974).
10. Victor L. Streeter and Benjamin E. Wylie "Hydraulic Transients", Mc. Graw Hill book Company (1967)
11. Patrick J. Roache, "Computational Fluid Dynamics", Hermosa Publishers, Albuquerque (1980)
12. S. Nakamura, "Computational Methods in Engineering and Science", John Wiley & Sons (1977).
13. Granino A. Korn and Theresa M. Korn "Mathematical Handbook for Scientists and Engineers", Mc. Graw Hill Company (1968).
14. S. Free and A. L. Schor, "A Stable Numerical Method for one-Dimensional Sodium Boiling Simulation", Nuclear Engineering Department at MIT. Presented at the 11th LMB meeting at Grenoble, France (1984).

APPENDIX ADerivation of the momentum equation using the staggered mesh in the continuity equation.

The mass equation is written for the control volume located between cell centers (i) and (i+1) as represented in figure 2.4.

$$\left. \frac{\Delta \rho}{\Delta t} \right|_{i+1/2} + \left[\frac{\Delta}{\Delta x} (\rho U) \right]_{i+1/2} = 0 \quad (\text{A-1})$$

The momentum equation is written for the same control volume in a conservative form:

$$\left. \frac{\Delta}{\Delta t} (\rho U) \right|_{i+1/2} + \left[\frac{\Delta}{\Delta x} (\rho U U) \right]_{i+1/2} = R \quad (\text{A-2})$$

where R includes the pressure gradient and the friction term which remain unchanged. Expanding (A-2) yields:

$$\begin{aligned} (U \cdot \frac{\Delta \rho}{\Delta t})_{i+1/2} + (\rho \cdot \frac{\Delta U}{\Delta t})_{i+1/2} + U_{i+1/2} \cdot \left[\frac{\Delta}{\Delta x} (\rho U) \right]_{i+1/2} \\ + (\rho U)_{i+1/2} \cdot \left[\frac{\Delta U}{\Delta x} \right]_{i+1/2} = R \end{aligned} \quad (\text{A-3})$$

Multiplying equation (A-1) by $U_{i+1/2}$ and subtracting it from equation (A-3) we obtain the momentum equation in a non-conservative form:

$$\rho_{i+1/2} \cdot \frac{\Delta U}{\Delta t} \Big|_{i+1/2} + (\rho U)_{i+1/2} \left[\frac{\Delta U}{\Delta x} \right]_{i+1/2} = R \quad (\text{A-4})$$

We see that there is no difference between the usual momentum equation (2.41) and equation (A-4). This transformation was therefore determined not to be worthwhile pursuing.

APPENDIX BThermodynamic Derivations

Pressure is considered as a function of density and energy so that:

$$P = P(\rho, e) \quad (B-1)$$

The total derivative of P is:

$$dP = \left. \frac{\partial P}{\partial \rho} \right|_e \cdot d\rho + \left. \frac{\partial P}{\partial e} \right|_\rho \cdot de \quad (B-2)$$

Let \dot{M} be the mass input to the volume V and e_{in} the corresponding energy input, we have:

$$\rho^{n+1} = (\rho^n \cdot V + \dot{M} \cdot \Delta t) / V = \rho^n + \frac{\dot{M}}{V} \cdot \Delta t \quad (B-3)$$

and

$$(\rho e)^{n+1} = (\rho e)^n + \frac{\dot{M}}{V} \cdot \Delta t h_{in} \quad (B-4)$$

Assuming an isentropic flow, equation (B-4) yields:

$$[(\rho e)^{n+1}] - [(\rho e)^n] = d(\rho e) = e d\rho + \rho de = 0 \quad (B-5)$$

Equation (B-5) yields:

$$\frac{d\rho}{de} = - \frac{\rho}{e} \quad (B-6)$$

using equation (B-6), equation (B-2) can be re-written as

$$dP = \left[\left. \frac{\partial P}{\partial \rho} \right|_e \cdot \left(- \frac{\rho}{e} \right) + \left. \frac{\partial P}{\partial e} \right|_\rho \right] \cdot de \quad (B-7)$$

Note that ρ and e with subscripts refers to mixture.

In eq.(B-7) $\frac{\partial P}{\partial \rho}\bigg|_e$ and $\frac{\partial P}{\partial e}\bigg|_\rho$ have to be evaluated.

In [5] $\frac{\partial \rho}{\partial P}\bigg|_e$ has been calculated:

$$\frac{\partial \rho}{\partial P}\bigg|_e = \frac{\partial \rho}{\partial \rho_v}\bigg|_e \cdot \frac{d\rho_v}{dP} + \frac{\partial \rho}{\partial \rho_l}\bigg|_e \cdot \frac{d\rho_l}{dP} + \frac{\partial \rho}{\partial e_l}\bigg|_\rho \cdot \frac{de_l}{dP} + \frac{\partial \rho}{\partial e_v}\bigg|_\rho \cdot \frac{de_v}{dP} \quad (\text{B-8})$$

where:

$$\frac{\partial \rho}{\partial \rho_v} = \rho_l^2 (e_v - e_l) (e - e_l) / \text{Denom}^2$$

$$\frac{\partial \rho}{\partial \rho_l} = \rho_v^2 (e_v - e_l) (e_v - e) / \text{Denom}^2$$

$$\frac{\partial \rho}{\partial e_l} = \rho_v \rho_l (\rho_l - \rho_v) (e - e_l) / \text{Denom}^2$$

$$\frac{\partial \rho}{\partial e_v} = \rho_l \rho_v (\rho_l - \rho_v) (e_v - e) / \text{Denom}^2$$

$$\text{Denom} = \rho_l (e - e_l) + \rho_v (e_v - e)$$

$$\frac{d\rho_a}{dP} = \frac{\partial \rho_a}{\partial P}\bigg|_{T_a} + \frac{\partial \rho_a}{\partial T_a}\bigg|_P \cdot \frac{dT_{\text{sat}}}{dP}$$

$$\frac{de_a}{dP} = \frac{\partial e_a}{\partial P}\bigg|_{T_a} + \frac{\partial e_a}{\partial T_a}\bigg|_P \cdot \frac{dT_{\text{sat}}}{dP}$$

$$a = v \text{ or } l \quad (\text{B-9})$$

$\frac{\partial \rho_a}{\partial P}\bigg|_{T_a}$ and $\frac{\partial e_a}{\partial P}\bigg|_{T_a}$ can be easily calculated from state functions

in [5] written as:

$$\begin{aligned}\rho_a &= \rho_a (P, T_a) \\ e_a &= h_a (T_a) - \frac{P}{\rho_a}\end{aligned}\quad (B-10)$$

Calculation of $\left. \frac{\partial e}{\partial P} \right|_{\rho}$:

The internal energy can be considered as a function of pressure and density. Thus the following is inferred:

$$de = \left. \frac{\partial e}{\partial P} \right|_{\rho} \cdot dP + \left. \frac{\partial e}{\partial \rho} \right|_{P} \cdot d\rho \quad (B-11)$$

The internal energy of a mixture can be written as:

$$e = [\alpha \rho_v e_v + (1 - \alpha) \rho_l e_l] / \rho \quad (B-12)$$

where

$$\alpha = \frac{\rho_l - \rho}{\rho_l - \rho_v} \quad (B-13)$$

the expression for $\left. \frac{\partial e}{\partial P} \right|_{\rho}$ can be obtained using equations (B-12) and (B-13). Since $T_l = T_v = T_{sat}$:

$$\begin{aligned}\left. \frac{\partial \rho_a}{\partial P} \right|_{\rho} &= \frac{d\rho_a}{dP} \\ \left. \frac{\partial e_a}{\partial P} \right|_{\rho} &= \frac{de_a}{dP} \quad a = v \text{ or } l\end{aligned}\quad (B-14)$$

$$\text{let } \Delta\rho = \rho_l - \rho_v \text{ and } \Delta e = e_l - e_v \quad (B-15)$$

Using equations (B-15), (B-14), (B-13) and (B-12) we have:

$$\begin{aligned} \left. \frac{\partial e}{\partial P} \right|_{\rho} &= \frac{1}{\Delta \rho} \left[\frac{d\rho_{\ell}}{dP} \left(e_{\ell} - \rho \rho_{\ell} \Delta e - \frac{A}{\rho (\Delta \rho)^2} \right) - \frac{d\rho_{\nu}}{dP} \left(e_{\nu} + \rho \rho_{\ell} \Delta e + \frac{A}{\rho (\Delta \rho)^2} \right) \right. \\ &\quad \left. + \frac{de_{\ell}}{dP} \rho_{\ell} (1 - \rho \rho_{\nu}) - \frac{de_{\nu}}{dP} \rho_{\nu} (1 - \rho \rho_{\ell}) \right] \end{aligned} \quad (\text{B-16})$$

$$\text{where } A = (\rho_{\ell} - \rho) \rho_{\nu} e_{\nu} + (\rho - \rho_{\nu}) \rho_{\ell} e_{\ell} \quad (\text{B-17})$$

Note that the expressions for $\frac{de_a}{dP}$ and $\frac{de_a}{dP}$ ($a = \nu$ or ℓ) have been derived above. Thus a final expression for dP has been obtained in our particular case.

APPENDIX CDerivation of Sonic Velocity

$$h = e + pv$$

$$dh = de + pdv + vdp$$

$$Tds = de + pdv$$

$$ds = 0 \text{ if isentropic}$$

$$\rightarrow de = -pdv \text{ or } \left. \frac{dv}{de} \right|_s = -\frac{1}{p} \quad (\text{C-1})$$

$$dh = \frac{dp}{\rho} \quad (\text{C-2})$$

$$\rho = \rho(p, e) \quad (\text{C-3})$$

$$d\rho = \left. \frac{\partial \rho}{\partial p} \right|_e dp + \left. \frac{\partial \rho}{\partial e} \right|_p de \quad (\text{C-4})$$

$$\frac{d\rho}{dp} = \left. \frac{\partial \rho}{\partial p} \right|_e + \left. \frac{\partial \rho}{\partial e} \right|_p \cdot \frac{de}{dp} \quad (\text{C-5})$$

$$\left. \frac{dp}{d\rho} \right|_s = \frac{1}{\left(\left. \frac{\partial \rho}{\partial p} \right|_e + \left(\left. \frac{\partial \rho}{\partial e} \right|_p \cdot \left. \frac{de}{dp} \right|_s \right)} = c^2 \quad (\text{C-6})$$

$$dv = \left. \frac{\partial v}{\partial p} \right|_e dp + \left. \frac{\partial v}{\partial e} \right|_p de \quad (\text{C-7})$$

for s constant, using (C-1), (C-7) yields:

$$\left. \frac{dv}{de} \right|_s = -\frac{1}{p} = \left(\left. \frac{\partial v}{\partial p} \right|_e \right) \left. \frac{dp}{de} \right|_s + \left(\left. \frac{\partial v}{\partial e} \right|_p \right) \quad (\text{C-8})$$

Then $\left(\frac{dp}{de} \right)_s$ can be written as:

$$\begin{aligned} \left. \frac{dp}{de} \right|_s &= \left(-\frac{1}{p} - \left(\left. \frac{\partial v}{\partial e} \right|_p \right) \right) / \left(\left. \frac{\partial v}{\partial p} \right|_e \right) \\ &= \left(-\frac{1}{p} + \frac{1}{\rho^2} \left(\left. \frac{\partial \rho}{\partial e} \right|_p \right) \right) / \left(-\frac{1}{\rho^2} \left(\left. \frac{\partial \rho}{\partial p} \right|_e \right) \right) \end{aligned} \quad (\text{C-9})$$

$$\left. \frac{dp}{de} \right|_s = \frac{\rho^2/p - \left(\left. \frac{\partial \rho}{\partial e} \right|_p \right)}{\left(\left. \frac{\partial \rho}{\partial p} \right|_e \right)}$$

$$\left(\left. \frac{\partial \rho}{\partial e} \right|_p \right) \cdot \left. \frac{de}{dp} \right|_s = \frac{\left(\left. \frac{\partial \rho}{\partial e} \right|_p \right) \cdot \left(\left. \frac{\partial \rho}{\partial p} \right|_e \right)}{\rho^2/p - \left(\left. \frac{\partial \rho}{\partial e} \right|_p \right)} \quad (\text{C-10})$$

Using equations (C-10), (C-6) yields:

$$c^2 = \left. \frac{dp}{d\rho} \right|_s = \frac{\rho^2/p - (\partial\rho/\partial e)_p}{(\partial\rho/\partial p)_e (\rho^2/p - (\partial\rho/\partial e)_p) + (\partial\rho/\partial e)_p \cdot (\partial\rho/\partial p)_e}$$

or:

$$\left. \frac{dp}{d\rho} \right|_s = \frac{1}{\rho_p} \left(1 - \rho_e \frac{p}{\rho^2} \right)$$

where $\rho_p = \left. \frac{\partial\rho}{\partial p} \right|_e$ and $\rho_e = \left. \frac{\partial\rho}{\partial e} \right|_p$

We now calculate the sonic velocity in terms of the enthalpy.

The enthalpy is defined as:

$$h = e + P/\rho \quad (C-11)$$

$$dh = de + \frac{1}{\rho} dP - \frac{P}{\rho^2} d\rho \quad (C-12)$$

We know that: $Tds = de - \frac{P}{\rho^2} d\rho$ (C-13)

We are considering an isentropic process: $ds = 0$ (C-14)

Equations (C-12), (C-13) and (C-14) yield:

$$dh = dP/\rho \quad (C-15)$$

The enthalpy is a function of pressure and density:

$$h = h(P, \rho) \quad (C-16)$$

Differentiating equation (16) gives:

$$dh = \left. \frac{\partial h}{\partial P} \right|_{\rho} \cdot dP + \left. \frac{\partial h}{\partial \rho} \right|_P \cdot d\rho \quad (C-17)$$

Re-arranging eq. (C-17) and recalling that we are considering an isentropic process yields:

$$\left. \frac{\partial h}{\partial \rho} \right|_P = \frac{dh}{d\rho} - \left. \frac{\partial h}{\partial P} \right|_{\rho} \cdot \left. \frac{dP}{d\rho} \right|_s \quad (C-18)$$

From equation (C-15), equation (C-18) can be written as:

$$\left. \frac{\partial h}{\partial \rho} \right|_P = \left. \frac{dP}{d\rho} \right|_s \cdot \left(\frac{1}{\rho} - \left. \frac{\partial h}{\partial P} \right|_{\rho} \right) \quad (C-19)$$

We finally obtain after re-arranging equation (C-19):

$$\frac{dP}{d\rho} = \frac{\left. \frac{\partial h}{\partial \rho} \right|_P}{\frac{1}{\rho} - \left. \frac{\partial h}{\partial P} \right|_\rho} = c^2 \quad (\text{C-20})$$

APPENDIX DApproximation Method of Krylov and Bogolyubov [13]

To solve a differential equation of the form

$$\frac{d^2y}{dt^2} + \omega^2 y + \mu f(y, \frac{dy}{dt}) = 0 \quad (D-1)$$

where ω is a given constant, and the last term is a small non-linear perturbation, we write

$$y = r(t) \cdot \cos \phi(t) \quad (D-2)$$

Assuming that errors of the order of μ^2 are negligible, the "amplitude" $r(t)$ and the "total phase" $\phi(t)$ are then obtained from the first-order differential equations

$$\frac{dr}{dt} = \frac{\mu}{2\pi\omega} = \int_0^{2\pi} [f(r\cos\lambda, -r\omega\sin\lambda) \cdot \sin\lambda] \cdot d\lambda = -r \cdot a_1(r)/2 \quad (D-3)$$

$$\frac{d\phi}{dt} = \omega + \frac{\mu}{2\pi r\omega} = \int_0^{2\pi} [f(r\cos\lambda, -r\omega\sin\lambda) \cdot \cos\lambda] \cdot d\lambda = \sqrt{a_2(r)} \quad (D-4)$$

For a given value $r(0) = r_0$, the solution of the equivalent linear differential equation

$$\frac{d^2y}{dt^2} + a_1(r_0) \frac{dy}{dt} + a_2(r_0) \cdot y = 0 \quad (D-5)$$

approximates the solution of the given differential equation (D-1) with an error of the order of μ^2 .

In our case, we have:

$$\mu = 1/\rho_2 \quad (D-6)$$

$$\text{and } f(y, \frac{dy}{dt}) = (a_1 \dot{p} + a_3 \dot{p}^2)/a_0 \quad (D-7)$$

Substituting equations (D-6) and (D-7) into equation (D-3) yields after integrating:

$$\frac{dr}{dt} = -a_1 r / 2a_0 = -ra_1(r)/2$$

$$\therefore a_1(r) = a_1/a_0 \quad (D-8)$$

Similarly, substituting equations (D-6) and (D-7) into equation (D-4) yields after integration:

$$\frac{d\phi}{dt} = a_2/a_0 = \sqrt{a_2(r)}$$

$$\therefore a_2(r) = a_2/a_0 \quad (D-9)$$

Recalling then equation (D-5) and using equations (D-8) and (D-9), the equivalent linear differential equation for \ddot{P} is:

$$\ddot{P} + a_1 \dot{P}/a_0 + a_2 \bar{P}/a_0 = 0 \quad (D-10)$$

APPENDIX E: Implemented and modified subroutinesListing of the subroutine for the
time step algorithm

```
subroutine cdnstn(alp,alpn,nc,nzp2,ncdns)
implicit real*8 (a-h,o-z)
integer ncdns
dimension alp(nzp2,nc),alpn(nzp2,nc)
ncdns=0
sma=0.0
do 20 i=1,nzp2
do 10 j=1,nc
if (alpn(i,j).gt.0) go to 10
if ((alpn(i,j)-alp(i,j)).lt.0) ncdns=1
10 continue
20 continue
do 40 i=1,nzp2
do 30 j=1,nzp2
sma=sma+alpn(i,j)
30 continue
40 continue
if (sma.eq.0) ncdns=1
50 continue
return
end
```

Heat removal capability implemented in THERMIT-4E

```

subroutine initrc (rf,rrdrf,vmf,vpf,qz,qt,qr,rn,dz,twf,tr,trn,
1             ifcar,iarf,nrzf,nrmzf,nf,nfm1,drzf,qpp,q,
2             nc,narf,nz,nfmx,nfm1mx,nrzhmx)
c
c initialize rod conduction arrays
c and make initial call to gap conductance calculation
c
c implicit real*8 (a-h,o-z)
c
c common /prop/   ftd,fpuo2,fpress,  cpr,  expr,  grgh,  pgas,
1             gmix(4),  hgap,  burn,  effb,  frac
c
c dimension rf(nfmx,1),rrdrf(nfm1mx,1),vmf(nfmx,1),vpf(nfmx,1),
1   qz(1),qt(narf,1),qr(nfm1mx,1),rn(narf,1),dz(1),twf(nz,1),
2   tr(nfmx,nz,1),trn(nfmx,nz,1),ifcar(1),iarf(1),nrzf(1),
3   nrmzf(nrzhmx,1),nf(1),nfm1(1),drzf(nrzhmx,1),qpp(nz,1)
c data pi/3.14159265/, rpi2/.159154943/
c data zero,half,one /0.0d0,0.5d0,1.0d0/
c
c geometry arrays
c
do 100 j=1,narf
  rf(1,j) = zero
  m = 2
  do 10 k=1,nrzh(j)
    dr = drzf(k,j)/nrmzf(k,j)
    do 10 l=1,nrmzf(k,j)
      rf(m,j) = rf(m-1,j) + dr
      m = m + 1
10  continue
  nfm1j = nfm1(j)
  do 20 k=1,nfm1j
20  rrdrf(k,j) = half*(rf(k+1,j)+rf(k,j))/(rf(k+1,j)-rf(k,j))
  vmf(1,j) = zero
  rp = half*(rf(2,j) + rf(1,j))
  vpf(1,j) = half*(rp*rp - rf(1,j)*rf(1,j))
  if(nfm1j.eq.1) go to 35
  do 30 k=2,nfm1j
    rp = half*(rf(k+1,j) + rf(k,j))
    rm = half*(rf(k,j) + rf(k-1,j))
    vpf(k,j) = half*(rp*rp - rf(k,j)*rf(k,j))
    vmf(k,j) = half*(rf(k,j)*rf(k,j) - rm*rm)
30  continue
35  rm = half*(rf(nf(j),j) + rf(nfm1j,j))
  vmf(nf(j),j) = half*(rf(nf(j),j)*rf(nf(j),j) - rm*rm)
  vpf(nf(j),j) = zero
c
c radial and transverse heat source distribution arrays
c
  sum = zero
  do 40 k=1,nfm1j
40  sum=sum+qr(k,j)*pi*(rf(k+1,j)*rf(k+1,j)-rf(k,j)*rf(k,j))
  if(sum.eq.zero) go to 55
  rsum = one/sum
  do 50 k=1,nfm1j
50  qr(k,j) = qr(k,j)*rsum
  sum = zero
55  do 60 k=1,nc
60  sum = sum + qt(j,k)*rn(j,k)
  if(sum.eq.zero) go to 100

```

```

        rsum = one/sum
        do 70 k=1,nc
70         qt(j,k) = qt(j,k)*rsum
100        continue
c
c axial heat source distribution array
c
        ncond = nz+1
        do 190 j=1,nz-1
            jj=j+1
            if(qz(j)*qz(jj).ge.0) go to 190
            ncond=jj
            go to 195
190        continue
195        sum = zero
            do 200 j=1,ncond-1
                jj = j + 1
                sum = sum + qz(j)*dz(jj)
200        continue
            rsum = dabs(one/sum)
            do 210 j=1,ncond-1
210         qz(j) = qz(j)*rsum
                nzp = nz + 1
                if(ncond.eq.nzp) go to 235
                sum = zero
                do 220 j=ncond,nz
                    jj = j + 1
                    sum = sum + qz(j)*dz(jj)
220        continue
                rsum = dabs(one/sum)
                do 230 j=ncond,nz
230         qz(j) = qz(j)*rsum
235        continue
c
c set iarf: this array assigns a region number to each axial level
c
        if(narf.eq.1) go to 255
        do 250 j=2,narf
            do 250 k=ifcar(j-1),ifcar(j)-1
250         iarf(k) = j-1
255        do 260 k=ifcar(narf),nz
260         iarf(k) = narf
c
c set initial rod temperatures
c
        do 300 i=1,nc
            do 300 j=1,nz
                do 300 k=1,nf(iarf(j))
                    trn(k,j,i) = twf(j,i)
                    tr(k,j,i) = twf(j,i)
300        continue
c
c set up heat flux distribution for "fast" steady-state
c
        do 400 ic=1,nc
            do 400 iz=1,nz
                iarfz = iarf(iz)
                qp = q*qz(iz)*qt(iarfz,ic)
                qpp(iz,ic) = qp*rp12/rf( nf(iarfz),iarfz )
400        continue

```

Heat extraction
capability implemented

```
c
c initialize gap conductance calculation
c radia below are from sisf-w1 experiment, typical of fast reactors
c
  radfu = 2.465e-3
  radcl = 2.540e-3
c
  call mp2(.true.,burn,d1,d2,d3,d4,d5,grgh,radfu,radcl,d6,d7,d8,
1         d9,d10,d11,d12,d13,d14)
  return
end
```

Excerpt of the modified timstp subroutine

Activation of the process for the time step increase

```

      dtconv = one/(rtscvz + rtscvy + rtscvx)
50  dtconv = dmin1(c1m*dtconv,dtmax)
      if (ncdns.ne.1) go to 55
      delt=dtconv
      go to 56
c
55  delt = dmin1(dtconv,dtnew )
56  if (delt.lt.0.9*dtconv) ird = 1
      kred = kred + ird
      dtmina = dabs(dtmin)
      if (dtmin.eq.zero) dtmina = 0.001*dtconv
      if (delt.ge.dtmina) go to 100
      if (dtmin.ge.zero) go to 60
      lerr = .true.
      ierr = 10
      return
60  delt = dtmina
c
100 if (dtold.gt.zero) tsmult = delt/dtold
      return
      end

```

Appendix F: Code's input and outputs for typical cases.

Input for test of subcooled liquid coming
into a stagnant two-phase mixture (Fig. 6.1a).

```

1
two-mesh calculation with pressure b.c.'s
$intgin nc=1 nz=2 nr=1 narf=0 nx=1 nrzs=1 iss=1 ixfl=0 ibb=0
ichnge=1 ishpr=11111 istrpr=1 nitmax=-5 ipfso1=34 noumax=0
  neq=4  ieqvax=1.0 number=0 kfold=4 $
$realin epsn=0.10e0 grav=0.0 hdt=2.6e-3 pdr=1.15 hdr=20.0
radf=4.325e-3 delpr=1.0 delro=1.0 delem=1.0 errmax=0.5e-1 $
1      $ ncr
0      $ indent
26.47e-3 $ dx
22.92e-3 $ dy
0.12e0 0.03e0 0.03e0 0.12e0 $ dz
2(0.0e0) $ arx
2(0.0e0) $ ary
3(169.8475e-6) $ arz
2(0.0e+0) $ vol
5.263e-3 $ hedz
3.616e-3 $ wedz
1.60e+5 1.40e+5 1.40e+5 1.40e+5 $ pressure
2(0.0e0) 2(0.3e0) $ alpha
2(800.0e0) 2(1195.92e+0) $ tfluid
2(0.0e0) 0.0e0 $ velocity
$timdat tend=1.0e-1 dtmin=-1.0e-7 dtmax=1.0e-2 dtsp=1.0 dtlp=0.0 iredmx=10 $
$timdat tend=-1.0 $
0

```

INITIAL CONDITIONS FOR TEST 6.1a

```

time step no = 0      real time = 0.000000 sec      time step size = 0.000000+00 sec      cpu time = 0 00 sec
number of newton iterations = 0      0 time step reductions due to error 0
number of inner iterations = 0 0 0      0 reduced time steps since last print

total reactor power = 0.000 kW      inlet flow rate = 0.000 g/s      maximum temperatures ic iz
total heat transfer = 0.000 kW      outlet flow rate = 0.000 g/s      rod: 0 00 at 0 0
flow enthalpy rise = 0.000 kW      total system mass = 6.822 g      wall: 0 00 at 0 0
flow energy rise = 0.000 kW      global mass error = 0.0000+00 g      liquid: 1195.92 at 1 2
    
```

```

maximum relative changes over the time step      maximum relative linearization errors
in pressure: 0.000D+00      in pressure: 0.000D+00
in mixture density: 0.000D+00      in mass/volume: 0.000D+00
in mixture energy: 0.000D+00      in energy/volume: 0.000D+00
    
```

ic	iz	z(mm)	P(bar)	void	qual(%)	em	rom	T vap	T liq	T sat	vvz	vlz	rov	rol	flow(g/s)
1	1	0.0	1.60000	0.0000	0.000	1048857.	826.11	800.00	800.00	1211.97	0.000	0.000	0.5768	826.11	0.000
1	2	15.0	1.40000	0.0000	0.000	1048857.	825.91	800.00	800.00	1195.92	0.000	0.000	0.5047	825.91	0.000
1	3	45.0	1.40000	0.3000	0.022	1550819.	512.86	1195.92	1195.92	1195.92	0.000	0.000	0.3692	732.49	0.000
1	4	60.0	1.40000	0.3000	0.022	1550819.	512.86	1195.92	1195.92	1195.92			0.3692	732.49	

FINAL STEADY-STATE FOR TEST 6.1a

time step no = 24 real time = 0.100057 sec time step size = 0.43697D-02 sec cpu time = 3.83 sec
 number of newton iterations = 2 0 time step reductions due to error = 0
 number of inner iterations = 2 0 0 0 reduced time steps since last print

total reactor power = 0.000 kW inlet flow rate = 873.783 g/s maximum temperaturens ic iz
 total heat transfer = 0.000 kW outlet flow rate = 873.783 g/s rod: 0.00 at 0 0
 flow enthalpy rise = -0.012 kW total system mass = 8.418 g wall: 0.00 at 0 0
 flow energy rise = -0.000 kW global mass error = -0.344D-17 g liquid: 800.00 at 1 1

maximum relative changes over the time step
 in pressure: 0.387D-06
 in mixture density: 0.710D-09
 in mixture energy: 0.100D-09

maximum relative linearization errors
 in pressure: 0.721D-19
 in mass/volume: 0.387D-18
 in energy/volume: 0.508D-19

ic	iz	z(mm)	P(bar)	void	qual(%)	sm	rom	T vap	T liq	T sat	vvz	viz	rov	rol	flow(g/s)
1	1	0.0	1.60000	0.0000	0.000	1048857.	826.11	800.00	800.00	1211.97	6.227	6.227	0.4176	826.11	873.783
1	2	15.0	1.51670	0.0000	0.000	1048857.	826.03	800.00	800.00	1205.49	6.228	6.228	0.3975	826.03	873.783
1	3	45.0	1.48334	0.0000	0.000	1048857.	825.99	800.00	800.00	1202.82	6.228	6.228	0.3894	825.99	873.783
1	4	60.0	1.40000	0.0000	0.000	1048857.	825.91	800.00	800.00	1195.92			0.3692	825.91	

CONDENSATION TEST (Fig. 6.1b): INPUTS

```

1
condensation test
$intgin nc=1 nz=2 nr=1 narf=1 nx=1 nrzs=1 lss=1 ixfl=0 ibb=2 ihtf=1
ichnge=1 ishpr=11111 istrpr=1 nitmax=-2 ipfsol=10 noumax=0
  neq=4 ieqvax=0.0 number=0 kfold=4 $
$realin epsn=0.10e0 grav=0.0 hdt=2.6e-3 pdr=1.15 hdr=20.0
radf=4.325e-3 delpr=1.0 delro=1.0 delem=1.0 errmax=0.5e-1 winlet=16.616e-3 $
$rodinp q0=9000.0 $
1          $ ncr
0          $ indent
1$ifcar
1$nrzf
1$nrmaf
3$mnrzf
26.47e-3   $ dx
22.92e-3   $ dy
0.12e0 0.10e0 0.1e0 0.12e0 $ dz
2(0.0e0)   $ arx
2(0.0e0)   $ ary
3(169.8475e-6) $ arz
2(0.0e+0)   $ vol
5.263e-3   $ hedz
3.616e-3   $ wedz
1.6e5 2(1.4e+5) 1.4e+5   $ pressure
2(0.5) 2(0.0e0) $ alpha
1195.920 1(1195.92) 2(1040.0) $ tfluid
3(0.118e0) $ velocity
1(1200.00) 1(1040.0) $twf
0.0 -1.0 $qz
1.0 $qt
1.0 $qr
1.0 $rn
1.625e-3 $drzf
$timdat tend=10.0e0 dtmin=-1.0e-6 dtmax=1.0e0 dtsp=20.0 dtlp=0.1e1 iredmx=20 $
$timdat tend=-1.0 $
0

```

INITIAL CONDITIONS FOR TEST 6.1b

time step no = 0 real time = 0.000000 sec time step size = 0.000000+00 sec cpu time = 0 00 sec
 number of newton iterations = 0 0 time step reductions due to error 0
 number of inner iterations = 0 0 0 0 reduced time steps since last print

total reactor power = 9.000 kW inlet flow rate = 7.344 g/s maximum temperatures ic iz
 total heat transfer = -9.000 kW outlet flow rate = 16.553 g/s rod: 0.00 at 0 0
 flow enthalpy rise = 5.963 kW total system mass = 20.252 g wall: 0.00 at 0 0
 flow energy rise = 5.963 kW global mass error = 0.0000+00 g liquid: 1195.92 at 1 1

maximum relative changes over the time step
 in pressure: 0.0000+00
 in mixture density: 0.0000+00
 in mixture energy: 0.0000+00

maximum relative linearization errors
 in pressure: 0.0000+00
 in mass/volume: 0.0000+00
 in energy/volume: 0.0000+00

ic	iz	z(mm)	P(bar)	void	qual(%)	em	rom	T vap	T liq	T sat	vvz	viz	rov	rol	flow(g/s)
1	1	0.0	1.40000	0.5000	0.050	1552141.	366.43	1195.92	1195.92	1195.92	0.118	0.118	0.3692	732.49	7.344
1	2	50.0	1.40000	0.5000	0.050	1552141.	366.43	1195.92	1195.92	1195.92	0.118	0.118	0.3692	732.49	7.344
1	3	150.0	1.40000	0.0000	0.000	1048857.	825.91	800.00	800.00	1195.92	0.118	0.118	0.5047	825.91	16.553
1	4	200.0	1.40000	0.0000	0.000	1048857.	825.91	800.00	800.00	1195.92			0.5047	825.91	

FINAL STEADY-STATE FOR TEST 6.1b

time step no = 295 real time = 9.986820 sec time step size = 0.314050-01 sec cpu time = 21.59 sec
 number of newton iterations = 2 0 time step reductions due to error 0
 number of inner iterations = 2 0 0 0 reduced time steps since last print

total reactor power = 9.000 kW inlet flow rate = 16.616 g/s maximum temperatures ic iz
 total heat transfer = -9.000 kW outlet flow rate = 16.616 g/s rod: 1195.96 at 1 1
 flow enthalpy rise = -9.000 kW total system mass = 19.233 g wall: 1195.96 at 1 1
 flow energy rise = -8.963 kW global mass error = -0.2730-14 g liquid: 1195.96 at 1 1

maximum relative changes over the time step maximum relative linearization errors
 in pressure: 0.1000-09 in pressure: 0.5240-16
 in mixture density: 0.3160-07 in mass/volume: 0.2180-13
 in mixture energy: 0.1380-06 in energy/volume: 0.4450-18

ic	iz	z(mm)	P(bar)	void	qual(%)	em	rom	T vap	T liq	T sat	vvz	vlz	rov	rol	flow(g/s)
1	1	0.0	1.40112	0.4868	0.048	1552141.	376.06	1196.01	1196.01	1196.01	3.152	0.259	0.3695	732.47	16.616
1	2	50.0	1.40058	0.5849	0.071	1553148.	304.30	1195.96	1195.96	1195.96	2.630	0.320	0.3693	732.48	16.616
1	3	150.0	1.39993	0.0000	0.000	1037139.	828.06	790.70	790.70	1195.91	0.118	0.118	0.3692	828.06	16.616
1	4	200.0	1.40000	0.0000	0.000	1037139.	828.06	790.70	790.70	1195.92			0.3692	828.06	

INPUTS FOR BOILING-CONDENSATION TEST (Fig. 6c)

```

1
boiling and condensation test
$intgin nc=1 nz=2 nr=1 narf=1 nx=1 nrzs=1 iss=1 ixfl=0 ibb=2 ihtf=1
ichnge=1 ishpr=11111 istrpr=1 nitmax=-2 ipfsol=10 noumax=0
      neq=4 ieqvax=0.0 numder=0 kfold=4 $
$realin epsn=0.10e0 grav=0.0 hdt=2.6e-3 pdr=1.15 hdr=20.0
radf=4.325e-3 delpr=1.0 delro=1.0 delem=1.0 errmax=0.5e-1 winlet=16.616e-3 $
$rodinp q0=9000.0 $
1          $ ncr
0          $ indent
1$ifcar
1$nrzf
1$nrmaf
3$mnrzf
26.47e-3   $ dx
22.92e-3   $ dy
0.12e0 0.10e0 0.1e0 0.12e0 $ dz
2(0.0e0)   $ arx
2(0.0e0)   $ ary
3(169.8475e-6) $ arz
2(0.0e+0)   $ voi
5.263e-3   $ hedz
3.616e-3   $ wedz
1.6e5 2(1.4e+5) 1.4e+5   $ pressure
2(0.00) 2(0.0e0) $ alpha
800.00 1(1040.00) 2(1040.0) $ tfluid
3(0.118e0) $ velocity
1(1200.00) 1(1040.0) $twf
1.0 -1.0 $qz
1.0 $qt
1.0 $qr
1.0 $rn
1.625e-3 $drzf
$timdat tend=10.0e0 dtmin=-1.0e-6 dtmax=1.0e0 dtsp=20.0 dtlp=0.1e1 iredmx=20 $
$timdat tend=-1.0 $
0

```


FINAL STEADY STATE FOR TEST 6.1c

time step no = 2826 real time = 5.001014 sec time step size = 0.14897D-02 sec cpu time = 154.92 sec
 number of newton iterations = 2 0 time step reductions due to error 0
 number of inner iterations = 1 0 0 1 reduced time steps since last print

total reactor power = 9.000 kW inlet flow rate = 16.616 g/s maximum temperatures ic iz
 total heat transfer = -0.000 kW outlet flow rate = 16.610 g/s rod: 1519.13 at 1 1
 flow enthalpy rise = 0.018 kW total system mass = 17.280 g wall: 1232.65 at 1 1
 flow energy rise = 0.018 kW global mass error = 0.198D-13 g liquid: 1196.07 at 1 1

maximum relative changes over the time step maximum relative linearization errors
 in pressure: 0.429D-09 in pressure: 0.601D-09
 in mixture density: 0.591D-06 in mass/volume: 0.398D-12
 in mixture energy: 0.244D-05 in energy/volume: 0.999D-19

ic	iz	z(mm)	P(bar)	void	qual(%)	em	rom	T vap	T liq	T sat	vvz	viz	rov	rol	flow(g/s)
1	1	0.0	1.40204	0.0000	0.000	1076470.	820.83	821.94	821.94	1196.09	1.088	0.119	0.3697	820.83	16.616
1	2	50.0	1.40185	0.7318	0.137	1556336.	196.85	1196.07	1196.07	1196.07	4.951	0.491	0.3696	732.46	16.616
1	3	150.0	1.39975	0.0000	0.000	1077928.	820.56	823.10	823.10	1195.89	0.119	0.119	0.3691	820.56	16.610
1	4	200.0	1.40000	0.0000	0.000	1077928.	820.56	823.10	823.10	1195.92			0.3692	820.56	

INPUTS FOR BOILING-CONDENSATION TEST (Fig. 6.1c)

(ten cells)

```

1
boiling and condensation test
$intgin nc=1 nz=10 nr=1 narf=1 nx=1 nrzs=1 iss=1 ixfl=0 ibb=2 ihtf=1
ichnge=1 ishpr=11111 istrpr=1 nitmax=-2 ipfsol=10 noumax=0
  neq=4 ieqvax=0.0 numder=0 kfold=4 $
$realin epsn=0.10e0 grav=0.0 hdt=2.6e-3 pdr=1.15 hdr=20.0
radf=4.325e-3 delpr=1.0 delro=1.0 delem=1.0 errmax=0.5e-1 winlet=16.616e-3 $
$rodinp q0=9000.0 $
1          $ ncr
0          $ indent
1$ifcar
1$nrzf
1$nrmaf
3$mnrzf
26.47e-3   $ dx
22.92e-3   $ dy
0.12e0 10(0.10e0) 0.12e0 $ dz
10(0.0e0)   $ arx
10(0.0e0)   $ ary
11(169.8475e-6) $ arz
10(0.0e+0)   $ vol
5.263e-3    $ hedz
3.616e-3    $ wedz
1.6e5 10(1.4e+5) 1.4e+5   $ pressure
6(0.00) 6(0.0e0) $ alpha
800.00 5(1040.00) 6(1040.0) $ tfluid
11(0.118e0) $ velocity
5(1200.00) 5(1040.0) $twf
  5(1.0)   5(-1.0) $qz
1.0 $qt
1.0 $qr
1.0 $rn
1.625e-3 $drzf
$timdat tend=5.0e0 dtmin=-1.0e-6 dtmax=1.0e0 dtsp=20.0 dtlp=0.1e1 fredmx=20 $
$timdat tend=-1.0 $
0

```

INITIAL CONDITIONS FOR TEST 6.1c
(10 cells)

```

time step no =      0      real time = 0.000000 sec      time step size = 0.000000+00 sec      cpu time =      0.00 sec
number of newton iterations =      0      0 time step reductions due to error 0
number of inner iterations =      0      0      0      0 reduced time steps since last print

total reactor power =      9.000 kW      inlet flow rate =      16.557 g/s      maximum temperatures      ic      iz
total heat transfer =      0.000 kW      outlet flow rate =      15.426 g/s      rod:      0.00 at      0      0
flow enthalpy rise =      3.469 kW      total system mass =      130.731 g      wall:      0.00 at      0      0
flow energy rise =      3.469 kW      global mass error =      0.0000+00 g      liquid: 1040.00 at      1      1

```

```

maximum relative changes over the time step      maximum relative linearization errors
in pressure:      0.0000+00      in pressure:      0.0000+00
in mixture density: 0.0000+00      in mass/volume: 0.0000+00
in mixture energy: 0.0000+00      in energy/volume: 0.0000+00

```

ic	iz	z(mm)	P(bar)	void	qual(%)	em	rom	T vap	T liq	T sat	vvz	viz	rov	rol	flow(g/s)
1	1	0.0	1.60000	0.0000	0.000	1048857.	826.11	800.00	800.00	1211.97	0.118	0.118	0.5768	826.11	16.557
1	2	50.0	1.40000	0.0000	0.000	1350604.	769.70	1040.00	1040.00	1195.92	0.118	0.118	0.4116	769.70	15.426
1	3	150.0	1.40000	0.0000	0.000	1350604.	769.70	1040.00	1040.00	1195.92	0.118	0.118	0.4116	769.70	15.426
1	4	250.0	1.40000	0.0000	0.000	1350604.	769.70	1040.00	1040.00	1195.92	0.118	0.118	0.4116	769.70	15.426
1	5	350.0	1.40000	0.0000	0.000	1350604.	769.70	1040.00	1040.00	1195.92	0.118	0.118	0.4116	769.70	15.426
1	6	450.0	1.40000	0.0000	0.000	1350604.	769.70	1040.00	1040.00	1195.92	0.118	0.118	0.4116	769.70	15.426
1	7	550.0	1.40000	0.0000	0.000	1350604.	769.70	1040.00	1040.00	1195.92	0.118	0.118	0.4116	769.70	15.426
1	8	650.0	1.40000	0.0000	0.000	1350604.	769.70	1040.00	1040.00	1195.92	0.118	0.118	0.4116	769.70	15.426
1	9	750.0	1.40000	0.0000	0.000	1350604.	769.70	1040.00	1040.00	1195.92	0.118	0.118	0.4116	769.70	15.426
1	10	850.0	1.40000	0.0000	0.000	1350604.	769.70	1040.00	1040.00	1195.92	0.118	0.118	0.4116	769.70	15.426
1	11	950.0	1.40000	0.0000	0.000	1350604.	769.70	1040.00	1040.00	1195.92	0.118	0.118	0.4116	769.70	15.426
1	12	1000.0	1.40000	0.0000	0.000	1350604.	769.70	1040.00	1040.00	1195.92			0.4116	769.70	

FINAL STEADY-STATE FOR TEST 6.1c
(10 cells)

```

time step no = 5410      real time = 25.001880 sec      time step size = 0.432200-02 sec      cpu time = 967.13 sec
number of newton iterations = 2      0 time step reductions due to error 0
number of inner iterations = 1 0 0      0 reduced time steps since last print

total reactor power = 9.000 kW      inlet flow rate = 16.616 g/s      maximum temperatures ic iz
total heat transfer = -0.000 kW      outlet flow rate = 16.616 g/s      rod: 1268.99 at 1 2
flow enthalpy rise = -0.004 kW      total system mass = 64.796 g      wall: 1211.69 at 1 2
flow energy rise = -0.004 kW      global mass error = 0.1810-14 g      liquid: 1197.38 at 1 2
    
```

```

maximum relative changes over the time step      maximum relative linearization errors
in pressure: 0.1000-09      in pressure: 0.1540-16
in mixture density: 0.1000-09      in mass/volume: 0.2700-15
in mixture energy: 0.1000-09      in energy/volume: 0.1660-18
    
```

ic	iz	z(mm)	P(bar)	void	qual(%)	em	rom	T vap	T liq	T sat	vvz	viz	rov	rol	flow(g/s)
1	1	0.0	1.41769	0.0000	0.000	1349212.	769.98	1038.90	1038.90	1197.41	0.127	0.127	0.3735	769.98	16.616
1	2	50.0	1.41758	0.0000	0.000	1457536.	749.70	1124.17	1124.17	1197.40	0.536	0.130	0.3735	749.70	16.616
1	3	150.0	1.41742	0.3100	0.023	1552777.	505.30	1197.38	1197.38	1197.38	2.401	0.193	0.3734	732.16	16.616
1	4	250.0	1.41702	0.7179	0.130	1557636.	206.84	1197.35	1197.35	1197.35	8.987	0.462	0.3733	732.17	16.616
1	5	350.0	1.41480	0.8044	0.209	1561045.	143.49	1197.16	1197.16	1197.16	15.149	0.651	0.3728	732.21	16.616
1	6	450.0	1.41072	0.8630	0.319	1565649.	100.63	1196.82	1196.82	1196.82	20.824	0.909	0.3718	732.29	16.616
1	7	550.0	1.40460	0.8331	0.252	1561891.	122.56	1196.30	1196.30	1196.30	14.792	0.763	0.3703	732.41	16.616
1	8	650.0	1.40153	0.7959	0.196	1559010.	149.80	1196.05	1196.05	1196.05	8.292	0.638	0.3696	732.47	16.616
1	9	750.0	1.39999	0.5676	0.066	1552858.	316.92	1195.91	1195.91	1195.91	1.484	0.308	0.3692	732.50	16.616
1	10	850.0	1.40008	0.0000	0.000	1457309.	749.72	1123.99	1123.99	1195.92	0.130	0.130	0.3692	749.72	16.616
1	11	950.0	1.40013	0.0000	0.000	1348984.	770.00	1038.72	1038.72	1195.93	0.127	0.127	0.3692	770.00	16.616
1	12	1000.0	1.40000	0.0000	0.000	1348984.	770.00	1038.72	1038.72	1195.92			0.3692	770.00	

INPUTS FOR BOILING TEST (Fig. 6.1e)

```

1
boiling test
$intgin nc=1 nz=2 nr=1 narf=1 nx=1 nrzs=1 iss=1 ixfl=0 ibb=2 ihtf=1
1chnge=1 ishpr=11111 istrpr=1 nitmax=-2 ipfsol=10 noumax=0
    neq=4 feqvax=0.0 numder=0 kfold=4 $
$realin epsn=0.10e0 grav=0.0 hdt=2.6e-3 pdr=1.15 hdr=20.0
radf=4.325e-3 delpr=1.0 delro=1.0 delem=1.0 errmax=0.5e-1 winlet=16.616e-3 $
$rodinp q0=9000.0 $
1          $ ncr
0          $ indent
1$ifcar
1$nrzf
1$nrmaf
3$mnrzf
26.47e-3   $ dx
22.92e-3   $ dy
0.12e0 0.10e0 0.1e0 0.12e0 $ dz
2(0.0e0)   $ arx
2(0.0e0)   $ ary
3(169.8475e-6) $ arz
2(0.0e+0)   $ vol
5.263e-3   $ hedz
3.616e-3   $ wedz
1.6e5 2(1.4e+5) 1.4e+5   $ pressure
2(0.00) 2(0.0e0) $ alpha
800.00 1(1040.00) 2(1040.0) $ tfluid
3(0.118e0) $ velocity
1(1200.00) 1(1040.0) $twf
    1.0 0.0 $qz
1.0 $qt
1.0 $qr
1.0 $rn
1.625e-3 $drzf
$timdat tend=10.0e0 dtmin=-1.0e-6 dtmax=1.0e0 dtsp=20.0 dtlp=0.1e1 iredmx=20 $
$timdat tend=-1.0 $
0

```

INITIAL CONDITIONS FOR BOILING TEST 6.1 e

F-14

time step no = 0 real time = 0.000000 sec time step size = 0.000000+00 sec cpu time = 0.00 sec
 number of newton iterations = 0 0 time step reductions due to error 0
 number of inner iterations = 0 0 0 0 reduced time steps since last print

total reactor power = 9.000 kW inlet flow rate = 16.557 g/s maximum temperatures ic iz
 total heat transfer = 9.000 kW outlet flow rate = 15.426 g/s rod: 0.00 at 0 0
 flow enthalpy rise = 3.489 kW total system mass = 26.146 g wall: 0.00 at 0 0
 flow energy rise = 3.489 kW global mass error = 0.0000+00 g liquid: 1040.00 at 1 1

maximum relative changes over the time step
 in pressure: 0.0000+00
 in mixture density: 0.0000+00
 in mixture energy: 0.0000+00

maximum relative linearization errors
 in pressure: 0.0000+00
 in mass/volume: 0.0000+00
 in energy/volume: 0.0000+00

ic	iz	z(mm)	P(bar)	void	qual(%)	em	rom	T vap	T liq	T sat	vvz	viz	rov	rol	flow(g/s)
1	1	0.0	1.60000	0.0000	0.000	1048857.	826.11	800.00	800.00	1211.97	0.118	0.118	0.5768	826.11	16 557
1	2	50.0	1.40000	0.0000	0.000	1350604.	769.70	1040.00	1040.00	1195.92	0.118	0.118	0.4116	769.70	15 426
1	3	150.0	1.40000	0.0000	0.000	1350604.	769.70	1040.00	1040.00	1195.92	0.118	0.118	0.4116	769.70	15 426
1	4	200.0	1.40000	0.0000	0.000	1350604.	769.70	1040.00	1040.00	1195.92			0.4116	769.70	

FINAL STEADY-STATE FOR TEST 6.1e

time step no = 2467 real time = 5.001642 sec time step size = 0.17583D-02 sec cpu time = 137.94 sec
 number of newton iterations = 2 0 time step reductions due to error 0
 number of inner iterations = 1 0 0 0 reduced time steps since last print

total reactor power = 9.000 kW inlet flow rate = 16.616 g/s maximum temperatures ic iz
 total heat transfer = 9.000 kW outlet flow rate = 16.616 g/s rod: 1578.06 at 1 1
 flow enthalpy rise = 8.976 kW total system mass = 1.394 g wall: 1291.58 at 1 1
 flow energy rise = 8.287 kW global mass error = -0.209D-16 g liquid: 1199.68 at 1 1

maximum relative changes over the time step
 in pressure: 0.100D-09
 in mixture density: 0.100D-09
 in mixture energy: 0.100D-09

maximum relative linearization errors
 in pressure: 0.116D-12
 in mass/volume: 0.415D-16
 in energy/volume: 0.187D-18

ic	iz	z(mm)	P(bar)	void	qual(%)	em	ron	T vap	T liq	T sat	vvz	viz	rov	rol	flow(g/s)
1	1	0.0	1.45406	0.8482	0.291	1569069.	111.35	1200.43	1200.43	1200.43	23.754	0.812	0.3823	731.47	16.616
1	2	50.0	1.44494	0.9436	0.882	1594373.	41.59	1199.68	1199.68	1199.68	51.186	1.928	0.3801	731.64	16.616
1	3	150.0	1.41939	0.9452	0.873	1592084.	40.47	1197.55	1197.55	1197.55	52.076	1.980	0.3739	732.12	16.616
1	4	200.0	1.40000	0.9485	0.920	1592084.	38.07	1195.92	1195.92	1195.92			0.3692	732.50	

INPUT FOR BOILING TEST (6.1e)

(ten cells)

```
1
boiling test
$intgin nc=1 nz=10 nr=1 narf=1 nx=1 nrzs=1 iss=1 ixfl=0 ibb=2 ihtf=1
ichnge=1 ishpr=11111 istrpr=1 nitmax=-2 ipfsol=34 noumax=0
neq=4 ieqvax=0.0 numder=0 kfold=4 $
$realin epsn=0.10e0 grav=0.0 hdt=2.6e-3 pdr=1.15 HDR=20.0
radf=4.325e-3 delpr=1.0 delro=1.0 delem=1.0 errmax=0.5e-1 winlet=16.616e-3 $
$rodinp q0=15000.0 $
1 $ ncr
0 $ indent
1$ifcar
1$nrzf
1$nrmaf
3$mnrf
26.47e-3 $ dx
22.92e-3 $ dy
0.12e0 10(0.1e0) 0.12e0 $ dz
10(0.0e0) $ arx
10(0.0e0) $ ary
11(169.8475e-6) $ arz
10(0.0e+0) $ vol
5.263e-3 $ hedz
3.616e-3 $ wedz
1.50e5 10(1.4e+5) 1.4e+5 $ pressure
6(0.00) 6(0.0e0) $ alpha
800.0 1(800.0) 10(800.0) $ tfluid
11(0.118e0) $ velocity
5(800.00) 5(800.0) $ twf
5(1.0) 5(0.0) $ qz
1.0 $qt
1.0 $qr
1.0 $rn
1.625e-3 $drzf
$timdat tend=50.0e0 dtmin=-1.0e-6 dtmax=1.0e0 dtsp=20.0 dtip=0.1e1 iredmx=20 $
$timdat tend=-1.0 $
0
```

F-16

INITIAL CONDITIONS (6.1e)

```

time step no = 0      real time = 0.000000 sec      time step size = 0.000000+00 sec      cpu time = 0.00 sec
number of newton iterations = 0      0 time step reductions due to error 0
number of inner iterations = 0 0 0      0 reduced time steps since last print
    
```

```

total reactor power = 15.000 kW      inlet flow rate = 16.555 g/s      maximum temperatures ic iz
total heat transfer = 15.000 kW      outlet flow rate = 16.553 g/s      rod: 0.00 at 0 0
flow enthalpy rise = -0.002 kW      total system mass = 140.279 g      wall: 0.00 at 0 0
flow energy rise = -0.002 kW      global mass error = 0.0000+00 g      liquid: 800.00 at 1 1
    
```

```

maximum relative changes over the time step
in pressure: 0.0000+00
in mixture density: 0.0000+00
in mixture energy: 0.0000+00
    
```

```

maximum relative linearization errors
in pressure: 0.0000+00
in mass/volume: 0.0000+00
in energy/volume: 0.0000+00
    
```

ic	iz	z(mm)	P(bar)	void	qual(%)	em	rom	T vap	T liq	T sat	vvz	viz	rov	rol	flow(g/s)
1	1	0.0	1.50000	0.0000	0.000	1048857.	826.01	800.00	800.00	1204.16	0.118	0.118	0.5408	826.01	16.555
1	2	50.0	1.40000	0.0000	0.000	1048857.	825.91	800.00	800.00	1195.92	0.118	0.118	0.5047	825.91	16.553
1	3	150.0	1.40000	0.0000	0.000	1048857.	825.91	800.00	800.00	1195.92	0.118	0.118	0.5047	825.91	16.553
1	4	250.0	1.40000	0.0000	0.000	1048857.	825.91	800.00	800.00	1195.92	0.118	0.118	0.5047	825.91	16.553
1	5	350.0	1.40000	0.0000	0.000	1048857.	825.91	800.00	800.00	1195.92	0.118	0.118	0.5047	825.91	16.553
1	6	450.0	1.40000	0.0000	0.000	1048857.	825.91	800.00	800.00	1195.92	0.118	0.118	0.5047	825.91	16.553
1	7	550.0	1.40000	0.0000	0.000	1048857.	825.91	800.00	800.00	1195.92	0.118	0.118	0.5047	825.91	16.553
1	8	650.0	1.40000	0.0000	0.000	1048857.	825.91	800.00	800.00	1195.92	0.118	0.118	0.5047	825.91	16.553
1	9	750.0	1.40000	0.0000	0.000	1048857.	825.91	800.00	800.00	1195.92	0.118	0.118	0.5047	825.91	16.553
1	10	850.0	1.40000	0.0000	0.000	1048857.	825.91	800.00	800.00	1195.92	0.118	0.118	0.5047	825.91	16.553
1	11	950.0	1.40000	0.0000	0.000	1048857.	825.91	800.00	800.00	1195.92	0.118	0.118	0.5047	825.91	16.553
1	12	1000.0	1.40000	0.0000	0.000	1048857.	825.91	800.00	800.00	1195.92			0.5047	825.91	

Initial conditions for
boiling test. (with gravity)

```

time step no =      0      real time =  0.000000 sec      time step size = 0.000000+00 sec      cpu time =      0.00 sec
number of newton iterations =  0      0 time step reductions due to error  0
number of inner iterations =  0  0  0      0 reduced time steps since last print

```

```

total reactor power =      10.000 kW      inlet flow rate =      16.555 g/s      maximum temperatures      lc      iz
total heat transfer =      10.000 kW      outlet flow rate =      16.553 g/s      rod:      0.00 at      0  0
flow enthalpy rise =      -0.002 kW      total system mass =      140.279 g      wall:      0.00 at      0  0
flow energy rise =      -0.002 kW      global mass error =  0.0000+00 g      liquid: 800.00 at      1  1

```

```

maximum relative changes over the time step
in pressure:      0.0000+00
in mixture density: 0.0000+00
in mixture energy: 0.0000+00

```

```

maximum relative linearization errors
in pressure:      0.0000+00
in mass/volume:  0.0000+00
in energy/volume: 0.0000+00

```

F-19

lc	iz	z(mm)	P(bar)	void	qual(%)	em	rom	T vap	T liq	T sat	vvz	vlz	rov	rol	flow(g/s)
1	1	0.0	1.50000	0.0000	0.000	1048857.	826.01	800.00	800.00	1204.16	0.118	0.118	0.5408	826.01	16.555
1	2	50.0	1.40000	0.0000	0.000	1048857.	825.91	800.00	800.00	1195.92	0.118	0.118	0.5047	825.91	16.553
1	3	150.0	1.40000	0.0000	0.000	1048857.	825.91	800.00	800.00	1195.92	0.118	0.118	0.5047	825.91	16.553
1	4	250.0	1.40000	0.0000	0.000	1048857.	825.91	800.00	800.00	1195.92	0.118	0.118	0.5047	825.91	16.553
1	5	350.0	1.40000	0.0000	0.000	1048857.	825.91	800.00	800.00	1195.92	0.118	0.118	0.5047	825.91	16.553
1	6	450.0	1.40000	0.0000	0.000	1048857.	825.91	800.00	800.00	1195.92	0.118	0.118	0.5047	825.91	16.553
1	7	550.0	1.40000	0.0000	0.000	1048857.	825.91	800.00	800.00	1195.92	0.118	0.118	0.5047	825.91	16.553
1	8	650.0	1.40000	0.0000	0.000	1048857.	825.91	800.00	800.00	1195.92	0.118	0.118	0.5047	825.91	16.553
1	9	750.0	1.40000	0.0000	0.000	1048857.	825.91	800.00	800.00	1195.92	0.118	0.118	0.5047	825.91	16.553
1	10	850.0	1.40000	0.0000	0.000	1048857.	825.91	800.00	800.00	1195.92	0.118	0.118	0.5047	825.91	16.553
1	11	950.0	1.40000	0.0000	0.000	1048857.	825.91	800.00	800.00	1195.92	0.118	0.118	0.5047	825.91	16.553
1	12	1000.0	1.40000	0.0000	0.000	1048857.	825.91	800.00	800.00	1195.92			0.5047	825.91	

Steady state of boiling test with gravity (6.1e): 10 cells

time step no = 4222 real time = 30.000652 sec time step size = 0.610990-02 sec cpu time = 769.65 sec
 number of newton iterations = 2 0 time step reductions due to error 0
 number of inner iterations = 1 0 0 0 reduced time steps since last print

total reactor power = 10.000 kW inlet flow rate = 16.616 g/s maximum temperatures ic iz
 total heat transfer = 10.000 kW outlet flow rate = 16.616 g/s rod: 1275.73 at 1 4
 flow enthalpy rise = 9.995 kW total system mass = 60.349 g wall: 1212.06 at 1 4
 flow energy rise = 9.717 kW global mass error = 0.1520-13 g liquid: 1198.35 at 1 4

maximum relative changes over the time step
 in pressure: 0.100D-09
 in mixture density: 0.100D-09
 in mixture energy: 0.100D-09

maximum relative linearization errors
 in pressure: 0.119D-12
 in mass/volume: 0.140D-14
 in energy/volume: 0.130D-15

F-20

ic	iz	z(mm)	P(bar)	void	qual(%)	em	rom	T vap	T liq	T sat	vvz	vlz	rov	rol	flow(g/s)
1	1	0.0	1.45830	0.0000	0.000	1168701.	803.78	895.38	895.38	1200.78	0.122	0.122	0.3833	803.78	16.616
1	2	50.0	1.44961	0.0000	0.000	1289062.	781.28	991.20	991.20	1200.06	0.125	0.125	0.3812	781.28	16.616
1	3	150.0	1.44194	0.0000	0.000	1409422.	758.72	1086.41	1086.41	1199.43	0.129	0.129	0.3794	758.72	16.616
1	4	250.0	1.43449	0.0000	0.000	1529782.	736.25	1180.42	1180.42	1198.81	5.986	0.133	0.3776	736.25	16.616
1	5	350.0	1.42898	0.5384	0.060	1555733.	338.05	1198.35	1198.35	1198.35	9.427	0.284	0.3762	731.94	16.616
1	6	450.0	1.42548	0.7809	0.182	1560984.	160.70	1198.06	1198.06	1198.06	14.611	0.583	0.3754	732.01	16.616
1	7	550.0	1.42084	0.7866	0.188	1560742.	156.52	1197.67	1197.67	1197.67	14.580	0.599	0.3743	732.09	16.616
1	8	650.0	1.41677	0.7877	0.189	1560334.	155.70	1197.33	1197.33	1197.33	14.625	0.602	0.3733	732.17	16.616
1	9	750.0	1.41269	0.7882	0.189	1559888.	155.38	1196.99	1196.99	1196.99	14.685	0.603	0.3723	732.25	16.616
1	10	850.0	1.40860	0.7894	0.190	1559479.	154.52	1196.64	1196.64	1196.64	14.730	0.606	0.3713	732.33	16.616
1	11	950.0	1.40449	0.7874	0.187	1558900.	156.00	1196.30	1196.30	1196.30	14.837	0.601	0.3703	732.41	16.616
1	12	1000.0	1.40000	0.7971	0.198	1558900.	148.91	1195.92	1195.92	1195.92			0.3692	732.50	

Input for condensation-boiling test

```
1
boiling and condensation test
$intgin nc=1 nz=10 nr=1 narf=1 nx=1 nrzs=1 iss=1 ixfl=0 ibb=0 ihtf=1
ichnge=1 ishpr=11111 istrpr=1 nitmax=-2 ipfsol=34 noumax=0
      neq=4 leqvax=0.0 numder=0 kfold=4 $
$realin epsn=0.10e0 grav=0.0 hdt=2.6e-3 pdr=1.15 hdr=20.0
radf=4.325e-3 delpr=1.0 delro=1.0 delem=1.0 errmax=0.5e-1 winlet=16.616e-3 $
$rodinp q0=3000.0 $
1          $ ncr
0          $ indent
1$ifcar
1$nrzf
1$nrmaf
3$mnrzf
26.47e-3    $ dx
22.92e-3    $ dy
0.12e0 10(0.1e0) 0.12e0 $ dz
10(0.0e0)    $ arx
10(0.0e0)    $ ary
11(169.8475e-6) $ arz
10(0.0e+0)    $ vol
5.263e-3    $ hedz
3.616e-3    $ wedz
1.5e5 10(1.4e+5) 1.4e+5    $ pressure
6(0.50) 6(0.5e0) $ alpha
1204.16 1(1195.92) 10(1195.92) $ tfluid
11(0.118e0) $ velocity
5(800.00) 5(800.0) $ twf
5(-1.0) 5(1.0) $ qz
1.0 $qt
1.0 $qr
1.0 $rn
1.625e-3 $drzf
$timdat tend=5.0e0 dtmin=-1.0e-6 dtmax=1.0e0 dtsp=20.0 dtlp=0.1e1 iredmx=20 $
$timdat tend=-1.0 $
0
```

Initial conditions for condensation-boiling test

time step no = 0 real time = 0.000000 sec time step size = 0.000000D+00 sec cpu time = 0.00 sec
 number of newton iterations = 0 0 time step reductions due to error 0
 number of inner iterations = 0 0 0 0 reduced time steps since last print

total reactor power = 3.000 kW inlet flow rate = 7.325 g/s maximum temperatures ic iz
 total heat transfer = 0.000 kW outlet flow rate = 7.344 g/s rod: 0.00 at 0 0
 flow enthalpy rise = -0.051 kW total system mass = 62.238 g wall: 0.00 at 0 0
 flow energy rise = -0.051 kW global mass error = 0.0000D+00 g liquid: 1195.92 at 1 1

maximum relative changes over the time step

in pressure: 0.000D+00
 in mixture density: 0.000D+00
 in mixture energy: 0.000D+00

maximum relative linearization errors

in pressure: 0.000D+00
 in mass/volume: 0.000D+00
 in energy/volume: 0.000D+00

F-22

ic	iz	z(mm)	P(bar)	void	qual(%)	em	rom	T vap	T liq	T sat	vvz	viz	rov	rol	flow(g/s)
1	1	0.0	1.50000	0.5000	0.054	1562990.	365.50	1204.16	1204.16	1204.16	0.118	0.118	0.3934	730.61	7.325
1	2	50.0	1.40000	0.5000	0.050	1552141.	366.43	1195.92	1195.92	1195.92	0.118	0.118	0.3692	732.49	7.344
1	3	150.0	1.40000	0.5000	0.050	1552141.	366.43	1195.92	1195.92	1195.92	0.118	0.118	0.3692	732.49	7.344
1	4	250.0	1.40000	0.5000	0.050	1552141.	366.43	1195.92	1195.92	1195.92	0.118	0.118	0.3692	732.49	7.344
1	5	350.0	1.40000	0.5000	0.050	1552141.	366.43	1195.92	1195.92	1195.92	0.118	0.118	0.3692	732.49	7.344
1	6	450.0	1.40000	0.5000	0.050	1552141.	366.43	1195.92	1195.92	1195.92	0.118	0.118	0.3692	732.49	7.344
1	7	550.0	1.40000	0.5000	0.050	1552141.	366.43	1195.92	1195.92	1195.92	0.118	0.118	0.3692	732.49	7.344
1	8	650.0	1.40000	0.5000	0.050	1552141.	366.43	1195.92	1195.92	1195.92	0.118	0.118	0.3692	732.49	7.344
1	9	750.0	1.40000	0.5000	0.050	1552141.	366.43	1195.92	1195.92	1195.92	0.118	0.118	0.3692	732.49	7.344
1	10	850.0	1.40000	0.5000	0.050	1552141.	366.43	1195.92	1195.92	1195.92	0.118	0.118	0.3692	732.49	7.344
1	11	950.0	1.40000	0.5000	0.050	1552141.	366.43	1195.92	1195.92	1195.92	0.118	0.118	0.3692	732.49	7.344
1	12	1000.0	1.40000	0.5000	0.050	1552141.	366.43	1195.92	1195.92	1195.92			0.3692	732.49	

Final steady-state for condensation-boiling test

time step no = 1009 real time = 5.002808 sec time step size = 0.48844D-02 sec cpu time = 186.27 sec
 number of newton iterations = 2 0 time step reductions due to error 0
 number of inner iterations = 1 0 0 0 reduced time steps since last print

total reactor power = 3.000 kW inlet flow rate = 115.855 g/s maximum temperatures ic iz
 total heat transfer = 0.000 kW outlet flow rate = 115.855 g/s rod: 1226.94 at 1 6
 flow enthalpy rise = -0.009 kW total system mass = 79.584 g wall: 1207.84 at 1 6
 flow energy rise = -0.084 kW global mass error = -0.139D-13 g liquid: 1203.11 at 1 1

maximum relative changes over the time step
 in pressure: 0.100D-09
 in mixture density: 0.100D-09
 in mixture energy: 0.100D-09

maximum relative linearization errors
 in pressure: 0.638D-15
 in mass/volume: 0.138D-14
 in energy/volume: 0.724D-19

ic	iz	z(mm)	P(bar)	void	qual(%)	em	rom	T vap	T liq	T sat	vvz	viz	rov	rol	flow(g/s)
1	1	0.0	1.50000	0.5003	0.054	1562990.	365.30	1204.16	1204.16	1204.16	14.670	1.860	0.3934	730.61	115.855
1	2	50.0	1.48700	0.4703	0.047	1561332.	387.28	1203.11	1203.11	1203.11	12.879	1.756	0.3903	730.85	115.855
1	3	150.0	1.47728	0.4261	0.039	1559941.	419.73	1202.32	1202.32	1202.32	10.859	1.621	0.3879	731.03	115.855
1	4	250.0	1.46936	0.3615	0.030	1558668.	466.99	1201.68	1201.68	1201.68	8.601	1.459	0.3860	731.18	115.855
1	5	350.0	1.46336	0.2771	0.020	1557585.	528.75	1201.19	1201.19	1201.19	5.426	1.289	0.3846	731.29	115.855
1	6	450.0	1.45926	0.0000	0.000	1555702.	731.46	1200.45	1200.45	1200.85	2.819	0.933	0.3836	731.46	115.855
1	7	550.0	1.45833	0.2212	0.015	1556808.	569.72	1200.78	1200.78	1200.78	7.683	1.196	0.3834	731.39	115.855
1	8	650.0	1.45154	0.3530	0.028	1556709.	473.40	1200.22	1200.22	1200.22	10.831	1.438	0.3817	731.51	115.855
1	9	750.0	1.44260	0.4402	0.041	1556318.	409.78	1199.48	1199.48	1199.48	13.765	1.660	0.3795	731.68	115.855
1	10	850.0	1.43133	0.5058	0.053	1555652.	361.90	1198.55	1198.55	1198.55	16.658	1.877	0.3768	731.89	115.855
1	11	950.0	1.41736	0.5405	0.060	1554474.	336.60	1197.38	1197.38	1197.38	20.269	2.016	0.3734	732.16	115.855
1	12	1000.0	1.40000	0.6679	0.101	1554474.	243.48	1195.92	1195.92	1195.92			0.3692	732.50	

Initial conditions for loop test (700 W)

TIME STEP NO = 0 REAL TIME = 0.000000 SEC TIME STEP SIZE = 0.000000+00 SEC CPU TIME = 0.00 SEC
 NUMBER OF NEWTON ITERATIONS = 0 0 TIME STEP REDUCTIONS DUE TO ERROR 0
 NUMBER OF INNER ITERATIONS = 0 0 0 0 REDUCED TIME STEPS SINCE LAST PRINT

TOTAL REACTOR POWER = 0.700 KW INLET FLOW RATE = 0.845 G/S MAXIMUM TEMPERATURES IC IZ
 TOTAL HEAT TRANSFER = 0.700 KW OUTLET FLOW RATE = 0.845 G/S ROD: 0.00 AT 0 0
 FLOW ENTHALPY RISE = 0.000 KW TOTAL SYSTEM MASS = 26.483 G WALL: 0.00 AT 0 0
 FLOW ENERGY RISE = 0.000 KW GLOBAL MASS ERROR = 0.0000+00 G LIQUID: 693.15 AT 1 1

MAXIMUM RELATIVE CHANGES OVER THE TIME STEP
 IN PRESSURE: 0.0000+00
 IN MIXTURE DENSITY: 0.0000+00
 IN MIXTURE ENERGY: 0.0000+00

MAXIMUM RELATIVE LINEARIZATION ERRORS
 IN PRESSURE: 0.0000+00
 IN MASS/VOLUME: 0.0000+00
 IN ENERGY/VOLUME: 0.0000+00

IC	IZ	Z(MM)	P(BAR)	VOID	QUAL(%)	EM	ROM	T VAP	T LIQ	T SAT	VVZ	VLZ	ROV	ROL	FLOW(G/S)
1	1	0.0	1.01325	0.0000	0.000	913556.	850.14	693.15	693.15	1158.78	0.120	0.120	0.4107	850.14	0.845
1	2	308.7	1.01325	0.0000	0.000	913556.	850.14	693.15	693.15	1158.78	0.120	0.120	0.4107	850.14	0.845
1	3	846.2	1.01325	0.0000	0.000	913556.	850.14	693.15	693.15	1158.78	0.120	0.120	0.4107	850.14	0.845
1	4	1383.7	1.01325	0.0000	0.000	913556.	850.14	693.15	693.15	1158.78	0.120	0.120	0.4107	850.14	0.845
1	5	1921.2	1.01325	0.0000	0.000	913556.	850.14	693.15	693.15	1158.78	0.120	0.120	0.4107	850.14	0.845
1	6	2458.7	1.01325	0.0000	0.000	913556.	850.14	693.15	693.15	1158.78	0.120	0.120	0.4107	850.14	0.845
1	7	2967.5	1.01325	0.0000	0.000	913556.	850.14	693.15	693.15	1158.78	0.120	0.120	0.4107	850.14	0.845
1	8	3367.5	1.01325	0.0000	0.000	913556.	850.14	693.15	693.15	1158.78	0.120	0.120	0.4107	850.14	0.845
1	9	3717.5	1.01325	0.0000	0.000	913556.	850.14	693.15	693.15	1158.78	0.120	0.120	0.4107	850.14	0.845
1	10	4017.5	1.01325	0.0000	0.000	913556.	850.14	693.15	693.15	1158.78	0.120	0.120	0.4107	850.14	0.845
1	11	4167.5	1.01325	0.0000	0.000	913556.	850.14	693.15	693.15	1158.78			0.4107	850.14	

Final steady-state for loop test (700 W)

```

TIME STEP NO = 7164          REAL TIME = 50.000788 SEC          TIME STEP SIZE = 0.628990-02 SEC          CPU TIME = 1388.52 SEC
NUMBER OF NEWTON ITERATIONS = 2          O TIME STEP REDUCTIONS DUE TO ERROR 0
NUMBER OF INNER ITERATIONS = 1 0 0          O REDUCED TIME STEPS SINCE LAST PRINT

TOTAL REACTOR POWER = 0.700 KW          INLET FLOW RATE = 0.845 G/S          MAXIMUM TEMPERATURES IC IZ
TOTAL HEAT TRANSFER = 0.700 KW          OUTLET FLOW RATE = 0.845 G/S          ROD: 1165.16 AT 1 8
FLOW ENTHALPY RISE = 0.700 KW          TOTAL SYSTEM MASS = 22.021 G          WALL: 1161.97 AT 1 8
FLOW ENERGY RISE = 0.685 KW          GLOBAL MASS ERROR = 0.417D-12 G          LIQUID: 1161.56 AT 1 8
    
```

MAXIMUM RELATIVE CHANGES OVER THE TIME STEP

```

IN PRESSURE: 0.369D-08
IN MIXTURE DENSITY: 0.113D-06
IN MIXTURE ENERGY: 0.142D-06
    
```

MAXIMUM RELATIVE LINEARIZATION ERRORS

```

IN PRESSURE: 0.355D-08
IN MASS/VOLUME: 0.105D-11
IN ENERGY/VOLUME: 0.856D-18
    
```

IC	IZ	Z(MM)	P(BAR)	VOID	QUAL(%)	EM	ROM	T VAP	T LIQ	T SAT	VVZ	VLZ	ROV	ROL	FLOW(G/S)
1	1	0.0	0.98732	0.0000	0.000	913556.	850.12	693.15	693.15	1155.91	0.120	0.120	0.2674	850.12	0.845
1	2	308.7	0.96243	0.0000	0.000	1128239.	810.81	863.14	863.14	1153.09	0.126	0.126	0.2611	810.81	0.845
1	3	846.2	0.96175	0.0000	0.000	1128239.	810.81	863.14	863.14	1153.01	0.126	0.126	0.2609	810.81	0.845
1	4	1383.7	1.00379	0.0000	0.000	1128203.	810.86	863.11	863.11	1157.74	0.126	0.126	0.2715	810.86	0.845
1	5	1921.2	1.04584	0.0000	0.000	1128110.	810.91	863.04	863.04	1162.31	0.126	0.126	0.2820	810.91	0.845
1	6	2458.7	1.08901	0.0000	0.000	913569.	850.21	693.16	693.16	1166.86	0.120	0.120	0.2927	850.21	0.845
1	7	2967.5	1.08823	0.0000	0.000	913569.	850.21	693.16	693.16	1166.78	0.120	0.120	0.2925	850.21	0.845
1	8	3367.5	1.05615	0.0000	0.000	1386908.	762.55	1068.68	1068.68	1163.41	7.382	0.134	0.2846	762.55	0.845
1	9	3717.5	1.03885	0.8323	0.187	1513989.	124.42	1161.56	1161.56	1161.56	21.060	0.782	0.2802	740.38	0.845
1	10	4017.5	1.02142	0.8376	0.192	1511745.	120.56	1159.67	1159.67	1159.67	21.463	0.806	0.2759	740.81	0.845
1	11	4167.5	1.01325	0.8548	0.217	1511745.	107.84	1158.78	1158.78	1158.78			0.2738	741.02	

Initial conditions for loop test (600 W)

```

TIME STEP NO =      0      REAL TIME =  0.000000 SEC      TIME STEP SIZE = 0.000000+00 SEC      CPU TIME =      0.00 SEC
NUMBER OF NEWTON ITERATIONS =  0      O TIME STEP REDUCTIONS DUE TO ERROR  0
NUMBER OF INNER ITERATIONS =  0  0  0      O REDUCED TIME STEPS SINCE LAST PRINT

TOTAL REACTOR POWER =      0.600 KW      INLET FLOW RATE =      0.845 G/S      MAXIMUM TEMPERATURES  IC  IZ
TOTAL HEAT TRANSFER =      0.600 KW      OUTLET FLOW RATE =      0.845 G/S      ROD:      0.00 AT  0  0
FLOW ENTHALPY RISE =      0.000 KW      TOTAL SYSTEM MASS =      26.483 G      WALL:      0.00 AT  0  0
FLOW ENERGY RISE =      0.000 KW      GLOBAL MASS ERROR =  0.0000+00 G      LIQUID:  693.15 AT  1  1
    
```

MAXIMUM RELATIVE CHANGES OVER THE TIME STEP

```

IN PRESSURE:      0.0000+00
IN MIXTURE DENSITY: 0.0000+00
IN MIXTURE ENERGY: 0.0000+00
    
```

MAXIMUM RELATIVE LINEARIZATION ERRORS

```

IN PRESSURE:      0.0000+00
IN MASS/VOLUME:  0.0000+00
IN ENERGY/VOLUME: 0.0000+00
    
```

IC	IZ	Z(MM)	P(BAR)	VOID	QUAL(%)	EM	ROM	T VAP	T LIQ	T SAT	VVZ	VLZ	ROV	ROL	FLOW(G/S)
1	1	0.0	1.01325	0.0000	0.000	913556.	850.14	693.15	693.15	1158.78	0.120	0.120	0.4107	850.14	0.845
1	2	308.7	1.01325	0.0000	0.000	913556.	850.14	693.15	693.15	1158.78	0.120	0.120	0.4107	850.14	0.845
1	3	846.2	1.01325	0.0000	0.000	913556.	850.14	693.15	693.15	1158.78	0.120	0.120	0.4107	850.14	0.845
1	4	1383.7	1.01325	0.0000	0.000	913556.	850.14	693.15	693.15	1158.78	0.120	0.120	0.4107	850.14	0.845
1	5	1921.2	1.01325	0.0000	0.000	913556.	850.14	693.15	693.15	1158.78	0.120	0.120	0.4107	850.14	0.845
1	6	2458.7	1.01325	0.0000	0.000	913556.	850.14	693.15	693.15	1158.78	0.120	0.120	0.4107	850.14	0.845
1	7	2967.5	1.01325	0.0000	0.000	913556.	850.14	693.15	693.15	1158.78	0.120	0.120	0.4107	850.14	0.845
1	8	3367.5	1.01325	0.0000	0.000	913556.	850.14	693.15	693.15	1158.78	0.120	0.120	0.4107	850.14	0.845
1	9	3717.5	1.01325	0.0000	0.000	913556.	850.14	693.15	693.15	1158.78	0.120	0.120	0.4107	850.14	0.845
1	10	4017.5	1.01325	0.0000	0.000	913556.	850.14	693.15	693.15	1158.78	0.120	0.120	0.4107	850.14	0.845
1	11	4167.5	1.01325	0.0000	0.000	913556.	850.14	693.15	693.15	1158.78			0.4107	850.14	

Final steady-state for loop test (600 W)

TIME STEP NO = 4087 REAL TIME = 49.998278 SEC TIME STEP SIZE = 0.10646D-01 SEC CPU TIME = 800.08 SEC
 NUMBER OF NEWTON ITERATIONS = 2 O TIME STEP REDUCTIONS DUE TO ERROR 0
 NUMBER OF INNER ITERATIONS = 1 0 0 O REDUCED TIME STEPS SINCE LAST PRINT

TOTAL REACTOR POWER =	0.600 KW	INLET FLOW RATE =	0.845 G/S	MAXIMUM TEMPERATURES IC IZ
TOTAL HEAT TRANSFER =	0.600 KW	OUTLET FLOW RATE =	0.845 G/S	ROD: 1163.70 AT 1 8
FLOW ENTHALPY RISE =	0.600 KW	TOTAL SYSTEM MASS =	22.483 G	WALL: 1160.97 AT 1 8
FLOW ENERGY RISE =	0.592 KW	GLOBAL MASS ERROR =	0.230D-12 G	LIQUID: 1160.56 AT 1 8

MAXIMUM RELATIVE CHANGES OVER THE TIME STEP

IN PRESSURE: 0.177D-08
 IN MIXTURE DENSITY: 0.382D-06
 IN MIXTURE ENERGY: 0.234D-06

MAXIMUM RELATIVE LINEARIZATION ERRORS

IN PRESSURE: 0.169D-08
 IN MASS/VOLUME: 0.327D-12
 IN ENERGY/VOLUME: 0.533D-17

IC	IZ	Z(MM)	P(BAR)	VOID	QUAL(%)	EM	ROM	T VAP	T LIQ	T SAT	VVZ	VLZ	ROV	ROL	FLOW(G/S)
1	1	0.0	0.97967	0.0000	0.000	913556.	850.11	693.15	693.15	1155.05	0.120	0.120	0.2654	850.11	0.845
1	2	308.7	0.95478	0.0000	0.000	1128239.	810.80	863.14	863.14	1152.21	0.126	0.126	0.2592	810.80	0.845
1	3	846.2	0.95411	0.0000	0.000	1128239.	810.80	863.14	863.14	1152.13	0.126	0.126	0.2590	810.80	0.845
1	4	1383.7	0.99615	0.0000	0.000	1128203.	810.85	863.11	863.11	1156.89	0.126	0.126	0.2696	810.85	0.845
1	5	1921.2	1.03819	0.0000	0.000	1128113.	810.91	863.04	863.04	1161.49	0.126	0.126	0.2801	810.91	0.845
1	6	2458.7	1.08137	0.0000	0.000	913569.	850.21	693.16	693.16	1166.06	0.120	0.120	0.2908	850.21	0.845
1	7	2967.5	1.08058	0.0000	0.000	913569.	850.21	693.16	693.16	1165.98	0.120	0.120	0.2906	850.21	0.845
1	8	3367.5	1.04824	0.0000	0.000	1319288.	775.21	1015.19	1015.19	1162.57	7.084	0.132	0.2826	775.21	0.845
1	9	3717.5	1.02955	0.7101	0.092	1508356.	214.87	1160.56	1160.56	1160.56	12.572	0.464	0.2779	740.61	0.845
1	10	4017.5	1.01854	0.7200	0.095	1506975.	207.63	1159.36	1159.36	1159.36	12.681	0.480	0.2752	740.88	0.845
1	11	4167.5	1.01325	0.7519	0.112	1506975.	184.06	1158.78	1158.78	1158.78			0.2738	741.02	

F-27

Input for loop test (26 cells, 600 W)

```

2
SINGLE PHASE MEASUREMENT FOR SODIUM NATURAL CONVECTION
  IN A VERTICAL LOOP:ORNL/TM-7018
$INTGIN NC=1,NZ=26,NR=1,NARF=1,NX=1,NRZS=1,IHTF=1,
        IHTS=3,ISS=1,IXFL=0,IDUMP=1,IBB=2,
        ISTRPR=0,ISHPR=10111,NITMAX=-2,IPFSOL=34,
        NEQ=4,NUMBER=0,IHTRPR=0
$REALIN HDT=3.25E-3,PDR=1.2533,HDR=1.OE+10,DELPR=0.5,
        RNUSS=7.0,RADF=1.625E-4,WINLET=8.50E-4,GRAV=110.0
$RODINP QO=600.0 $
1$NCR
0$INDENT
1$IFCAR
1$NRZF
1$NRMAF
3$MNRZF
1$INX
7$MNRZS
4$NRMZS
4.07327E-3      $DX
4.07327E-3      $DY
1.OE-6 0.6175 4(0.4575) 6(0.6175) 4(0.4575) 0.6175 5(0.194)
5(0.3) 1.OE-6      $DZ
26(0.0)          $ARX
26(0.0)          $ARY
27(8.285E-6)     $ARZ
5.122162E-6 4(3.794962E-6) 6(5.12212E-6) 4(3.794962E-6)
5.122162E-6 5(1.60923E-6) 5(2.4885E-6)      $VOL
3.25E-3          $HEDZ
3.25E-3          $WEDZ
28(1.01325E+05) $P
28(0.0)          $ALP
28(693.15)       $TEMP
27(12.OE-2)      $VEL
-9.8 5(0.0) 5(9.8) 5(0.0) 11(-9.8)          $GRAV
26(693.15)       $TWF
16(0.0) 5(1.0) 5(0.0)          $QZ
1.0              $QT
1.0              $QR
1.0              $RN
1.625E-3         $DRZF
1.62929E-2       $PCX
2.03E-2          $DRZS
1.OE+6 14(0.0) 1.OE+6 10(0.0)          $HOUT
863.15 14(500.0) 693.15 10(500.0)       $TOUT
26(693.15)       $TWS
26(2.5E+6)       $HLSS
$1IMDAT TEND=200.0,DTMIN=1.OE-6,DTMAX=1.0,DTSP=20.0,DTLP=1.0,IREDMX=20 $
$TIMDAT TEND=-1.0$
0

```

F-28

Initial conditions for loop test (600 W)

```

TIME STEP NO =      0      REAL TIME =  0.000000 SEC      TIME STEP SIZE = 0.000000+00 SEC      CPU TIME =      0.00 SEC
NUMBER OF NEWTON ITERATIONS =      0      0 TIME STEP REDUCTIONS DUE TO ERROR  0
NUMBER OF INNER ITERATIONS =      0      0      0      0 REDUCED TIME STEPS SINCE LAST PRINT
TOTAL REACTOR POWER =      0.600 KW      INLET FLOW RATE =      0.845 G/S      MAXIMUM TEMPERATURES IC IZ
TOTAL HEAT TRANSFER =      0.600 KW      OUTLET FLOW RATE =      0.845 G/S      ROD:      0.00 AT      0      0
FLOW ENTHALPY RISE =      0.000 KW      TOTAL SYSTEM MASS =      78.065 G      WALL:      0.00 AT      0      0
FLOW ENERGY RISE =      0.000 KW      GLOBAL MASS ERROR =  0.0000+00 G      LIQUID:  693.15 AT      1      1
    
```

```

MAXIMUM RELATIVE CHANGES OVER THE TIME STEP
IN PRESSURE:      0.0000+00
IN MIXTURE DENSITY: 0.0000+00
IN MIXTURE ENERGY: 0.0000+00
    
```

```

MAXIMUM RELATIVE LINEARIZATION ERRORS
IN PRESSURE:      0.0000+00
IN MASS/VOLUME:   0.0000+00
IN ENERGY/VOLUME: 0.0000+00
    
```

IC	IZ	Z(MM)	P(BAR)	VOID	QUAL(%)	EM	ROM	T VAP	T LIQ	T SAT	VVZ	VLZ	ROV	ROL	FLOW(G/S)
1	1	0.0	1.01325	0.0000	0.000	913556.	850.14	693.15	693.15	1158.78	0.120	0.120	0.4107	850.14	0.845
1	2	308.7	1.01325	0.0000	0.000	913556.	850.14	693.15	693.15	1158.78	0.120	0.120	0.4107	850.14	0.845
1	3	846.2	1.01325	0.0000	0.000	913556.	850.14	693.15	693.15	1158.78	0.120	0.120	0.4107	850.14	0.845
1	4	1303.8	1.01325	0.0000	0.000	913556.	850.14	693.15	693.15	1158.78	0.120	0.120	0.4107	850.14	0.845
1	5	1761.3	1.01325	0.0000	0.000	913556.	850.14	693.15	693.15	1158.78	0.120	0.120	0.4107	850.14	0.845
1	6	2218.8	1.01325	0.0000	0.000	913556.	850.14	693.15	693.15	1158.78	0.120	0.120	0.4107	850.14	0.845
1	7	2756.2	1.01325	0.0000	0.000	913556.	850.14	693.15	693.15	1158.78	0.120	0.120	0.4107	850.14	0.845
1	8	3373.7	1.01325	0.0000	0.000	913556.	850.14	693.15	693.15	1158.78	0.120	0.120	0.4107	850.14	0.845
1	9	3991.2	1.01325	0.0000	0.000	913556.	850.14	693.15	693.15	1158.78	0.120	0.120	0.4107	850.14	0.845
1	10	4608.7	1.01325	0.0000	0.000	913556.	850.14	693.15	693.15	1158.78	0.120	0.120	0.4107	850.14	0.845
1	11	5226.2	1.01325	0.0000	0.000	913556.	850.14	693.15	693.15	1158.78	0.120	0.120	0.4107	850.14	0.845
1	12	5843.8	1.01325	0.0000	0.000	913556.	850.14	693.15	693.15	1158.78	0.120	0.120	0.4107	850.14	0.845
1	13	6381.3	1.01325	0.0000	0.000	913556.	850.14	693.15	693.15	1158.78	0.120	0.120	0.4107	850.14	0.845
1	14	6838.8	1.01325	0.0000	0.000	913556.	850.14	693.15	693.15	1158.78	0.120	0.120	0.4107	850.14	0.845
1	15	7296.3	1.01325	0.0000	0.000	913556.	850.14	693.15	693.15	1158.78	0.120	0.120	0.4107	850.14	0.845
1	16	7753.8	1.01325	0.0000	0.000	913556.	850.14	693.15	693.15	1158.78	0.120	0.120	0.4107	850.14	0.845
1	17	8291.3	1.01325	0.0000	0.000	913556.	850.14	693.15	693.15	1158.78	0.120	0.120	0.4107	850.14	0.845
1	18	8697.0	1.01325	0.0000	0.000	913556.	850.14	693.15	693.15	1158.78	0.120	0.120	0.4107	850.14	0.845
1	19	8891.0	1.01325	0.0000	0.000	913556.	850.14	693.15	693.15	1158.78	0.120	0.120	0.4107	850.14	0.845
1	20	9085.0	1.01325	0.0000	0.000	913556.	850.14	693.15	693.15	1158.78	0.120	0.120	0.4107	850.14	0.845
1	21	9279.0	1.01325	0.0000	0.000	913556.	850.14	693.15	693.15	1158.78	0.120	0.120	0.4107	850.14	0.845
1	22	9473.0	1.01325	0.0000	0.000	913556.	850.14	693.15	693.15	1158.78	0.120	0.120	0.4107	850.14	0.845
1	23	9720.0	1.01325	0.0000	0.000	913556.	850.14	693.15	693.15	1158.78	0.120	0.120	0.4107	850.14	0.845
1	24	10020.0	1.01325	0.0000	0.000	913556.	850.14	693.15	693.15	1158.78	0.120	0.120	0.4107	850.14	0.845
1	25	10320.0	1.01325	0.0000	0.000	913556.	850.14	693.15	693.15	1158.78	0.120	0.120	0.4107	850.14	0.845
1	26	10620.0	1.01325	0.0000	0.000	913556.	850.14	693.15	693.15	1158.78	0.120	0.120	0.4107	850.14	0.845
1	27	10920.0	1.01325	0.0000	0.000	913556.	850.14	693.15	693.15	1158.78	0.120	0.120	0.4107	850.14	0.845
1	28	11070.0	1.01325	0.0000	0.000	913556.	850.14	693.15	693.15	1158.78	0.120	0.120	0.4107	850.14	0.845

FINAL STEADY-STATE FOR LOOP TEST (600 W)

TIME STEP NO = 16556 REAL TIME = 195.995733 SEC TIME STEP SIZE = 0.10863D-01 SEC CPU TIME = 8344.33 SEC
 NUMBER OF NEWTON ITERATIONS = 2 O TIME STEP REDUCTIONS DUE TO ERROR 0
 NUMBER OF INNER ITERATIONS = 1 0 0 O REDUCED TIME STEPS SINCE LAST PRINT

TOTAL REACTOR POWER =	0.600 KW	INLET FLOW RATE =	0.850 G/S	MAXIMUM TEMPERATURES IC IZ
TOTAL HEAT TRANSFER =	0.600 KW	OUTLET FLOW RATE =	0.850 G/S	ROD: 1167.08 AT 1 21
FLOW ENTHALPY RISE =	0.600 KW	TOTAL SYSTEM MASS =	66.231 G	WALL: 1165.11 AT 1 21
FLOW ENERGY RISE =	0.592 KW	GLOBAL MASS ERROR =	0.155D-16 G	LIQUID: 1164.81 AT 1 21

MAXIMUM RELATIVE CHANGES OVER THE TIME STEP
 IN PRESSURE: 0.100D-09
 IN MIXTURE DENSITY: 0.100D-09
 IN MIXTURE ENERGY: 0.100D-09

MAXIMUM RELATIVE LINEARIZATION ERRORS
 IN PRESSURE: 0.409D-12
 IN MASS/VOLUME: 0.396D-15
 IN ENERGY/VOLUME: 0.610D-18

IC	IZ	Z(MM)	P(BAR)	VOID	QUAL(%)	EM	ROM	T VAP	T LIO	T SAT	VVZ	VLZ	ROV	ROL	FLOW(G/S)
1	1	0.0	0.94834	0.0000	0.000	913556.	850.08	693.15	693.15	1151.47	0.121	0.121	0.2576	850.08	0.850
1	2	308.7	0.92344	0.0000	0.000	1128239.	810.77	863.14	863.14	1148.55	0.127	0.127	0.2513	810.77	0.850
1	3	846.2	0.92276	0.0000	0.000	1128239.	810.77	863.14	863.14	1148.47	0.127	0.127	0.2511	810.77	0.850
1	4	1303.8	0.92219	0.0000	0.000	1128239.	810.77	863.14	863.14	1148.41	0.127	0.127	0.2510	810.77	0.850
1	5	1761.3	0.92161	0.0000	0.000	1128239.	810.77	863.14	863.14	1148.34	0.127	0.127	0.2508	810.77	0.850
1	6	2218.8	0.92104	0.0000	0.000	1128239.	810.77	863.14	863.14	1148.27	0.127	0.127	0.2507	810.77	0.850
1	7	2756.2	0.92036	0.0000	0.000	1128239.	810.77	863.14	863.14	1148.19	0.127	0.127	0.2505	810.77	0.850
1	8	3373.7	0.96865	0.0000	0.000	1128239.	810.81	863.14	863.14	1153.80	0.127	0.127	0.2627	810.81	0.850
1	9	3991.2	1.01694	0.0000	0.000	1128239.	810.86	863.14	863.14	1159.19	0.127	0.127	0.2748	810.86	0.850
1	10	4608.7	1.06524	0.0000	0.000	1128239.	810.91	863.14	863.14	1164.37	0.127	0.127	0.2868	810.91	0.850
1	11	5226.2	1.11353	0.0000	0.000	1128239.	810.96	863.14	863.14	1169.37	0.127	0.127	0.2988	810.96	0.850
1	12	5843.8	1.16183	0.0000	0.000	1128239.	811.01	863.14	863.14	1174.21	0.127	0.127	0.3108	811.01	0.850
1	13	6381.3	1.16116	0.0000	0.000	1128239.	811.01	863.14	863.14	1174.14	0.127	0.127	0.3106	811.01	0.850
1	14	6838.8	1.16058	0.0000	0.000	1128239.	811.01	863.14	863.14	1174.08	0.127	0.127	0.3105	811.01	0.850
1	15	7296.3	1.16001	0.0000	0.000	1128239.	811.00	863.14	863.14	1174.03	0.127	0.127	0.3103	811.00	0.850
1	16	7753.8	1.15943	0.0000	0.000	1128239.	811.00	863.14	863.14	1173.97	0.127	0.127	0.3102	811.00	0.850
1	17	8291.3	1.15870	0.0000	0.000	913569.	850.28	693.16	693.16	1173.90	0.121	0.121	0.3100	850.28	0.850
1	18	8697.0	1.12460	0.0000	0.000	1054741.	824.55	804.67	804.67	1170.50	0.124	0.124	0.3016	824.55	0.850
1	19	8891.0	1.10893	0.0000	0.000	1195913.	798.36	917.06	917.06	1168.91	0.129	0.129	0.2977	798.36	0.850
1	20	9085.0	1.09377	0.0000	0.000	1337085.	771.92	1029.30	1029.30	1167.35	0.133	0.133	0.2939	771.92	0.850
1	21	9279.0	1.07911	0.0000	0.000	1478257.	745.49	1140.36	1140.36	1165.83	7.148	0.138	0.2903	745.49	0.850
1	22	9473.0	1.06938	0.6815	0.083	1513437.	235.77	1164.81	1164.81	1164.81	11.680	0.426	0.2879	739.63	0.850
1	23	9720.0	1.06027	0.6922	0.087	1512359.	227.93	1163.85	1163.85	1163.85	11.718	0.440	0.2856	739.85	0.850
1	24	10020.0	1.04986	0.6970	0.088	1510987.	224.42	1162.74	1162.74	1162.74	11.890	0.447	0.2830	740.11	0.850
1	25	10320.0	1.03943	0.7016	0.089	1509599.	221.09	1161.63	1161.63	1161.63	12.070	0.454	0.2804	740.36	0.850
1	26	10620.0	1.02898	0.7058	0.090	1508187.	218.10	1160.50	1160.50	1160.50	12.262	0.460	0.2778	740.62	0.850
1	27	10920.0	1.01852	0.7117	0.092	1506800.	213.77	1159.36	1159.36	1159.36	12.427	0.469	0.2752	740.88	0.850
1	28	11070.0	1.01325	0.7453	0.108	1506800.	188.96	1158.78	1158.78	1158.78			0.2738	741.02	

Input for loop test (26 cells, 640 W)

```

2
SINGLE PHASE MEASUREMENT FOR SODIUM NATURAL CONVECTION
  IN A VERTICAL LOOP:ORNL/TM-7018
$INTGIN NC=1,NZ=26,NR=1,NARF=1,NX=1,NRZS=1,IHTF=1,
        IHTS=3,ISS=1,IXFL=0,IDUMP=1,IBB=2,
        ISTRPR=0,ISHPR=10111,NITMAX=-2,IPFSOL=34,
        NEQ=4,NUMBER=0,IHTRPR=0
$REALIN HDT=3.25E-3,PDR=1.2533,HDR=1.OE+10,DELPR=0.5,
        RNUSS=7.0,RADF=1.625E-4,WINLET=8.5OE-4,GRAV=110.0
$RODINP QO=640.0
1$NCR
0$INDENT
1$IFCAR
1$NRZF
1$NRMAF
3$MNRZF
1$INX
7$MNRZS
4$NRMZS
4.07327E-3 $DX
4.07327E-3 $DY
1.0E-6 0.6175 4(0.4575) 6(0.6175) 4(0.4575) 0.6175 5(0.194)
5(0.3) 1.0E-6 $DZ
26(0.0) $ARX
26(0.0) $ARY
27(8.285E-6) $ARZ
5.122162E-6 4(3.794962E-6) 6(5.12212E-6) 4(3.794962E-6)
5.122162E-6 5(1.60923E-6) 5(2.4885E-6) $VOL
3.25E-3 $HEDZ
3.25E-3 $WEDZ
28(1.01325E+05) $P
28(0.0) $ALP
28(693.15) $TEMP
27(12.0E-2) $VEL
-9.8 5(0.0) 5(9.8) 5(0.0) 11(-9.8) $GRAV
26(693.15) $TWF
16(0.0) 5(1.0) 5(0.0) $QZ
1.0 $QT
1.0 $QR
1.0 $RN
1.625E-3 $DRZF
1.62929E-2 $PCX
2.03E-2 $DRZS
1.0E+6 14(0.0) 1.0E+6 10(0.0) $HOUT
863.15 14(500.0) 693.15 10(500.0) $TOUT
26(693.15) $TWS
26(2.5E+6) $HLSS
$TIMDAT TEND=10.0,DTMIN=1.0E-6,DTMAX=1.0,DTSP=20.0,DTLP=1.0,IREDMX=20
$TIMDAT TEND=-1.0
0

```

F-31

Initial conditions for loop test (26 cells)

TIME STEP NO = 0 REAL TIME = 0.000000 SEC TIME STEP SIZE = 0.000000+00 SEC CPU TIME = 0.00 SEC
 NUMBER OF NEWTON ITERATIONS = 0 0 TIME STEP REDUCTIONS DUE TO ERROR = 0
 NUMBER OF INNER ITERATIONS = 0 0 0 0 REDUCED TIME STEPS SINCE LAST PRINT

TOTAL REACTOR POWER = 0.640 KW INLET FLOW RATE = 0.845 G/S MAXIMUM TEMPERATURES IC IZ
 TOTAL HEAT TRANSFER = 0.640 KW OUTLET FLOW RATE = 0.845 G/S ROD: 0.00 AT 0 0
 FLOW ENTHALPY RISE = 0.000 KW TOTAL SYSTEM MASS = 78.065 G WALL: 0.00 AT 0 0
 FLOW ENERGY RISE = 0.000 KW GLOBAL MASS ERROR = 0.0000+00 G LIQUID: 693.15 AT 1 1

MAXIMUM RELATIVE CHANGES OVER THE TIME STEP
 IN PRESSURE: 0.0000+00
 IN MIXTURE DENSITY: 0.0000+00
 IN MIXTURE ENERGY: 0.0000+00

MAXIMUM RELATIVE LINEARIZATION ERRORS
 IN PRESSURE: 0.0000+00
 IN MASS/VOLUME: 0.0000+00
 IN ENERGY/VOLUME: 0.0000+00

IC	IZ	Z(MM)	P(BAR)	VOID	QUAL(%)	EM	ROM	T VAP	T LIQ	T SAT	VVZ	VLZ	ROV	ROL	FLOW(G/S)
1	1	0.0	1.01325	0.0000	0.000	913556.	850.14	693.15	693.15	1158.78	0.120	0.120	0.4107	850.14	0.845
1	2	308.7	1.01325	0.0000	0.000	913556.	850.14	693.15	693.15	1158.78	0.120	0.120	0.4107	850.14	0.845
1	3	846.2	1.01325	0.0000	0.000	913556.	850.14	693.15	693.15	1158.78	0.120	0.120	0.4107	850.14	0.845
1	4	1303.8	1.01325	0.0000	0.000	913556.	850.14	693.15	693.15	1158.78	0.120	0.120	0.4107	850.14	0.845
1	5	1761.3	1.01325	0.0000	0.000	913556.	850.14	693.15	693.15	1158.78	0.120	0.120	0.4107	850.14	0.845
1	6	2218.8	1.01325	0.0000	0.000	913556.	850.14	693.15	693.15	1158.78	0.120	0.120	0.4107	850.14	0.845
1	7	2756.2	1.01325	0.0000	0.000	913556.	850.14	693.15	693.15	1158.78	0.120	0.120	0.4107	850.14	0.845
1	8	3373.7	1.01325	0.0000	0.000	913556.	850.14	693.15	693.15	1158.78	0.120	0.120	0.4107	850.14	0.845
1	9	3991.2	1.01325	0.0000	0.000	913556.	850.14	693.15	693.15	1158.78	0.120	0.120	0.4107	850.14	0.845
1	10	4608.7	1.01325	0.0000	0.000	913556.	850.14	693.15	693.15	1158.78	0.120	0.120	0.4107	850.14	0.845
1	11	5226.2	1.01325	0.0000	0.000	913556.	850.14	693.15	693.15	1158.78	0.120	0.120	0.4107	850.14	0.845
1	12	5843.8	1.01325	0.0000	0.000	913556.	850.14	693.15	693.15	1158.78	0.120	0.120	0.4107	850.14	0.845
1	13	6381.3	1.01325	0.0000	0.000	913556.	850.14	693.15	693.15	1158.78	0.120	0.120	0.4107	850.14	0.845
1	14	6838.8	1.01325	0.0000	0.000	913556.	850.14	693.15	693.15	1158.78	0.120	0.120	0.4107	850.14	0.845
1	15	7296.3	1.01325	0.0000	0.000	913556.	850.14	693.15	693.15	1158.78	0.120	0.120	0.4107	850.14	0.845
1	16	7753.8	1.01325	0.0000	0.000	913556.	850.14	693.15	693.15	1158.78	0.120	0.120	0.4107	850.14	0.845
1	17	8291.3	1.01325	0.0000	0.000	913556.	850.14	693.15	693.15	1158.78	0.120	0.120	0.4107	850.14	0.845
1	18	8697.0	1.01325	0.0000	0.000	913556.	850.14	693.15	693.15	1158.78	0.120	0.120	0.4107	850.14	0.845
1	19	8891.0	1.01325	0.0000	0.000	913556.	850.14	693.15	693.15	1158.78	0.120	0.120	0.4107	850.14	0.845
1	20	9085.0	1.01325	0.0000	0.000	913556.	850.14	693.15	693.15	1158.78	0.120	0.120	0.4107	850.14	0.845
1	21	9279.0	1.01325	0.0000	0.000	913556.	850.14	693.15	693.15	1158.78	0.120	0.120	0.4107	850.14	0.845
1	22	9473.0	1.01325	0.0000	0.000	913556.	850.14	693.15	693.15	1158.78	0.120	0.120	0.4107	850.14	0.845
1	23	9720.0	1.01325	0.0000	0.000	913556.	850.14	693.15	693.15	1158.78	0.120	0.120	0.4107	850.14	0.845
1	24	10020.0	1.01325	0.0000	0.000	913556.	850.14	693.15	693.15	1158.78	0.120	0.120	0.4107	850.14	0.845
1	25	10320.0	1.01325	0.0000	0.000	913556.	850.14	693.15	693.15	1158.78	0.120	0.120	0.4107	850.14	0.845
1	26	10620.0	1.01325	0.0000	0.000	913556.	850.14	693.15	693.15	1158.78	0.120	0.120	0.4107	850.14	0.845
1	27	10920.0	1.01325	0.0000	0.000	913556.	850.14	693.15	693.15	1158.78	0.120	0.120	0.4107	850.14	0.845
1	28	11070.0	1.01325	0.0000	0.000	913556.	850.14	693.15	693.15	1158.78	0.120	0.120	0.4107	850.14	0.845

FINAL STEADY-STATE FOR LOOP TEST (640 W)

TIME STEP NO = 21805 REAL TIME = 200.000669 SEC TIME STEP SIZE = 0.85361D-02 SEC CPU TIME = 10960.49 SEC
 NUMBER OF NEWTON ITERATIONS = 2 O TIME STEP REDUCTIONS DUE TO ERROR = 0
 NUMBER OF INNER ITERATIONS = 1 0 0 O REDUCED TIME STEPS SINCE LAST PRINT

TOTAL REACTOR POWER =	0.640 KW	INLET FLOW RATE =	0.850 G/S	MAXIMUM TEMPERATURES IC 12
TOTAL HEAT TRANSFER =	0.640 KW	OUTLET FLOW RATE =	0.850 G/S	ROD: 1169.15 AT 1 20
FLOW ENTHALPY RISE =	0.639 KW	TOTAL SYSTEM MASS =	65.369 G	WALL: 1167.05 AT 1 20
FLOW ENERGY RISE =	0.629 KW	GLOBAL MASS ERROR =	0.988D-15 G	LIQUID: 1166.53 AT 1 20

MAXIMUM RELATIVE CHANGES OVER THE TIME STEP
 IN PRESSURE: 0.100D-09
 IN MIXTURE DENSITY: 0.100D-09
 IN MIXTURE ENERGY: 0.100D-09

MAXIMUM RELATIVE LINEARIZATION ERRORS
 IN PRESSURE: 0.233D-12
 IN MASS/VOLUME: 0.796D-15
 IN ENERGY/VOLUME: 0.651D-17

IC	IZ	Z(MM)	P(BAR)	VOID	QUAL(%)	EM	ROM	T VAP	T LIQ	T SAT	VVZ	VLZ	ROV	ROL	FLOW(G/S)
1	1	0.0	0.95451	0.0000	0.000	913556.	850.08	693.15	693.15	1152.18	0.121	0.121	0.2591	850.08	0.850
1	2	308.7	0.92962	0.0000	0.000	1128239.	810.77	863.14	863.14	1149.28	0.127	0.127	0.2529	810.77	0.850
1	3	846.2	0.92894	0.0000	0.000	1128239.	810.77	863.14	863.14	1149.20	0.127	0.127	0.2527	810.77	0.850
1	4	1303.8	0.92836	0.0000	0.000	1128239.	810.77	863.14	863.14	1149.13	0.127	0.127	0.2525	810.77	0.850
1	5	1761.3	0.92779	0.0000	0.000	1128239.	810.77	863.14	863.14	1149.07	0.127	0.127	0.2524	810.77	0.850
1	6	2218.8	0.92721	0.0000	0.000	1128239.	810.77	863.14	863.14	1149.00	0.127	0.127	0.2523	810.77	0.850
1	7	2756.2	0.92654	0.0000	0.000	1128239.	810.77	863.14	863.14	1148.92	0.127	0.127	0.2521	810.77	0.850
1	8	3373.7	0.92483	0.0000	0.000	1128239.	810.82	863.14	863.14	1154.50	0.127	0.127	0.2642	810.82	0.850
1	9	3991.2	1.02312	0.0000	0.000	1128239.	810.87	863.14	863.14	1159.86	0.127	0.127	0.2763	810.87	0.850
1	10	4608.7	1.07141	0.0000	0.000	1128239.	810.92	863.14	863.14	1165.02	0.127	0.127	0.2884	810.92	0.850
1	11	5226.2	1.11971	0.0000	0.000	1128239.	810.96	863.14	863.14	1170.00	0.127	0.127	0.3004	810.96	0.850
1	12	5843.8	1.16801	0.0000	0.000	1128239.	811.01	863.14	863.14	1174.81	0.127	0.127	0.3123	811.01	0.850
1	13	6381.3	1.16734	0.0000	0.000	1128239.	811.01	863.14	863.14	1174.75	0.127	0.127	0.3121	811.01	0.850
1	14	6838.8	1.16676	0.0000	0.000	1128239.	811.01	863.14	863.14	1174.69	0.127	0.127	0.3120	811.01	0.850
1	15	7296.3	1.16619	0.0000	0.000	1128239.	811.01	863.14	863.14	1174.63	0.127	0.127	0.3119	811.01	0.850
1	16	7753.8	1.16561	0.0000	0.000	1128239.	811.01	863.14	863.14	1174.58	0.127	0.127	0.3117	811.01	0.850
1	17	8291.3	1.16488	0.0000	0.000	913569.	850.29	693.16	693.16	1174.51	0.121	0.121	0.3115	850.29	0.850
1	18	8697.0	1.13080	0.0000	0.000	1064153.	822.83	812.15	812.15	1171.12	0.125	0.125	0.3031	822.83	0.850
1	19	8891.0	1.11518	0.0000	0.000	1214736.	794.85	932.06	932.06	1169.54	0.129	0.129	0.2992	794.85	0.850
1	20	9085.0	1.10010	0.0000	0.000	1365319.	766.64	1051.64	1051.64	1168.00	0.134	0.134	0.2955	766.64	0.850
1	21	9279.0	1.08582	0.0384	0.002	1511939.	710.88	1166.53	1166.53	1166.53	7.512	0.144	0.2919	739.23	0.850
1	22	9473.0	1.07688	0.7828	0.126	1516388.	175.62	1165.60	1165.60	1165.60	14.712	0.566	0.2897	739.45	0.850
1	23	9720.0	1.06652	0.7710	0.131	1515202.	169.58	1164.51	1164.51	1164.51	14.813	0.586	0.2871	739.70	0.850
1	24	10020.0	1.05488	0.7740	0.131	1513651.	167.46	1163.28	1163.28	1163.28	15.052	0.594	0.2842	739.98	0.850
1	25	10320.0	1.04313	0.7768	0.132	1512067.	165.45	1162.02	1162.02	1162.02	15.302	0.601	0.2813	740.27	0.850
1	26	10620.0	1.03127	0.7792	0.132	1510440.	163.71	1160.75	1160.75	1160.75	15.569	0.607	0.2784	740.57	0.850
1	27	10920.0	1.01932	0.7831	0.134	1508836.	160.90	1159.45	1159.45	1159.45	15.815	0.617	0.2754	740.86	0.850
1	28	11070.0	1.01325	0.8056	0.153	1508836.	144.29	1158.78	1158.78	1158.78			0.2738	741.02	